

This document downloaded from
vulcanhammer.net vulcanhammer.info
Chet Aero Marine



Don't forget to visit our companion site
<http://www.vulcanhammer.org>

Use subject to the terms and conditions of the respective websites.



**US Army Corps
of Engineers®**
Engineer Research and
Development Center



Comparison of Levee Underseepage Analysis Methods Using Blanket Theory and Finite Element Analysis

Thomas L. Brandon, Abeera Batool, Martha Jimenez,
Noah D. Vroman, and Maureen K. Corcoran

August 2018

The U.S. Army Engineer Research and Development Center (ERDC) solves the nation's toughest engineering and environmental challenges. ERDC develops innovative solutions in civil and military engineering, geospatial sciences, water resources, and environmental sciences for the Army, the Department of Defense, civilian agencies, and our nation's public good. Find out more at www.erdclibrary.usace.army.mil.

To search for other technical reports published by ERDC, visit the ERDC online library at <http://acwc.sdp.sirsi.net/client/default>.

Comparison of Levee Underseepage Analysis Methods Using Blanket Theory and Finite Element Analysis

Thomas L. Brandon, Abeera Batool, and Martha Jimenez

*Department of Civil and Environmental Engineering
Virginia Tech
750 Drillfield Dr.
Blacksburg, VA 24061-0105*

Noah D. Vroman

*U.S. Army Corps of Engineers
Mississippi Valley Division Dam and Levee Safety Production Center
4155 East Clay St.
Vicksburg, MS 39183*

Maureen K. Corcoran

*Geotechnical and Structures Laboratory
U.S. Army Engineer Research and Development Center
3909 Halls Ferry Road
Vicksburg, MS 39180-6199*

Final report

Approved for public release; distribution is unlimited.

Prepared for U.S. Army Corps of Engineers
Washington, DC 20314-1000

Under Engineering Manual 1110-2-1913

Abstract

This report provides a comparison of levee underseepage analysis methods using Blanket Theory and finite element analysis. Blanket Theory is a set of closed-form solutions for computing seepage pressures and flows beneath levees. These solutions were introduced in a U.S. Army Corps of Engineers (USACE) 1956 technical manual and are also shown in the 2000 version of USACE Engineer Manual, "Design and Construction of Levees." Derivations of Blanket Theory, which have not been previously documented, are thoroughly documented in this report. These derivations include the standard seven Blanket Theory cases and provide the key assumptions necessary for the accuracy of the solution; they highlight the errors in the Blanket Theory equations shown in the 2000 USACE engineering manual. An additional Blanket Theory case, which include a cutoff wall located beneath the levee, is derived in this report. Subsequently, an evaluation of the Blanket Theory solutions is made using finite element analysis. This evaluation included the standard seven Blanket Theory cases, the additional Blanket Theory case, and layered strata. This evaluation demonstrates where the analysis methods did or did not produce similar results. The finite element analysis method is further evaluated comparing different finite element analysis software. Finally, general guidelines for performing levee underseepage finite element analysis are provided in this report.

DISCLAIMER: The contents of this report are not to be used for advertising, publication, or promotional purposes. Citation of trade names does not constitute an official endorsement or approval of the use of such commercial products. All product names and trademarks cited are the property of their respective owners. The findings of this report are not to be construed as an official Department of the Army position unless so designated by other authorized documents.

DESTROY THIS REPORT WHEN NO LONGER NEEDED. DO NOT RETURN IT TO THE ORIGINATOR.

Contents

Abstract	ii
Figures and Tables.....	v
Preface.....	ix
Unit Conversion Factors	x
1 Introduction.....	1
2 Derivation of Blanket Theory Equations.....	3
2.1 Case histories	3
2.2 Cases 2, 3, and 4 - Impervious top stratum both riverside and landside	7
2.2.1 Case 2 - Impervious top stratum both riverside and landside	7
2.2.2 Case 3 - Impervious riverside top stratum and no landside top stratum	10
2.2.3 Case 4 — Impervious landside top stratum and no riverside top stratum	11
2.3 Semi-pervious top stratum (Cases 5, 6, 7, 8).....	13
2.3.1 Case 5 - Semi-pervious riverside top stratum and no landside top stratum.....	13
2.3.2 Case 6 - Semi-pervious landside top stratum and no riverside top stratum.....	16
2.3.3 Case 7 - Semi-pervious top strata both riverside and landside	19
2.3.4 Case 7a - Semi-pervious landside and riverside top stratum (top stratum extends infinitely landward of the levee)	21
2.3.5 Case 7b - Semi-pervious landside and riverside top stratum (seepage block in the pervious substratum located landward of the levee)	25
2.3.6 Case 7c - Semi-pervious landside and riverside top stratum	29
2.3.7 Case 8 - Semi-pervious top strata both riverside and landside with sheet pile at the center of levee	33
2.3.8 Case 8a - Semi-pervious landside and riverside top stratum (top stratum extends infinitely landward of the levee) with cutoff.....	36
2.3.9 Case 8b (L_3 = finite distance to seepage block).....	37
2.3.10 Case 8c (L_3 = finite distance to an open seepage exit)	38
2.4 Blanket Theory equations summary.....	39
3 Evaluation of Blanket Theory Solutions with Finite Elements Analyses	45
3.1 Introduction.....	45
3.2 Case 1 - No landside and riverside top stratum.....	47
3.3 Case 2 - Impervious landside and riverside top stratum	49
3.4 Case 3 - Impervious riverside top stratum and no landside top stratum	52
3.5 Case 4 - Impervious landside top stratum and no riverside top stratum	53
3.6 Case 5 - Semi-pervious riverside top stratum and no landside top stratum	55
3.7 Case 6 - Semi-pervious landside top stratum and no riverside top stratum	59
3.8 Case 7 - Semi-pervious top strata on riverside and landside.....	66
3.8.1 Case 7a - Semi-pervious landside and riverside top stratum (top stratum extends infinitely landward of the levee)	66
3.8.2 Case 7b - Semi-pervious landside and riverside top stratum (seepage block in the pervious substratum located landward of the levee)	70

3.8.3	Case 7c – Semi-pervious landside and riverside top stratum (seepage exit in the pervious substratum located landward of the levee)	73
3.9	Case 8 – Semi-pervious top strata on riverside and landside.....	78
3.9.1	Case 8b – Semi-pervious landside and riverside top stratum (seepage block in the pervious substratum located landward of the levee) with cutoff wall	79
3.9.2	Case 8c – Semi-pervious landside and riverside top stratum (seepage exit in the pervious substratum located landward of the levee) with cutoff wall	81
4	Comparison of SLIDE with SEEP/W	83
5	Issues with Numbers of Elements	85
6	General Guidelines for Finite Element Analysis.....	86
7	Boundary Conditions for Blanket Theory Cases	87
8	Layered Top Strata	91
9	Finite Element Boundary Conditions for Outfall Canals	100
	References	102
	Appendix A	103
	Appendix B	107
	Appendix C	121
	Report Documentation Page	

Figures and Tables

Figures

Figure 1. Case 1 - No top stratum.	4
Figure 2. Equipotential lines for levee section having $L_2/d > 1$	4
Figure 3. Equipotential lines for levee section having $L_2/d < 1$	5
Figure 4. Case 1 - No top stratum with three zones of fragments.	5
Figure 5. Case 2 Impervious top stratum on both riverside and landside.	8
Figure 6. Pressure diagram for confined flow condition.	9
Figure 7. Case 3 - Impervious riverside top stratum and no landside top stratum.	10
Figure 8. Case 4 - Impervious landside top stratum and no riverside top stratum.	11
Figure 9. Case 5 - Semi-pervious riverside top stratum and no landside top stratum.	14
Figure 10. Case 6 - Semi-pervious landside top stratum and no riverside top stratum.	16
Figure 11. Case 7 - Semi-pervious top strata both riverside and landside.	19
Figure 12. Case 7a - Semi-pervious top strata both riverside and landside with L_3 as infinite.	21
Figure 13. Landward side of the levee.	22
Figure 14. Case 7b - Semi-pervious top strata both riverside and landside with L_3 as finite distance to seepage block.	25
Figure 15. Case 7c - Semi-pervious top strata both riverside and landside with L_3 as a finite distance to an open seepage exit.	30
Figure 16. Case 8 - Semi-pervious top strata both riverside and landside with sheet pile at the center of levee.	34
Figure 17. Case 8a - Semi-pervious top strata both riverside and landside with sheet pile at the center of levee and L_3 as infinite.	37
Figure 18. Case 8b - Semi-pervious top strata both riverside and landside with sheet pile at the center of levee and L_3 as finite distance to seepage block.	38
Figure 19. Case 8c - Semi-pervious top strata both riverside and landside with sheetpile at the center of levee and L_3 as finite distance to an open seepage exit.	39
Figure 20. Equations for computation of underseepage flow and substratum pressures for Cases 1 through 4.	40
Figure 21. Equations for computation of underseepage flow and substratum pressures for Cases 5 and 6.	41
Figure 22. Equations for computation of underseepage flow and substratum pressures for Case 7.	42
Figure 23. Equations for computation of underseepage flow and substratum pressures for Case 8.	43
Figure 24. Generalized geometry and boundary conditions used in finite element analysis.	46
Figure 25. Geometry for Case 1 - No landside and riverside top stratum.	48
Figure 26. Calculated values of flow per unit length (Q_s) for different values of L_2/d for Case 1.	48
Figure 27. Comparison of different values of L_1 and L_3 for FEA.	49

Figure 28. Percent error in calculated flow per unit length (Q_s) for Blanket Theory with increasing L_2/d ratios.	49
Figure 29. Geometry for Case 2 - Impervious landside and riverside top stratum.	50
Figure 30. Calculated values of flow per unit length (Q_s) from Blanket Theory and finite element analysis for different values of L_3 for Case 2.	51
Figure 31. Excess head (h_o) or pressure head beneath blanket at toe for Case 2 calculated using FEA and Blanket Theory for different values of L_3 for $d = 25$ ft and $d = 100$ ft.	51
Figure 32. Geometry for Case 3 - Impervious riverside top stratum and no landside top stratum.	52
Figure 33. Calculated values of flow per unit length (Q_s) from Blanket Theory and finite element analysis for different values of L_1 for Case 3.	53
Figure 34. Geometry for Case 4 - Impervious landside top stratum and no riverside top stratum.	54
Figure 35. Calculated values of flow per unit length (Q_s) from Blanket Theory and finite element analysis for different values of L_3 for Case 4.	54
Figure 36. Excess head (h_o) or pressure head at toe calculated using FEA and Blanket Theory for different values of L_3	55
Figure 37. Geometry of Case 5 - Semi-pervious riverside top stratum and no landside top stratum.	56
Figure 38. Calculated values of flow per unit length (Q_s) for various permeability ratios from Blanket Theory and finite element analysis for Case 5 for $z_b = 10$ ft and $L_1 = 200$ ft.	57
Figure 39. Calculated values of flow per unit length (Q_s) for various permeability ratios from Blanket Theory and finite element analysis for Case 5 for $z_b = 10$ ft and $L_1 = 1,000$ ft.	58
Figure 40. Calculated values of flow per unit length (Q_s) for various permeability ratios from Blanket Theory and finite element analysis for Case 5 for $z_b = 20$ ft and $L_1 = 200$ ft.	58
Figure 41. Calculated values of flow per unit length (Q_s) for various permeability ratios from Blanket Theory and finite element analysis for Case 5 for $z_b = 20$ ft and $L_1 = 1,000$ ft.	59
Figure 42. Geometry for Case 6 - Semi-pervious landside top stratum and no riverside top stratum.	60
Figure 43. Calculated values of flow per unit length (Q_s) for various permeability ratios from Blanket Theory and finite element analysis for Case 6 for $z_b = 10$ ft and $L_3 = 1,000$ ft.	61
Figure 44. Calculated values of flow per unit length (Q_s) for various permeability ratios from Blanket Theory and finite element analysis for Case 6 for $z_b = 20$ ft and $L_3 = 1,000$ ft.	62
Figure 45. Excess head (h_o) or pressure head beneath blanket at toe for Case 6 calculated using FEA and Blanket Theory for different permeability ratios for $z_b = 10$ ft and $L_3 = 1,000$ ft.	62
Figure 46. Pressure head beneath blanket at toe for Case 6 calculated using FEA and Blanket Theory for different permeability ratios for $z_b = 20$ ft and $L_3 = 1,000$ ft.	63
Figure 47. Piezometric grade line for Case 6 where $L_3 = 200$ ft, $z_b = 10$ ft, and $k_f/k_b = 10$	64
Figure 48. Piezometric grade line for Case 6 where $L_3 = 200$ ft, $z_b = 10$ ft, and $k_f/k_b = 1000$	65
Figure 49. Piezometric grade line for Case 6 where $L_3 = 500$ ft, $z_b = 10$ ft, and $k_f/k_b = 1000$	65
Figure 50. Geometry and finite element boundary conditions for Case 7a.	66
Figure 51. Calculated values of flow per unit length (Q_s) for various permeability ratios from Blanket Theory and finite element analysis for Case 7a for $z_b = 10$ ft and $L_1 = 500$ ft.	67

Figure 52. Calculated values of flow per unit length (Q_s) for various permeability ratios from Blanket Theory and finite element analysis for Case 7a for $z_b = 20$ ft and $L_1 = 500$ ft.	68
Figure 53. Excess head (h_o) or pressure head beneath blanket at toe for Case 7a calculated using FEA and Blanket Theory for different permeability ratios for $z_b = 10$ ft and $L_1 = 500$ ft.	69
Figure 54. Excess head (h_o) or pressure head beneath blanket at toe for Case 7a calculated using FEA and Blanket Theory for different permeability ratios for $z_b = 20$ ft and $L_1 = 500$ ft.	69
Figure 55. Geometry and finite element boundary conditions for Case 7b.	70
Figure 56. Calculated values of flow per unit length (Q_s) for various permeability ratios from Blanket Theory and finite element analysis for Case 7b for $z_b = 10$ ft and $L_1 = 500$ ft and $L_3 = 500$ ft.	71
Figure 57. Calculated values of flow per unit length (Q_s) for various permeability ratios from Blanket Theory and finite element analysis for Case 7b for $z_b = 20$ ft and $L_1 = 500$ ft and $L_3 = 500$ ft.	72
Figure 58. Excess head (h_o) or pressure head beneath blanket at toe for Case 7b calculated using FEA and Blanket Theory for different permeability ratios for $z_b = 10$ ft, $L_1 = 500$ ft, and $L_3 = 500$ ft.	72
Figure 59. Excess head (h_o) or pressure head beneath blanket at toe for Case 7b calculated using FEA and Blanket Theory for different permeability ratios for $z_b = 20$ ft, $L_1 = 500$ ft, and $L_3 = 500$ ft.	73
Figure 60. Geometry and boundary conditions for Case 7c.	74
Figure 61. Calculated values of flow per unit length (Q_s) for various permeability ratios from Blanket Theory and finite element analysis for Case 7c for $z_b = 10$ ft and $L_1 = 500$ ft and $L_3 = 500$ ft.	74
Figure 62. Calculated values of flow per unit length (Q_s) for various permeability ratios from Blanket Theory and finite element analysis for Case 7c for $z_b = 20$ ft and $L_1 = 500$ ft and $L_3 = 500$ ft.	75
Figure 63. Excess head (h_o) or pressure head beneath blanket at toe for Case 7c calculated using FEA and Blanket Theory for different permeability ratios for $z_b = 10$ ft, $L_1 = 500$ ft, and $L_3 = 500$ ft.	76
Figure 64. Excess head (h_o) or pressure head beneath blanket at toe for Case 7c calculated using FEA and Blanket Theory for different permeability ratios for $z_b = 20$ ft, $L_1 = 500$ ft, and $L_3 = 500$ ft.	76
Figure 65. Pressure head at the top of the pervious layer for Case 7c calculated with finite element analysis and Blanket Theory for $z_b = 10$ ft and $k_f/k_b = 10$.	77
Figure 66. Pressure head at the top of the pervious layer for Case 7c calculated with finite element analysis and Blanket Theory for $z_b = 10$ ft and $k_f/k_b = 1000$.	78
Figure 67. Geometry and boundary conditions for Case 8b.	79
Figure 68. Calculated values of flow per unit length (Q_s) for various permeability ratios from Blanket Theory and finite element analysis for Case 8b for $z_b = 10$ ft and $L_1 = 500$ ft and $L_3 = 500$ ft.	80
Figure 69. Pressure head beneath blanket at toe for Case 8b calculated using FEA and Blanket Theory for different permeability ratios for $z_b = 10$ ft, $L_1 = 500$ ft, and $L_3 = 500$ ft.	80
Figure 70. Geometry and boundary conditions for Case 8c.	81

Figure 71. Calculated values of flow per unit length (Q_s) for various permeability ratios from Blanket Theory and finite element analysis for Case 8c for $z_b = 10$ ft and $L_1 = 500$ ft and $L_3 = 500$ ft.	82
Figure 72. Pressure head beneath blanket at toe for Case 8c calculated using FEA and Blanket Theory for different permeability ratios for $z_b = 10$ ft, $L_1 = 500$ ft, and $L_3 = 500$ ft.	82
Figure 73. Calculated flows for SLIDE and SEEP/W for Case 7c.	83
Figure 74. Pressure head at the toe of the levee calculated by SLIDE and SEEP/W for Case 7c.	84
Figure 75. Calculated flows for Case 6 showing the effect of number of elements.	85
Figure 76. Boundary conditions to be set for finite element seepage analysis.	87
Figure 77. General configuration of top strata used in the analyses.	91
Figure 78. Calculated values of flow per unit length (Q_s) from Blanket Theory and finite element analysis for combinations 1 to 22 for Case 6.	97
Figure 79. Excess head (h_o) or pressure head beneath blanket at toe for Case 6 calculated using FEA and Blanket Theory for combinations 1 to 22.	97
Figure 80. Calculated values of flow per unit length (Q_s) from Blanket Theory and finite element analysis for combinations 23 to 44 for Case 6.	98
Figure 81. Excess head (h_o) or pressure head beneath blanket at toe for Case 6 calculated using FEA and Blanket Theory for combinations 23 to 44.	98
Figure 82. Calculated values of flow per unit length (Q_s) from Blanket Theory and finite element analysis for combinations 45 to 66 for Case 6.	99
Figure 83. Excess head (h_o) or pressure head beneath blanket at toe for Case 6 calculated using FEA and Blanket Theory for combinations 45 to 66.	99

Tables

Table 1. Summary of parameters for combinations 1 to 22 used in the analyses of top strata having $z_1 = z_2 = 10$ ft.	93
Table 2. Summary of parameters for combinations 23 to 44 used in the analyses of top strata having $z_1 = 5$ ft and $z_2 = 15$ ft.	94
Table 3. Summary of parameters for combinations 45 to 66 used in the analyses of top strata having $z_1 = 15$ ft and $z_2 = 5$ ft.	95

Preface

The study was funded by both the Hurricane Protection Office (HPO) in U.S. Army Corps of Engineers (USACE), New Orleans District and Headquarters, USACE. The work began in 2009 and was completed by a joint effort between Geotechnical Engineering and Geosciences Branch (GEGB) of The U.S. Army Engineer Research and Development Center (ERDC) and Virginia Tech University. Virginia Tech University was funded for this study under contract W912HZ-09-P-0197. The technical monitor for the study was Mr. Noah Vroman.

The GEGB is under the Geosciences and Structures Division (GS), ERDC, Geotechnical and Structures Laboratory (ERDC-GSL). At the time of publication, Mr. Chad A. Gartrell was Chief, CEERD-GSG; Mr. James Davis was Chief, CEERD-GS; and Dr. Michael Sharp, CEERD-GZT, was the Technical Director for Civil Works. The Deputy Director of ERDC-GSL was Dr. William P. Grogan, and the Director was Mr. Bartley P. Durst.

COL Ivan P. Beckman was the Commander of ERDC, and Dr. David W. Pittman was the Director.

Unit Conversion Factors

Multiply	By	To Obtain
feet	0.3048	meters
gallons (US liquid)	3.785412 E-03	cubic meters
feet per second	0.24384	centimeters per second
pounds (mass) per cubic foot	16.01846	kilograms per cubic meter

1 Introduction

The U.S. Army Corps of Engineers (USACE) Engineer Manual (EM) 1110-2-1913, “Design and Construction of Levees” (USACE 2000), provides closed-form (Blanket Theory) solutions for seepage pressures and flows beneath levees. These solutions were originally developed in the USACE Technical Manual (TM) 3-424, “Investigation of Underseepage and Its Control” (USACE 1956), and have been used by the USACE for over 50 years in various forms.

USACE (1956) developed these solutions using a compilation of existing theories and methods, such as the Method of Fragments (Forchheimer 1917; Muskat 1937; Pavlovsky 1956; and Harr 1962), and Bennett’s (1946) and Barron’s (1948) contributions on effects of semi-pervious blankets. However, USACE (1956) did not provide derivations for these solutions, yet these solutions are still included in USACE (2000).

This study was conducted for the USACE Headquarters (HQ) and the New Orleans District (Hurricane Protection Office). The study was performed to assist in the update of USACE Engineer Manual (EM) 1110-2-1913, “Design and Construction of Levees,” and provide guidance to the Geotechnical Criteria and Analysis Team (GCAT) for efforts on the Hurricane Storm Dam Risk Reduction System (HSDRRS) located in Louisiana.

Following the events of Hurricane Katrina, EM 1110-2-1913 needed revision to incorporate lessons learned from the event and to update the manual to the current state-of-levee design and construction practices. The scope of this study initially focused on supporting the revision and update to the EM and included the following:

- providing derivations to the Blanket Theory equations shown in USACE (2000)
- correcting Blanket Theory equations in USACE (2000) that contained errors
- comparing Blanket Theory solutions to solutions from finite element seepage analysis
- providing general guidelines for finite element seepage analysis
- evaluating potential errors in Blanket Theory solutions of layered top stratum

The initial scope of the study was expanded to also support ongoing HSDRRS rebuilding efforts. The additional scope items included recommended finite element boundary conditions for the Outfall Canals located in the HSDRRS.

The authors benefited greatly from personal notes provided by Doug Spaulding (1976) that contained many of the derivations included in this report.

2 Derivation of Blanket Theory Equations

2.1 Case histories

In USACE (2000), solutions are given for nine different configurations of impervious and semi-pervious top stratum conditions. Several corrections were made to these solutions, and three additional configurations (Cases 8a, 8b, and 8c) have been added.

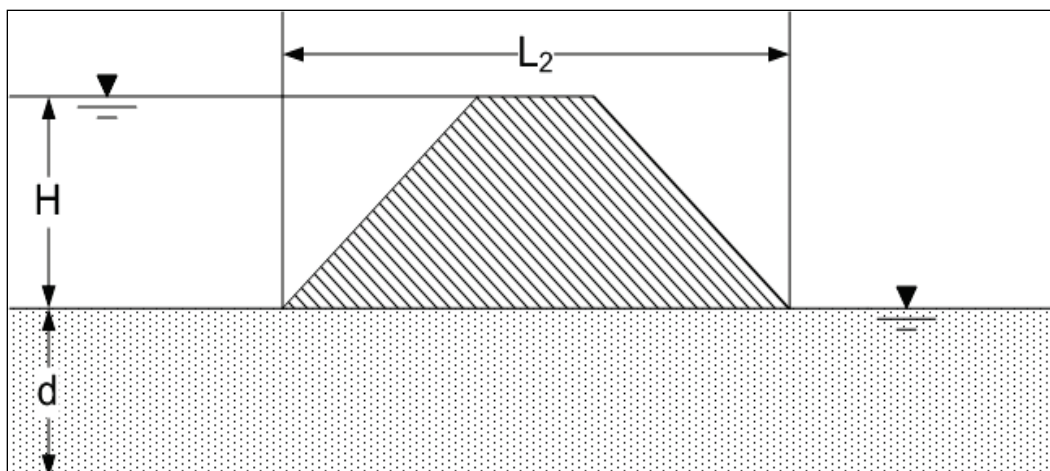
The following cases are addressed in this report:

- Case 1 - No landside and riverside top stratum
- Case 2 - Impervious landside and riverside top stratum
- Case 3 - Impervious riverside top stratum and no landside top stratum
- Case 4 - Impervious landside top stratum and no riverside top stratum
- Case 5 – Semi-pervious riverside top stratum and no landside top stratum
- Case 6 – Semi-pervious landside top stratum and no riverside top stratum
- Case 7a - Semi-pervious landside and riverside top stratum (top stratum extends infinitely landward of the levee)
- Case 7b - Semi-pervious landside and riverside top stratum (seepage block in the pervious substratum located landward of the levee)
- Case 7c – Semi-pervious landside and riverside top stratum (seepage exit in the pervious substratum located landward of the levee)
- Case 8a – Semi-pervious landside and riverside top stratum (top stratum extends infinitely landward of the levee) with cutoff
- Case 8b – Semi-pervious landside and riverside top stratum (seepage block in the pervious substratum located landward of the levee) with cutoff
- Case 8c – Semi-pervious landside and riverside top stratum (seepage exit in the pervious substratum located landward of the levee) with cutoff

The following derivations are for no top stratum, which is shown as Case 1 in USACE (2000) and USACE (1956). Figure 1 shows the basic geometry for Case 1. The technique to determine the flow for Case 1 is provided by Harr (1962) using the Method of Fragments, which is based on previous analyses by Forchheimer (1917) and Pavlovsky (1935, 1956). The fundamental assumption of this method, as stated by Harr (1962), is that equipotential

lines at various critical parts of the flow region can be approximated by vertical lines that divide the region into sections or *fragments*.

Figure 1. Case 1 - No top stratum.



The application of the Method of Fragments is limited to the cases where the base width of the levee (L_2) is greater than the thickness of the pervious substratum, d (i.e., $L_2/d \geq 1$). This is illustrated in Figures 2 and 3 by showing equipotential lines produced from a finite element analysis (FEA) for sections having $L_2/d > 1$ and $L_2/d < 1$.

Figure 2. Equipotential lines for levee section having $L_2/d > 1$.

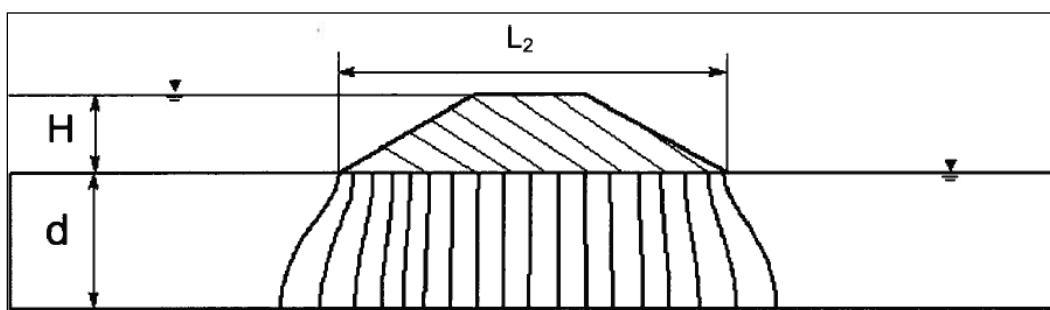
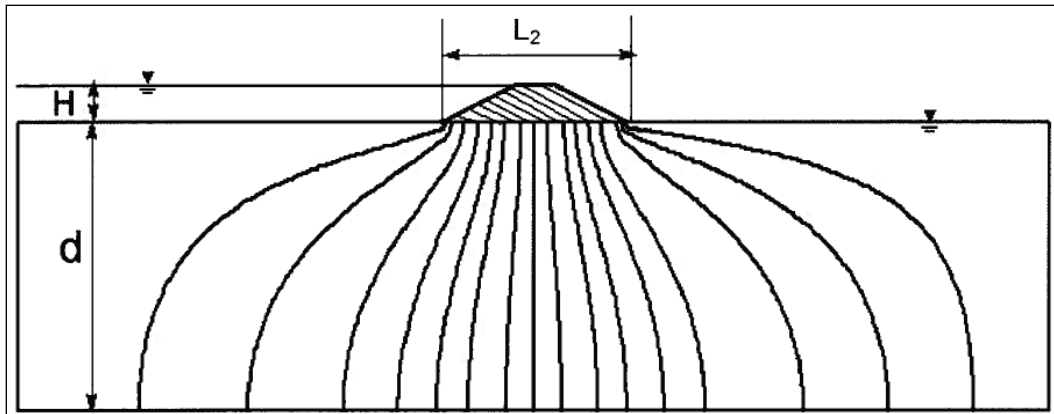
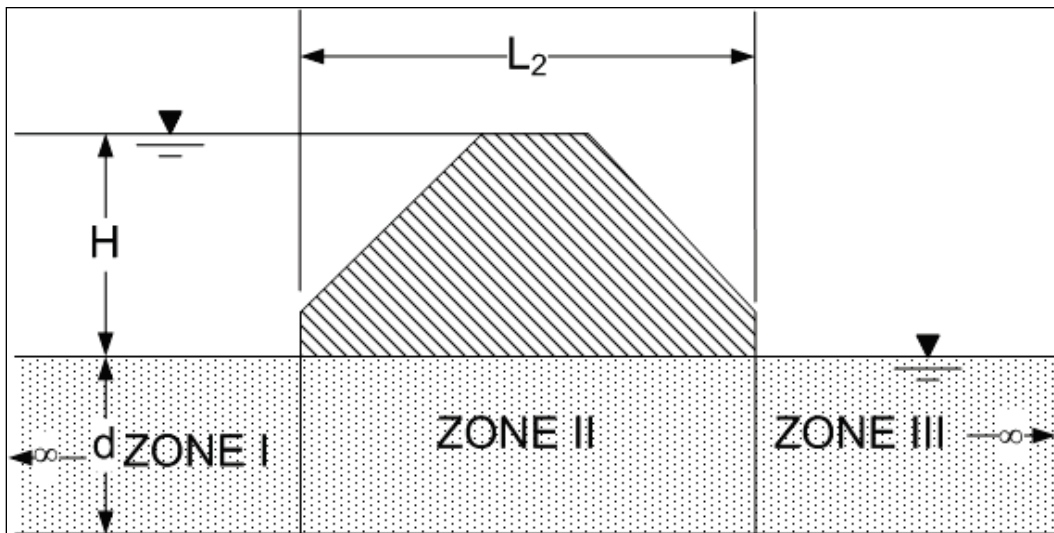


Figure 3. Equipotential lines for levee section having $L_2/d < 1$.

It is clear from these figures that the assumption that the equipotential lines are vertical is violated if $L_2/d < 1$, and hence the Method of Fragments and accordingly, Blanket Theory solutions, are limited to the case where $L_2/d \geq 1$.

The three zones or fragments for Case 1 are shown in Figure 4.

Figure 4. Case 1 - No top stratum with three zones of fragments.



The flow or seepage per unit length (Q_s) of the levee is computed using the following equation:

$$Q_s = \frac{k_f H}{\sum \Phi} \quad (1)$$

where:

k_f = Horizontal permeability of the pervious substratum

H = Net head on levee

Φ = Dimensionless form factor

Note that Equation 1 is same as the general seepage equation based on Darcy's Law, which is:

$$Q_s = \delta \cdot k_f \cdot H \quad (2)$$

where:

$$\delta = \frac{1}{\Sigma \Phi} = \text{Shape factor} \quad (3)$$

It is important to understand the correct application of the dimensionless *form factors* in order to use the Method of Fragments. The form factors were divided into different types by Harr (1962) using the procedure described by Pavlovsky (1935). Fragment types and associated form factors are presented in Table A-1 of Appendix A. This table is used as a reference to calculate form factors of various types of zones for the different cases addressed using Blanket Theory.

The form factor for Zone II is:

$$\Phi_{II} = \frac{L_2}{d} \text{ (Type - I Fragment)}$$

Similarly, the form factors for Zones I and III are:

$$\Phi_I = \Phi_{III} = 0.43 \text{ (Special case of Type - II Fragment with } s = 0)$$

The above-mentioned form factor is not present in Table A1. However, considerable effort was expended to trace the origin of this form factor. It was observed that an equation similar to Case 1 of Blanket Theory is present in Muskat (1937) with a reference to work by Forchheimer (1917). Some discussion related to work by Forchheimer (1917) is presented in Appendix B.

Substituting values of form factors into Equation 3:

$$\delta = \frac{1}{\Sigma\Phi} = \frac{1}{0.43 + \frac{L_2}{d} + 0.43} \quad (4)$$

$$\delta = \frac{1}{0.86 + \frac{L_2}{d}} \quad (5)$$

$$\delta = \frac{d}{0.86d + L_2} \quad (6)$$

Therefore, Equation 2 becomes:

$$Q_s = k_f H \frac{d}{(0.86d + L_2)} \quad (7)$$

where:

L_2 = base width of levee

d = thickness of pervious substratum

Equation 7 is the same equation shown in USACE (2000) for computation of seepage beneath the levee for Case 1.

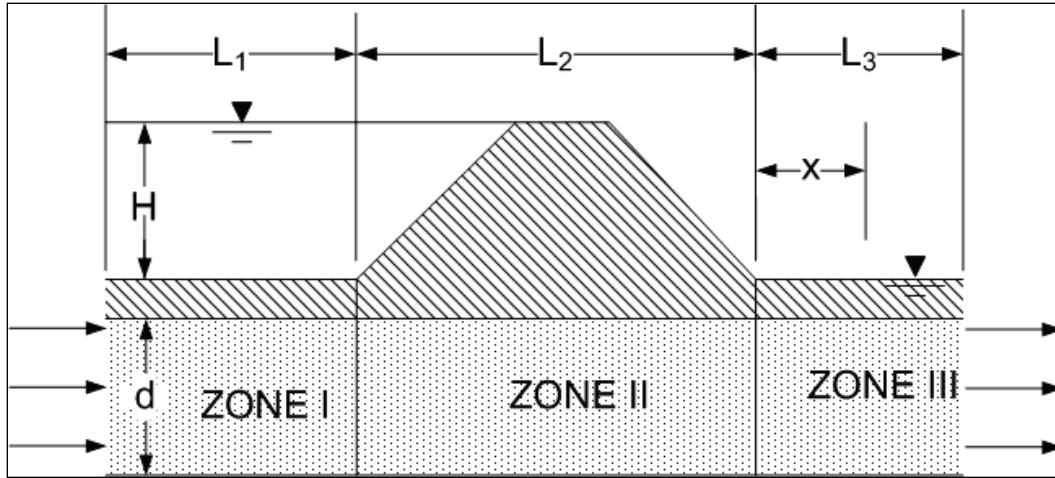
2.2 Cases 2, 3, and 4 - Impervious top stratum both riverside and landside

The following derivations are for impervious top stratum conditions. An impervious top stratum on both the riverside and landside of the levee is considered in Case 2, an impervious top stratum on only the riverside is considered in Case 3, while an impervious top stratum on only the landside is considered in Case 4. These case numbers are the same in both USACE (1956) and USACE (2000).

2.2.1 Case 2 - Impervious top stratum both riverside and landside

The geometry for Case 2 is shown in Figure 5 below.

Figure 5. Case 2 Impervious top stratum on both riverside and landside.



Case 2 is simply a direct application of Darcy's Law for confined flow conditions, similar to flow through a pipe. However, flow can also be determined using the form factors as discussed above. The form factors for zones I, II, and III are given by:

$$\Phi_I = L_1/d \text{ (Type - I Fragment)}$$

$$\Phi_{II} = L_2/d \text{ (Type - I Fragment)}$$

$$\Phi_{III} = L_3/d \text{ (Type - I Fragment)}$$

Substituting the values of the form factors in Equation 3:

$$\delta = \frac{1}{\Sigma \Phi} = \frac{1}{L_1/d + L_2/d + L_3/d} \quad (8)$$

$$\delta = \frac{d}{L_1 + L_2 + L_3} \quad (9)$$

Equation 2 becomes:

$$Q_s = k_f H \frac{d}{(L_1 + L_2 + L_3)} \quad (10)$$

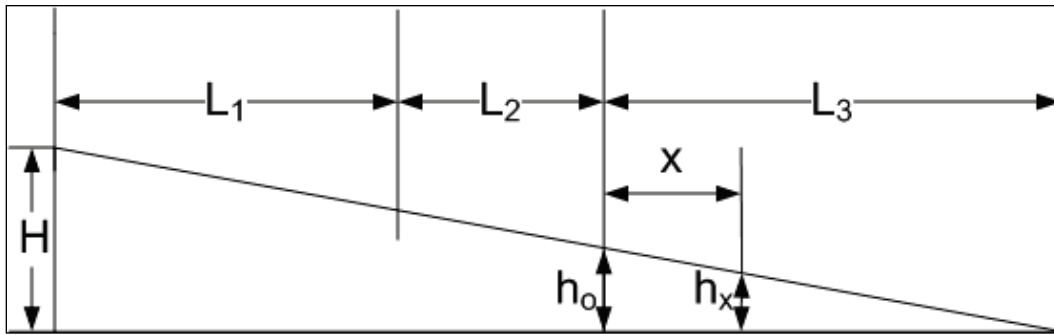
where:

L_1 = Distance from river to riverside levee toe

L_3 = Length of foundation and top stratum beyond landside levee toe

Similarly, the head at the toe of the levee is found by considering the pressure diagram (Piezometric Grade Line or PGL) as shown in Figure 6. The flow in the pervious layer is assumed to be solely horizontal; therefore, the head loss is linear with horizontal distance.

Figure 6. Pressure diagram for confined flow condition.



The pressure head becomes zero at a distance L_3 from the landside toe of the levee. Using the concept of similar triangles:

$$\frac{h_o}{H} = \frac{L_3}{L_1 + L_2 + L_3} \quad (11)$$

$$h_o = H \left(\frac{L_3}{L_1 + L_2 + L_3} \right) \quad (12)$$

where: h_o = excess head at landside levee toe.

Similarly, the head at any distance x from the toe of the levee is determined by

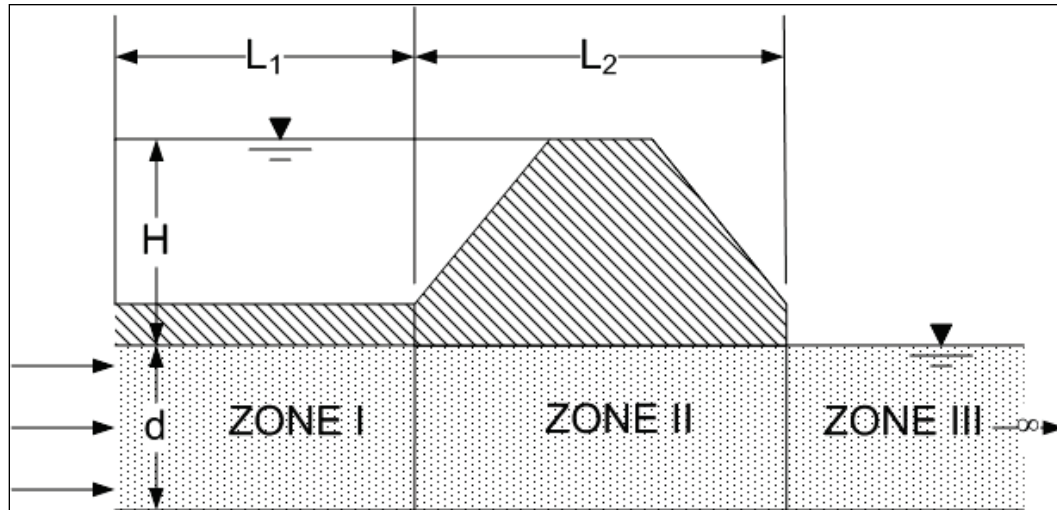
$$h_x = h_o \left(\frac{L_3 - x}{L_3} \right) \quad \text{For } x \leq L_3 \quad (13)$$

$$h_x = 0 \quad \text{For } x \geq L_3 \quad (14)$$

2.2.2 Case 3 - Impervious riverside top stratum and no landside top stratum

The geometry for Case 3 is shown in Figure 7 below.

Figure 7. Case 3 - Impervious riverside top stratum and no landside top stratum.



USACE (2000) uses the difference between the top of the blanket on the riverside and the water elevation on the riverside for the total head loss H for Case 3 as shown in Figure B5 of Appendix B. As shown in Figure B5, the head loss would be dependent on the thickness of the blanket. In Figure 7, the value of H is the difference between riverside and landside water level, or the total head loss from riverside to landside.

The flow can be calculated by using the form factors as discussed previously. The form factors for zones I, II, and III are given by:

$$\Phi_I = L_1 / d \text{ (Type - I Fragment)}$$

$$\Phi_{II} = L_2 / d \text{ (Type - I Fragment)}$$

$$\Phi_{III} = 0.43 \text{ (Special case of Type - II Fragment with } s = 0)$$

Substituting the values of the form factors in Equation 3:

$$\delta = \frac{1}{\sum \Phi} = \frac{1}{L_1/d + L_2/d + 0.43} \quad (15)$$

$$\delta = \frac{d}{L_1 + L_2 + 0.43d} \quad (16)$$

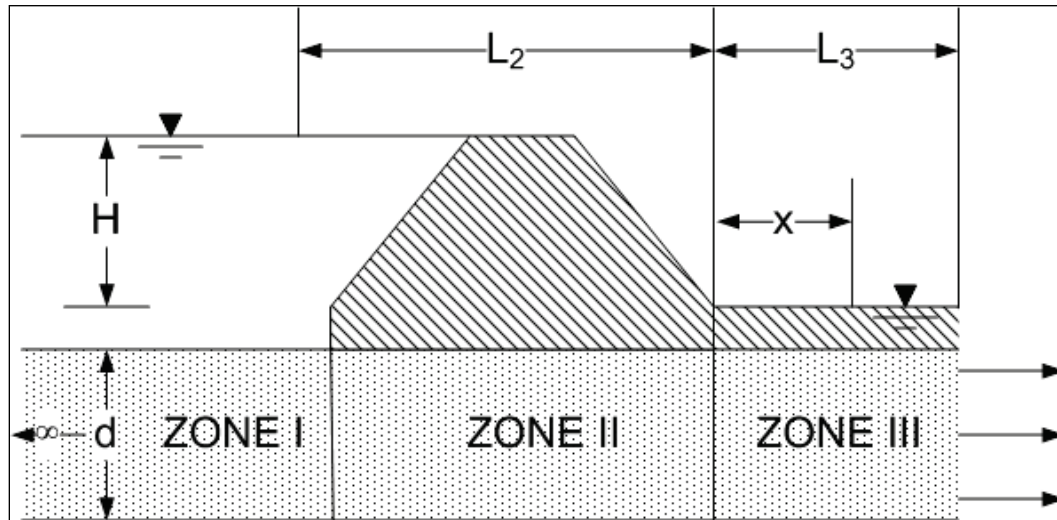
Equation 2 becomes:

$$Q_s = k_f H \frac{d}{(L_1 + L_2 + 0.43d)} \quad (17)$$

2.2.3 Case 4 — Impervious landside top stratum and no riverside top stratum

The geometry for Case 4 is shown in Figure 8. As in Case 3, the value of H is the difference between riverside and landside water level.

Figure 8. Case 4 - Impervious landside top stratum and no riverside top stratum.



The flow can be determined by using the form factors as discussed previously. The form factors for zones I, II, and III are:

$$\Phi_I = 0.43 \text{ (Special case of Type-II Fragment with } s = 0)$$

$$\Phi_{II} = L_2/d \text{ (Type-I Fragment)}$$

$$\Phi_{III} = L_3/d \text{ (Type-I Fragment)}$$

Substituting the values of form factors in Equation 3:

$$\delta = \frac{1}{\sum \Phi} = \frac{1}{0.43 + \frac{L_2}{d} + \frac{L_3}{d}} \quad (18)$$

$$\delta = \frac{d}{0.43d + L_2 + L_3} \quad (19)$$

Equation 2 becomes:

$$Q_s = k_f H \frac{d}{(0.43d + L_2 + L_3)} \quad (20)$$

Similarly, the head at the toe of the levee is found using the Method of Fragments. The head loss in m^{th} fragment is calculated as follows:

$$h_m = \frac{H\Phi_m}{\sum \Phi}$$

where:

Φ_m = Form factor for the m^{th} zone

$\sum \Phi$ = Summation of form factors for all the fragments (zones I, II, and III in this case).

So, head at the toe of the structure is determined as follows:

$$h_o = H - (h_1 + h_2)$$

Or simply,

$$h_o = h_3 = \frac{H\Phi_{III}}{\sum \Phi} \quad (21)$$

So, the form factors for zones I, II, and III as described above are given by:

$$\Phi_I = 0.43$$

$$\Phi_{II} = L_2/d$$

$$\Phi_{\text{III}} = L_3/d$$

Substituting the values of form factors into Equation 21:

$$h_o = \frac{H\Phi_{\text{III}}}{\sum \Phi} = \frac{H(L_3/d)}{0.43 + (L_2/d) + (L_3/d)}$$

$$\frac{h_o}{H} = \frac{L_3}{0.43d + L_2 + L_3}$$

$$h_o = H \left(\frac{L_3}{0.43d + L_2 + L_3} \right) \quad (22)$$

Similarly, the head at any distance x from the landside toe of the levee is determined by:

$$h_x = h_o \left(\frac{L_3 - x}{L_3} \right) \quad (23)$$

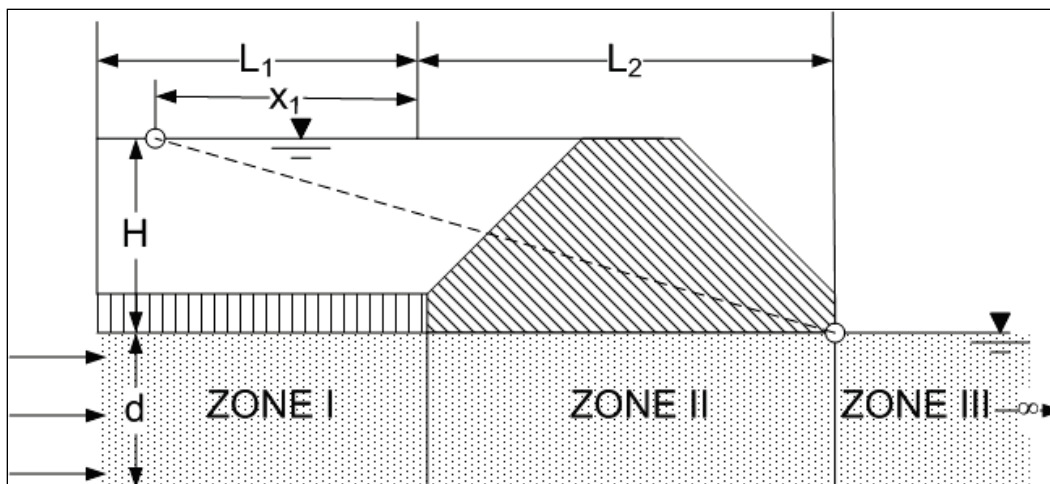
2.3 Semi-pervious top stratum (Cases 5, 6, 7, 8)

The following derivations are for semi-pervious top stratum conditions. A semi-pervious top stratum on only the riverside is considered in Case 5; a semi-pervious top stratum on only the landside represents Case 6; a semi-pervious top stratum on both the riverside and landside is considered in Case 7; and an additional configuration of Case 7 with a sheet pile at the center of the levee is considered in Case 8. Cases 7a, 7b, and 7c are shown in USACE (1956) as Cases 5, 6, and 7, respectively. Case 8 is an added configuration not shown in USACE (2000).

2.3.1 Case 5 - Semi-pervious riverside top stratum and no landside top stratum

The geometry for Case 5 is shown in Figure 9. As in Case 3 and Case 4, the value for H is the difference between the riverside water surface and the landside water surface.

Figure 9. Case 5 - Semi-pervious riverside top stratum and no landside top stratum.



The difference between Case 3 and 5 is that there was an impervious top stratum on the riverside in Case 3 while in Case 5, the top stratum is semi-pervious. Therefore, the distance from the river to the riverside levee toe (L_1) will no longer be equal to the effective seepage entry distance (x_1).

To simplify the calculations, the semi-pervious top stratum will be replaced by an equivalent impervious top stratum, such that the seepage beneath the levee will be the same. This is accomplished by computing x_1 , where x_1 is the equivalent length of an impervious top stratum for a semi-pervious stratum of length L_1 on the riverward side. Similarly, x_3 is the equivalent length of an impervious top stratum for a semi-pervious stratum of length L_3 on the landward side. So, x_1 and x_3 were equal to L_1 and L_3 for impervious cases, but the flow in the pervious layer will no longer be completely horizontal for cases having a semi-pervious top stratum, as there will also be some vertical flow occurring through the top stratum. Therefore, x_1 and x_3 must be calculated separately. This becomes very useful for applying Method of Fragments to calculate flow as well as determining head at the toe of the levee for cases having semi-pervious blankets (Cases 5 through 8). Confined flow conditions will only occur underneath the levee (because the levee is assumed to be completely impervious) and cannot be used elsewhere for these cases without assuming an equivalent impervious blanket.

The value of x_1 is determined from the following equations depending on the type of seepage entrance. The complete derivations of these equations are shown in Appendix B. Two different seepage entrance types are given below:

1. If the distance to the river from the riverside levee toe L_1 is known, and no riverside borrow pits or seepage block exists, x_1 is estimated as follows:

$$x_1 = \frac{\tan h(cL_1)}{c} \quad (24)$$

With c defined as:

$$c = \sqrt{\frac{k_{br}}{k_f z_{br} d}} \quad (25)$$

where:

k_{br} = transformed vertical permeability of riverside top stratum

k_f = horizontal permeability of pervious substratum

d = thickness of pervious substratum

z_{br} = transformed thickness of riverside top stratum

2. If a seepage block exists between the riverside levee toe and the river that prevents any seepage entrance into pervious foundation beyond the seepage block, x_1 can be estimated from the following equation:

$$x_1 = \frac{1}{c \tan h(cL_1)} \quad (26)$$

The next step after determining x_1 is to calculate flow for Case 5. The same procedure as described for the first four cases will be used. The only difference is that the form factor will be defined in terms of the distance to the effective seepage entrance (as calculated above) as opposed to L_1 .

The form factors for zones I, II, and III are given by

$$\Phi_I = x_1/d \text{ (Type-I Fragment)}$$

$$\Phi_{II} = L_2/d \text{ (Type-I Fragment)}$$

$$\Phi_{III} = 0.43 \text{ (Special case of Type-II Fragment with } s = 0)$$

Substituting the values of the form factors into Equation 3:

$$\delta = \frac{1}{\sum \Phi} = \frac{1}{x_1/d + L_2/d + 0.43} \quad (27)$$

$$\delta = \frac{d}{x_1 + L_2 + 0.43d} \quad (28)$$

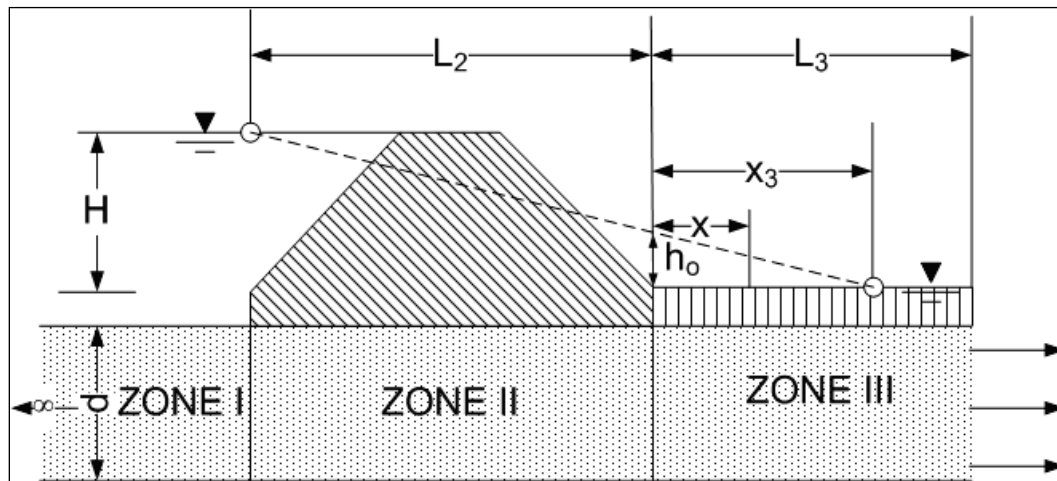
Equation 2 becomes:

$$Q_s = k_f H \frac{d}{(x_1 + L_2 + 0.43d)} \quad (29)$$

2.3.2 Case 6 - Semi-pervious landside top stratum and no riverside top stratum

The geometry for Case 6 is shown in Figure 10. If the water level is considered as shown in USACE (2000), then it becomes a *free surface problem*, because the phreatic surface would be present within the landside top stratum. This should not be the case if Blanket Theory is used.

Figure 10. Case 6 - Semi-pervious landside top stratum and no riverside top stratum.



Case 6 is similar to Case 4, except that the top stratum is impervious in Case 4 and semi-pervious in Case 6. Hence, effective seepage exit (x_3) will no longer be equal to the length of the top stratum beyond the levee toe (L_3) as explained in Case 5 and must be calculated separately.

The value of the equivalent length (x_3) of the impervious blanket is determined from the following equations, depending on the type of

seepage exit. The complete derivations of these equations are shown in Case 7 section of this report.

1. For L_3 = infinite distance

$$x_3 = 1 / c = \sqrt{\frac{k_f z_{bl} d}{k_{bl}}} \quad (30)$$

where:

$$c = \sqrt{\frac{k_{bl}}{k_f z_{bl} d}} \quad (31)$$

where:

- k_{bl} = transformed vertical permeability of the landside top stratum
- k_f = horizontal permeability of the pervious substratum
- d = thickness of the pervious substratum
- z_{bl} = transformed thickness of the landside top stratum

2. For L_3 = finite distance to a seepage block

$$x_3 = \frac{1}{c \tan h(cL_3)} \quad (32)$$

where: c is as defined above.

3. For L_3 = finite distance to an open seepage exit

$$x_3 = \frac{\tan h(cL_3)}{c} \quad (33)$$

Calculating the flow for Case 6 is similar to that described for the impervious blanket cases. However, the form factors will be defined in terms of the distance of the effective seepage exit x_3 (as calculated above) as opposed to L_3 .

The form factors for zones I, II, and III are given by:

$$\Phi_I = 0.43 \text{ (Special case of Type-II Fragment with } s = 0)$$

$$\Phi_{II} = L_2/d \text{ (Type-I Fragment)}$$

$$\Phi_{III} = x_3/d \text{ (Type-I Fragment)}$$

Substituting the values of form factors in Equation 3:

$$\delta = \frac{1}{\sum \Phi} = \frac{1}{0.43 + L_2/d + x_3/d} \quad (34)$$

$$\delta = \frac{d}{0.43d + L_2 + x_3} \quad (35)$$

Equation 2 becomes:

$$Q_s = k_f H \frac{d}{(0.43d + L_2 + x_3)} \quad (36)$$

Similarly, the excess head at the toe of the levee is found using the Method of Fragments in a similar manner as explained in Case 4, but with L_3 being replaced by x_3 :

$$\frac{h_o}{H} = \frac{x_3}{0.43d + L_2 + x_3} \quad (37)$$

$$h_o = H \left(\frac{x_3}{0.43d + L_2 + x_3} \right) \quad (38)$$

The head at any distance x from the toe of the levee is shown in USACE (2000) by:

$$h_x = h_o \left(\frac{x_3 - x}{x_3} \right)$$

However, in this equation the head loss will no longer be linear because of semi-pervious (compared to impervious) blanket on the landside. For Case 6, the semi-pervious blanket of length L_3 can be taken as an

impervious blanket of equivalent length x_3 . This can be a useful approach to determine the head at toe of the levee as well as under the levee because flow will be confined in this case and the linear PGL can be obtained. However, this cannot be used to determine the head at any distance x from the toe of the levee, as the linear PGL plotted for the equivalent impervious top stratum will be different than actual PGL for semi-pervious stratum beyond the levee toe (which will be non-linear because of flow occurring vertically through the semi-pervious top stratum).

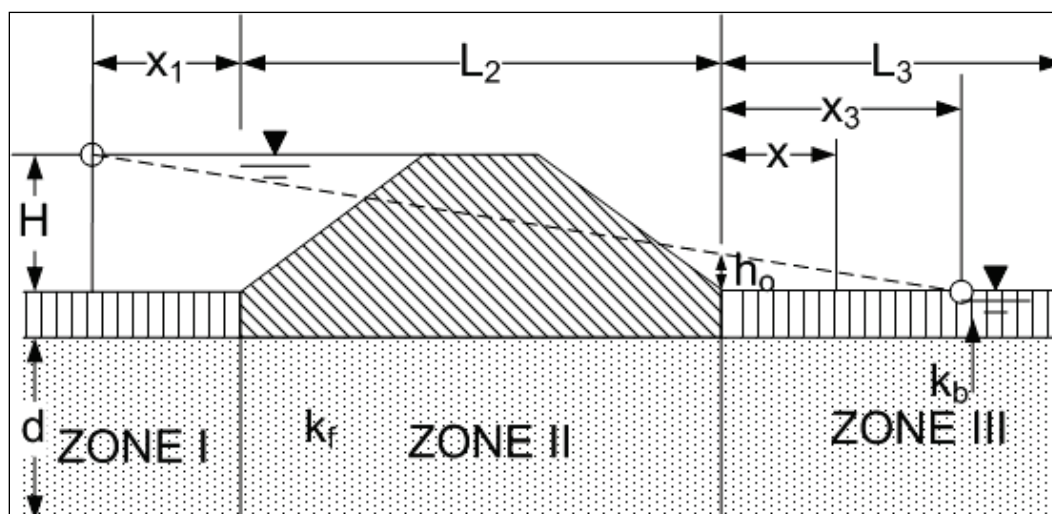
The head at any distance x can be calculated in a similar manner, as will be shown for Case 7 by considering the landward side of the levee, and the complete derivation of these equations will be discussed then. However, if we assume that an open seepage exit is present on the landside for Case 6, as it appears to be shown in Figure B6 of Appendix B in EM-1110-2-1913 (USACE 2000), then this becomes similar to Case 7c, and then the head at any distance x is determined by:

$$h_x = \frac{h_o \sin h(c(L_3 - x))}{\sin h(cL_3)} \quad (39)$$

2.3.3 Case 7 - Semi-pervious top strata both riverside and landside

The basic geometry for Case 7 is shown Figure 11. The permeability of the top stratum is shown as k_b in the subsequent figures; the subscripts “l” or “r” are used accordingly in the equations to represent landside and riverside top stratum permeability, respectively.

Figure 11. Case 7 - Semi-pervious top strata both riverside and landside.



The same procedures as described earlier in this report will be used to determine the quantity of underseepage for Case 7. As the semi-pervious strata is present on both landward and riverward sides, L_1 and L_3 will be replaced by x_1 and x_3 , respectively, to calculate the form factors.

Therefore, the form factors for zones I, II, and III are given by:

$$\Phi_I = x_1 / d \text{ (Type-I Fragment)}$$

$$\Phi_{II} = L_2 / d \text{ (Type-I Fragment)}$$

$$\Phi_{III} = x_3 / d \text{ (Type-I Fragment)}$$

Putting the values of the form factors in Equation 3:

$$\delta = \frac{1}{\sum \Phi} = \frac{1}{x_1/d + L_2/d + x_3/d} \quad (40)$$

$$\delta = \frac{d}{x_1 + L_2 + x_3} \quad (41)$$

Hence, Equation 2 becomes:

$$Q_s = k_f H \frac{d}{(x_1 + L_2 + x_3)} \quad (42)$$

Similarly, the head at the toe of the levee is found using the Method of Fragments and from similar triangles as follows:

$$\frac{h_o}{H} = \frac{x_3}{x_1 + L_2 + x_3} \quad (43)$$

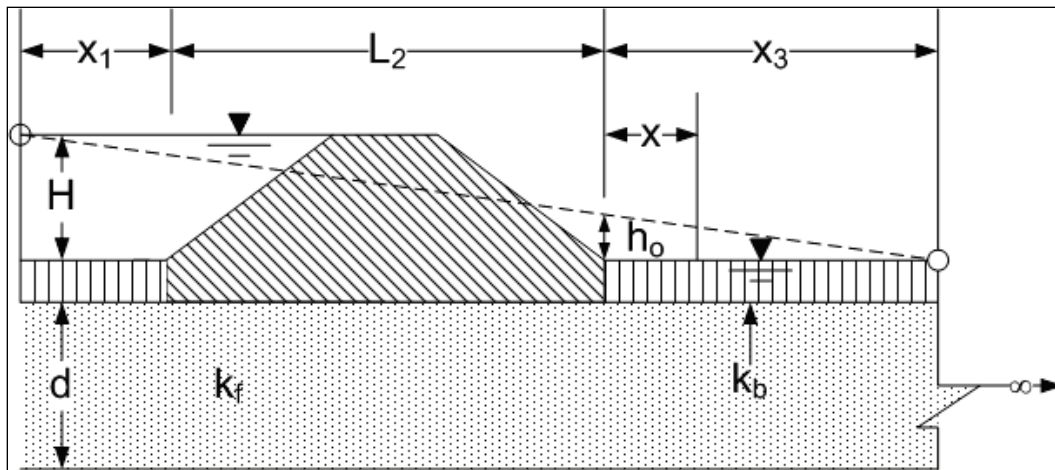
$$h_o = H \left(\frac{x_3}{x_1 + L_2 + x_3} \right) \quad (44)$$

There are three different subcases for Case 7 depending on the boundary conditions on the landward side. The value of x_3 is determined for each case depending on the type of seepage exit.

2.3.4 Case 7a - Semi-pervious landside and riverside top stratum (top stratum extends infinitely landward of the levee)

Figure 12 shows the geometry for Case 7a. This subcase is assumed to have an infinite horizontal dimension (L_3) on the landward side.

Figure 12. Case 7a - Semi-pervious top strata both riverside and landside with L_3 as infinite.

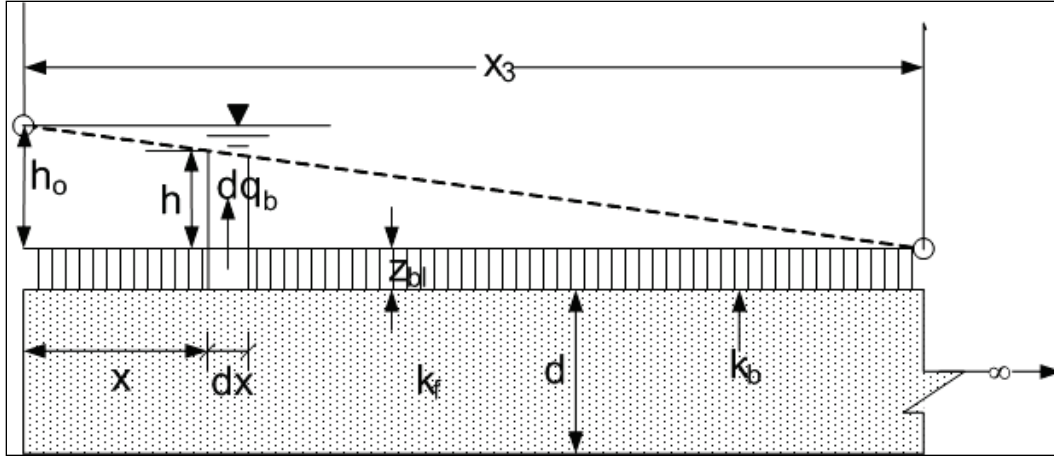


Two basic assumptions for this case are:

1. The flow through the top stratum is vertical, and the permeability of the top stratum (k_{bt}) is the vertical component of the permeability. This is considered to occur when the contrast in permeabilities between the top stratum and substratum is about an order of magnitude or greater (Bennett 1946).
2. The flow through the pervious substratum is horizontal. This is considered to occur when the contrast in permeabilities between the top stratum and substratum is about an order of magnitude or greater (Bennett 1946).

Consider the landward side of the levee, as shown in Figure 13, to illustrate the derivation.

Figure 13. Landward side of the levee.



From Darcy's Law, the vertical flow through the top stratum will be:

$$q = kiA$$

$$dq_b = k_{bl} \frac{h}{z_{bl}} dx$$

$$\frac{dq_b}{dx} = k_{bl} \frac{h}{z_{bl}} \quad (45)$$

Similarly, the horizontal flow through the pervious substratum is:

$$q_f = k_f d \frac{dh}{dx}$$

$$\frac{dq_f}{dx} = k_f d \frac{d^2 h}{dx^2} \quad (46)$$

The continuity equation for steady state will be:

$$\frac{dq_f}{dx} + \frac{dq_b}{dx} = 0 \quad (47)$$

Substituting the values of $\frac{dq_f}{dx}$ and $\frac{dq_b}{dx}$ from Equations 46 and 45, respectively:

$$k_f d \frac{d^2 h}{dx^2} - k_{bl} \frac{h}{z_{bl}} = 0 \quad (48)$$

Dividing $k_f d$ on both sides of the equation:

$$\frac{d^2 h}{dx^2} - \frac{k_{bl}}{k_f d z_{bl}} h = 0$$

$$\frac{d^2 h}{dx^2} - c^2 h = 0 \quad (49)$$

where $c = \sqrt{\frac{k_{bl}}{k_f d z_{bl}}}$.

The differential equation is solved as shown below.

Let $p = \frac{dh}{dx}$ and the auxiliary equation is:

$$p^2 - c^2 = 0. \quad (p^1 = \frac{dh}{dx}, p^2 = \frac{d^2 h}{dx^2}, p^0 = h = 1) \quad (50)$$

The roots of the above equation are c and $-c$.

The solution of the above differential equation is:

$$h = m e^{cx} + n e^{-cx} \quad (51)$$

Where, m and n are constants.

The boundary conditions for this case are:

For $x = 0$, $h = h_o$

For $x = \infty$, $h = 0$

Putting the first condition in Equation 51:

$$h_o = m + n \quad (52)$$

Similarly, putting the second condition in Equation 51:

$$0 = m \times \infty + n \times 0 \quad (53)$$

From the above equation, it is clear that m must be zero to have a finite value.

So,

$$\begin{aligned} m &= 0 \\ n &= h_o \end{aligned} \quad (54)$$

Therefore, the equation for head becomes:

$$\begin{aligned} h &= me^{cx} + ne^{-cx} \\ h_x &= h_o e^{-cx} \end{aligned} \quad (55)$$

where: $c = \sqrt{\frac{k_{bl}}{k_f z_{bl} d}}$

The distance from the landside levee toe to the effective seepage exit (x_3) can be determined by extrapolating the hydraulic grade line at $x = 0$ to the point where we have ground surface or tail water as shown in Figure 13. Again, note that the linear PGL is plotted to determine x_3 as this distance is considered to be equivalent length of impervious blanket.

Now,

$$\frac{dh}{dx} = \frac{-h_o}{x_3} \quad (56)$$

Also, we know that,

$$h = h_o e^{-cx} \quad (57)$$

So,

When $x = 0$,

$$\frac{dh}{dx} = -h_o c \quad (58)$$

Equating Equations 56 and 58, we get

$$\frac{-h_o}{x_3} = -h_o c \quad (59)$$

$$x_3 = \frac{1}{c} \quad (60)$$

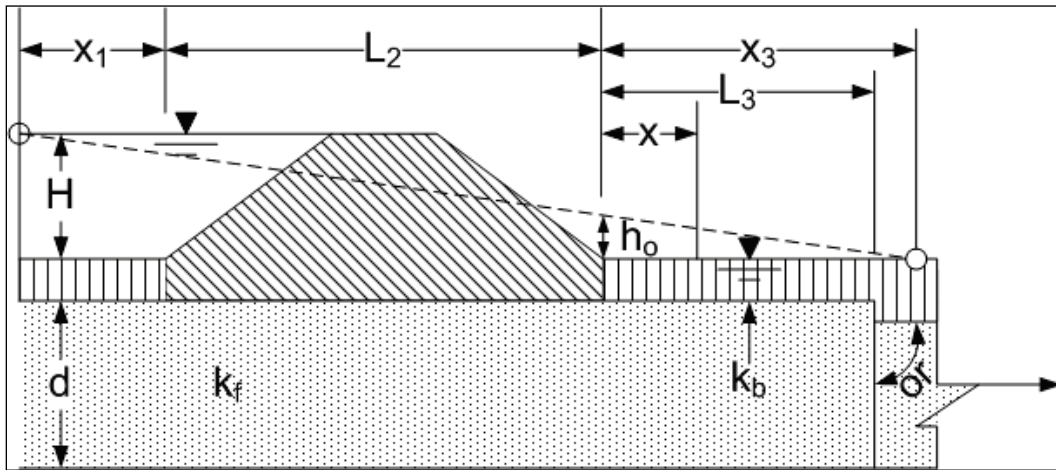
As $c = \sqrt{\frac{k_{bl}}{k_f z_{bl} d}}$, so

$$x_3 = \sqrt{\frac{k_f z_{bl} d}{k_{bl}}} \quad (61)$$

2.3.5 Case 7b - Semi-pervious landside and riverside top stratum (seepage block in the pervious substratum located landward of the levee)

Figure 14 shows the geometry for Case 7b. For this case, a seepage block (impervious boundary) is located at a distance L_3 from the toe of the levee.

Figure 14. Case 7b - Semi-pervious top strata both riverside and landside with L_3 as finite distance to seepage block.



The solution of the differential equation, as developed in Case 7a, is:

$$h = me^{cx} + ne^{-cx} \quad (62)$$

where: m and n are constants.

The boundary conditions for Case 7-b are:

For $x = 0$, $h = h_o$

For $x = L_3$, $\frac{dh}{dx} = 0$

Putting the first condition in Equation 51:

$$h_o = m + n \quad (63)$$

$$m = h_o - n \quad (64)$$

Similarly, putting the second condition in Equation 51:

$$\frac{dh}{dx} = mce^{cx} - nce^{-cx} \quad (65)$$

$$0 = mce^{cL_3} - nce^{-cL_3} \quad (66)$$

Substituting in the value of m from first boundary condition:

$$0 = (h_o - n)ce^{cL_3} - nce^{-cL_3} \quad (67)$$

$$0 = h_o ce^{cL_3} - nce^{cL_3} - nce^{-cL_3} \quad (68)$$

$$0 = h_o ce^{cL_3} - nc(e^{cL_3} + e^{-cL_3}) \quad (69)$$

$$h_o ce^{cL_3} = nc(e^{cL_3} + e^{-cL_3}) \quad (70)$$

$$h_o e^{cL_3} = n(e^{cL_3} + e^{-cL_3}) \quad (71)$$

Multiplying by $1/2$ on both sides:

$$\frac{1}{2}h_o e^{cL_3} = \frac{1}{2}n(e^{cL_3} + e^{-cL_3}) \quad (72)$$

As we know that,

$$\cos hx = \frac{e^x + e^{-x}}{2} \quad (73)$$

So,

$$n \cosh(cL_3) = \frac{1}{2} h_0 e^{cL_3} \quad (74)$$

$$n = \frac{h_0 e^{cL_3}}{2 \cosh(cL_3)} \quad (75)$$

Putting the values of m and n in Equation 51:

$$h = \left(h_0 - \frac{h_0 e^{cL_3}}{2 \cosh(cL_3)} \right) e^{cx} + \left(\frac{h_0 e^{cL_3}}{2 \cosh(cL_3)} \right) e^{-cx} \quad (76)$$

$$h = h_0 e^{cx} - \left(\frac{h_0 e^{cL_3}}{2 \cosh(cL_3)} \right) e^{cx} + \left(\frac{h_0 e^{cL_3}}{2 \cosh(cL_3)} \right) e^{-cx} \quad (77)$$

$$h = \frac{h_0}{2 \cosh(cL_3)} \left[e^{cx} 2 \cosh(cL_3) - e^{cL_3} e^{cx} + e^{cL_3} e^{-cx} \right] \quad (78)$$

Now,

$$e^{cx} 2 \cosh(cL_3) = e^{cx} (e^{cL_3} + e^{-cL_3}) \text{ Because } \cos hx = \frac{e^x + e^{-x}}{2}$$

$$e^{cx} 2 \cosh(cL_3) = e^{cx+cL_3} + e^{cx-cL_3} \quad (79)$$

Putting the value of the above expression in Equation 78

$$h = \frac{h_0}{2 \cosh(cL_3)} \left[e^{cx+cL_3} + e^{cx-cL_3} - e^{cx+cL_3} + e^{-cx+cL_3} \right] \quad (80)$$

$$h = \frac{h_0}{\cosh(cL_3)} \frac{\left[e^{-c(-x+L_3)} + e^{c(-x+L_3)} \right]}{2} \quad (81)$$

$$h_x = \frac{h_o \cos h(c(L_3 - x))}{\cos h(cL_3)} \quad (82)$$

For $x = L_3$

$$h_x = \frac{h_o}{\cos h(cL_3)} \text{ Because } \cos h(0) = 1 \quad (48)$$

The distance from the landside levee toe to the effective seepage exit (x_3) can be determined in a same manner as done for Case 7a.

So,

$$\frac{dh}{dx} = \frac{-h_o}{x_3} \quad (83)$$

Also, we know that,

$$h = \frac{h_o \cos h(c(L_3 - x))}{\cos h(cL_3)} \quad (84)$$

$$\frac{dh}{dx} = \frac{h_o}{\cos h(cL_3)} \frac{d}{dx} (\cos h(c(L_3 - x))) \quad (85)$$

Now,

$$\cos h(c(L_3 - x)) = \frac{e^{cL_3} e^{-cx} + e^{-cL_3} e^{cx}}{2} \quad (86)$$

$$\frac{d}{dx} \cos h(c(L_3 - x)) = \frac{e^{cL_3} (-c) e^{-cx} + e^{-cL_3} (c) e^{cx}}{2} \quad (87)$$

$$\frac{d}{dx} \cos h(c(L_3 - x)) = \frac{-c}{2} [e^{c(-x+L_3)} - e^{-c(-x+L_3)}] \quad (88)$$

$$\frac{d}{dx} \cos h(c(L_3 - x)) = -c \sin h(c(L_3 - x)) \quad (89)$$

For $x = 0$,

$$\frac{d}{dx} \cos h(c(L_3 - x)) = -c \sin h(cL_3) \quad (90)$$

Now, putting the value of above expression in Equation 85:

$$\frac{dh}{dx} = \frac{h_o}{\cos h(cL_3)} - c \sin h(cL_3) \quad (91)$$

$$\frac{dh}{dx} = -ch_o \tan h(cL_3) \quad (92)$$

As we know that,

$$\frac{dh}{dx} = \frac{-h_o}{x_3} \quad (93)$$

Putting the value of $\frac{dh}{dx}$ as derived in Equation 93:

$$-ch_o \tan h(cL_3) = \frac{-h_o}{x_3} \quad (94)$$

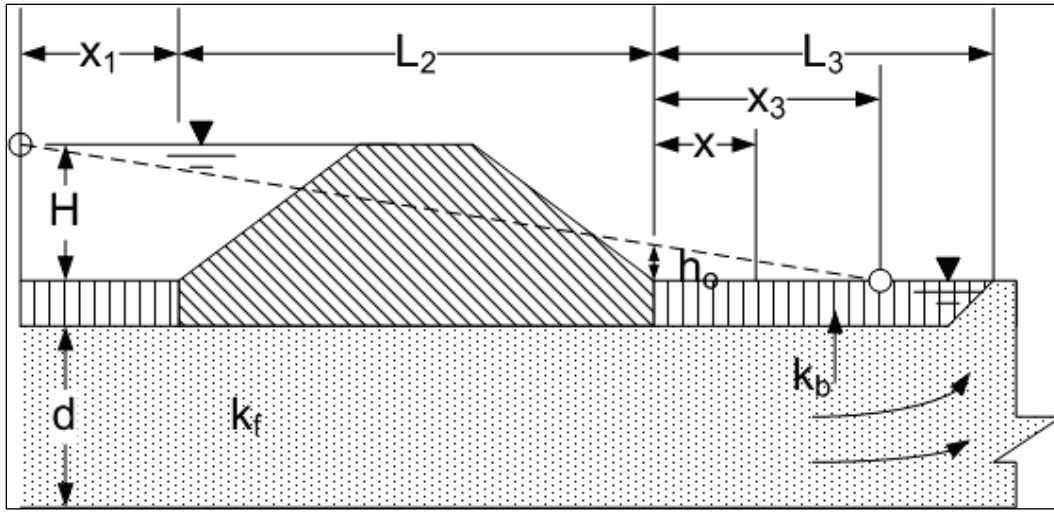
$$x_3 = \frac{1}{c \tan h(cL_3)} \quad (95)$$

where: $c = \sqrt{\frac{k_{bl}}{k_f z_{bl} d}}$

2.3.6 Case 7c – Semi-pervious landside and riverside top stratum

Figure 15 shows the geometry for Case 7c. In this case, an open seepage exit is located at a distance L_3 from the landside levee toe.

Figure 15. Case 7c - Semi-pervious top strata both riverside and landside with L_3 as a finite distance to an open seepage exit.



The solution of the differential equation as developed in Case 7a is $h = me^{cx} + ne^{-cx}$ where, m and n are constants.

The boundary conditions for Case 7c are as follows:

For $x = 0$, $h = h_0$

For $x = L_3$, $h = 0$

Putting the first condition in Equation 51:

$$h_0 = m + n \quad (96)$$

$$m = h_0 - n \quad (97)$$

Similarly, putting the second condition in Equation 51:

$$h = me^{cx} + ne^{-cx} \quad (98)$$

$$0 = me^{cL_3} + ne^{-cL_3} \quad (99)$$

Putting the value of m in the above equation:

$$0 = (h_0 - n)e^{cL_3} + ne^{-cL_3} \quad (100)$$

$$0 = h_o e^{cL_3} - n e^{cL_3} + n e^{-cL_3} \quad (101)$$

$$0 = h_o e^{cL_3} - n(e^{cL_3} - e^{-cL_3}) \quad (102)$$

$$h_o e^{cL_3} = n(e^{cL_3} - e^{-cL_3}) \quad (103)$$

$$n = \frac{h_o e^{cL_3}}{(e^{cL_3} - e^{-cL_3})} \quad (104)$$

$$\text{As, } \sin hx = \frac{e^x - e^{-x}}{2}$$

$$n = \frac{h_o e^{cL_3}}{2 \sin h(cL_3)} \quad (105)$$

Putting the values of m and n in Equation 51:

$$h = \left(h_o - \frac{h_o e^{cL_3}}{2 \sin h(cL_3)} \right) e^{cx} + \frac{h_o e^{cL_3}}{2 \sin h(cL_3)} e^{-cx} \quad (106)$$

$$h = \frac{h_o}{2 \sin h(cL_3)} (2e^{cx} \sin h(cL_3) - e^{cL_3} e^{cx} + e^{cL_3} e^{-cx}) \quad (107)$$

Now,

$$e^{cx} 2 \sin h(cL_3) = e^{cx} (e^{cL_3} - e^{-cL_3}) \quad (108)$$

$$\text{Because, } \sin hx = \frac{e^x - e^{-x}}{2}$$

$$e^{cx} 2 \sin h(cL_3) = e^{cx+cL_3} - e^{cx-cL_3} \quad (109)$$

Putting the value of the above expression in Equation 107:

$$h = \frac{h_o}{2 \sin h(cL_3)} (e^{cx+cL_3} - e^{cx-cL_3} - e^{cL_3+cx} + e^{cL_3-cx}) \quad (110)$$

$$h = \frac{h_o}{\sin h(cL_3)} \frac{(e^{c(L_3-x)} - e^{-c(L_3-x)})}{2} \quad (111)$$

$$h_x = \frac{h_o \sin h(c(L_3 - x))}{\sin h(cL_3)} \quad (112)$$

The distance from the landside levee toe to the effective seepage exit (x_3) can be determined in a same manner as for Case 7a.

So,

$$\frac{dh}{dx} = \frac{-h_o}{x_3} \quad (113)$$

Also, we know that,

$$h = \frac{h_o \sin h(c(L_3 - x))}{\sin h(cL_3)} \quad (114)$$

$$\frac{dh}{dx} = \frac{h_o}{\sin h(cL_3)} \frac{d}{dx}(\sin h(c(L_3 - x))) \quad (115)$$

Now,

$$\sin h(c(L_3 - x)) = \frac{e^{cL_3} e^{-cx} - e^{-cL_3} e^{cx}}{2} \quad (116)$$

$$\frac{d}{dx} \sin h(c(L_3 - x)) = \frac{e^{cL_3} (-c) e^{-cx} - e^{-cL_3} (c) e^{cx}}{2} \quad (117)$$

$$\frac{d}{dx} \sin h(c(L_3 - x)) = \frac{-c}{2} [e^{c(-x+L_3)} + e^{-c(-x+L_3)}] \quad (118)$$

$$\frac{d}{dx} \sin h(c(L_3 - x)) = -c \cos h(c(L_3 - x)) \quad (119)$$

Now, substituting the value of above expression in Equation 115:

$$\frac{dh}{dx} = \frac{h_o}{\sin h(cL_3)} - c \cos h(c(L_3 - x)) \quad (120)$$

For $x=0$,

$$\frac{dh}{dx} = \frac{h_o}{\sin h(cL_3)} - c \cos h(cL_3) \quad (121)$$

$$\frac{dh}{dx} = \frac{-ch_o}{\tan h(cL_3)} \quad (122)$$

As we know that,

$$\frac{dh}{dx} = \frac{-h_o}{x_3} \quad (123)$$

Putting the value of $\frac{dh}{dx}$ in Equation 122:

$$\frac{-ch_o}{\tan h(cL_3)} = \frac{-h_o}{x_3} \quad (124)$$

$$x_3 = \frac{\tan h(cL_3)}{c} \quad (125)$$

where:

$$c = \sqrt{\frac{k_{bl}}{k_f z_{bl} d}}$$

2.3.7 Case 8 - Semi-pervious top strata both riverside and landside with sheet pile at the center of levee

Figure 16 shows the geometry for a new case, Case 8, which is not included in USACE (2000). Case 8 is similar to Case 7, except that a sheet-pile cutoff is located beneath the center of the levee. This case was introduced to model I-walls and partially penetrating slurry walls.

where:

s = length of embedment of the sheet pile into the substratum

b = half base width of the levee = $L_2/2$

The modulus is found from Equation 68 and then the value of K/K' is determined using the tables of complete elliptic integrals of first kind. One such table is provided in Appendix A (Table A2).

Substituting the values of the form factors in Equation 3:

$$\delta = \frac{1}{\Sigma\Phi} = \frac{1}{x_1/d + K/K' + K/K' + x_3/d} \quad (127)$$

$$\delta = \frac{1}{x_1/d + 2K/K' + x_3/d} \quad (128)$$

Therefore, Equation 2 becomes:

$$Q_s = k_f H \frac{d}{\left(x_1 + 2d \left(\frac{K}{K'} \right) + x_3 \right)} \quad (129)$$

Similarly, the head at the toe of the levee is found using Method of Fragments. The head loss in m^{th} fragment is calculated as follows:

$$h_m = \frac{H\Phi_m}{\Sigma\Phi} \quad (130)$$

where:

Φ_m = Form factor for m^{th} zone

$\Sigma\Phi$ = Summation of form factors for all the fragments (zones I, II, III, and IV in this case).

Head loss through zone I, $h_1 = \frac{H\Phi_1}{\Sigma\Phi}$

$$\text{Head loss through zone II, } h_2 = \frac{H\Phi_2}{\sum \Phi}$$

$$\text{Head loss through zone III, } h_3 = \frac{H\Phi_3}{\sum \Phi}$$

$$\text{Head loss through zone IV, } h_4 = \frac{H\Phi_4}{\sum \Phi}$$

Accordingly, the head at the toe of the structure is determined as follows:

$$h_o = H - (h_1 + h_2 + h_3) \quad (131)$$

Or simply,

$$h_o = h_4 = \frac{H\Phi_4}{\sum \Phi} \quad (132)$$

There are three different subcases for Case 8, similar to Case 7, depending on the seepage boundary conditions on the landward side. The value of x_3 is determined for each case depending upon the type of seepage exit.

2.3.8 Case 8a – Semi-pervious landside and riverside top stratum (top stratum extends infinitely landward of the levee) with cutoff

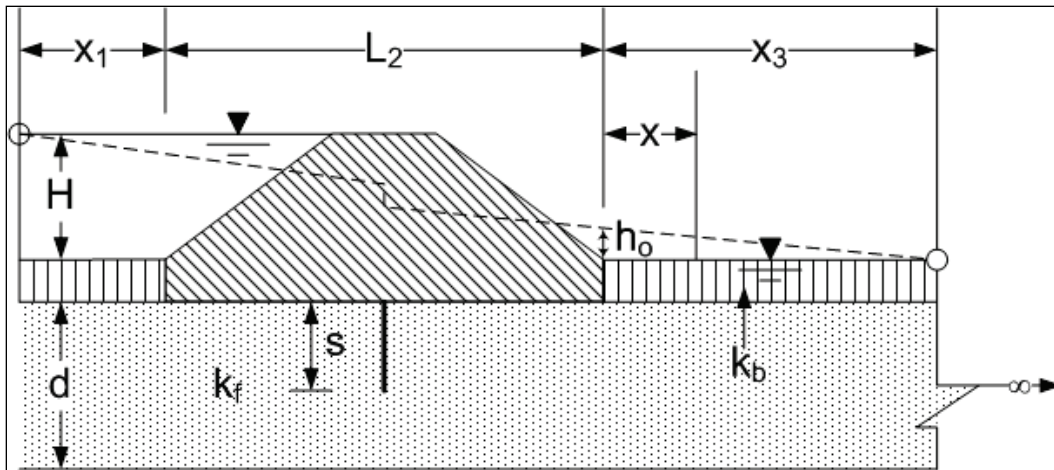
Figure 17 shows the geometry for Case 8a. For this case, the horizontal distance from the landside levee toe is considered to be infinite.

It is clear from the figure below that the landward side of Case 8a is identical to the landward side of Case 7a. Therefore, the equation to determine the head at any distance x will be the same for both cases. The equation for the head at distance $= x$ is as follows:

$$h_x = h_o e^{-cx} \quad (133)$$

where, $c = \sqrt{\frac{k_{bl}}{k_f z_{bl} d}}$ and h_o is determined from either equation 131 or 132.

Figure 17. Case 8a - Semi-pervious top strata both riverside and landside with sheet pile at the center of levee and L_3 as infinite.



The derivation of the above equation is explained in detail in the section of this report addressing Case 7a. The distance from the landside levee toe to the effective seepage exit (x_3) is also determined in a similar manner as in Case 7a, and the equation is as follows:

$$x_3 = \frac{1}{c} = \sqrt{\frac{k_f z_b d}{k_b}} \quad (134)$$

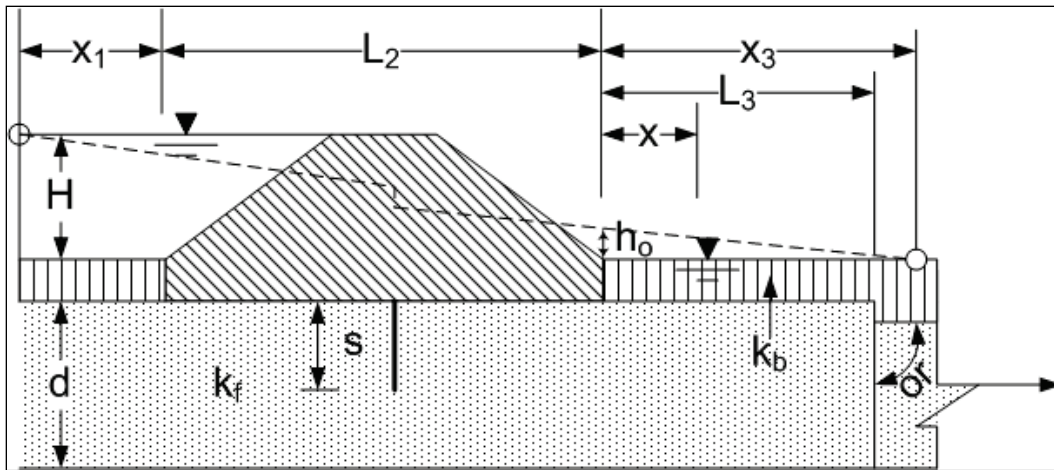
2.3.9 Case 8b (L_3 = finite distance to seepage block)

Figure 18 shows the basic geometry for Case 8b, in which seepage block is located a distance L_3 from the landward levee toe.

It is again clear from Figure 18 that the landward side of Case 8b is identical to the landward side of Case 7b. Therefore, the equation to determine the head at any distance x will be the same. The equation for the head at distance $= x$ is:

$$h_x = \frac{h_o \cos h(c(L_3 - x))}{\cos h(cL_3)} \quad (135)$$

Figure 18. Case 8b - Semi-pervious top strata both riverside and landside with sheet pile at the center of levee and L_3 as finite distance to seepage block.



For $x = L_3$

$$h_x = \frac{h_0}{\cosh(cL_3)} \text{ because } \cosh(0) = 1$$

The distance from the landside levee toe to the effective seepage exit (x_3) is also determined in a similar manner as in Case 7b, and the equation is:

$$x_3 = \frac{1}{c \tanh(cL_3)} \quad (136)$$

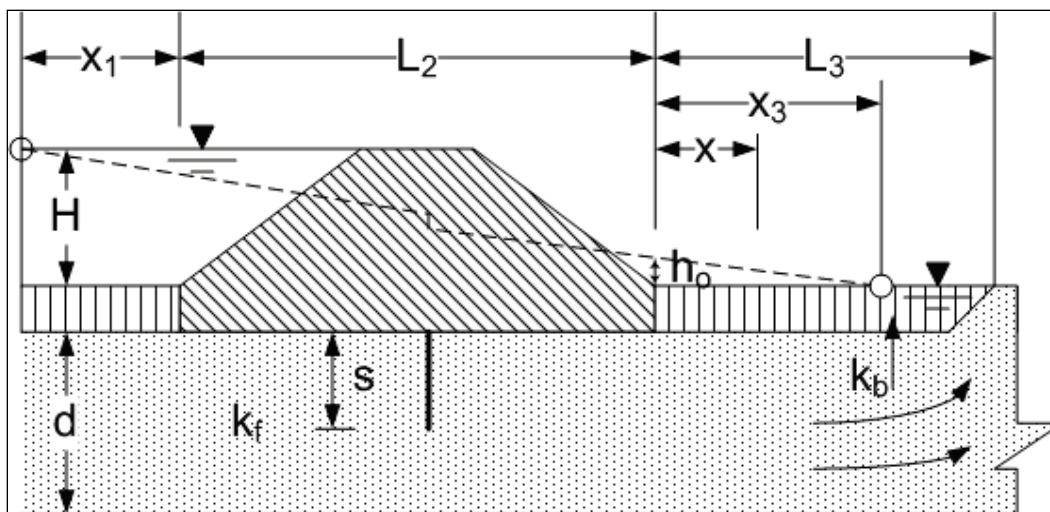
2.3.10 Case 8c (L_3 = finite distance to an open seepage exit)

Figure 19 shows the basic geometry used for the development of the equations for Case 8c. This case has an open seepage exit located a distance L_3 from the landward levee toe.

The seepage boundary conditions for Case 8c are the same as for Case 7c, therefore the equation to determine the head at any distance x is also the same. The equation for the head at distance = x is as follows:

$$h_x = \frac{h_0 \sinh(c(L_3 - x))}{\sinh(cL_3)} \quad (137)$$

Figure 19. Case 8c - Semi-pervious top strata both riverside and landside with sheetpile at the center of levee and L_3 as finite distance to an open seepage exit.



The distance from the landside levee toe to the effective seepage exit (x_3) is also determined in the same manner as for Case 7c by the following equation:

$$x_3 = \frac{\tan h(cL_3)}{c} \quad (138)$$

2.4 Blanket Theory equations summary

A summary of the equations, along with their respective figures for Cases 1 through 8, are shown in the following figures. Figure 20 summarizes Cases 1 through 4; Figure 21 is the summary of Cases 5 and 6; Figures 22 and 23 represent the summaries of Cases 7 and 8, respectively. The application of the Blanket Theory equations is limited to the cases where $\frac{L_2}{d} \geq 1$. This constraint is necessary to ensure that the equipotential lines are essentially vertical, which is one of the fundamental assumptions of the Method of Fragments.

The Blanket Theory assumption that flow through top stratum is vertical and through pervious substratum is horizontal is only true if the ratio of k_f to k_b is greater than or equal to 10. The validity of the assumptions becomes questionable for lower ratio of permeabilities. However, it is not clear from either the USACE (2000) or USACE (1956) what ratio of permeabilities between the pervious layer and the top blanket make the top blanket essentially impervious. In other words, no guidance is provided to select when the top blanket is considered to be impervious versus semi-pervious.

Figure 20. Equations for computation of underseepage flow and substratum pressures for Cases 1 through 4.

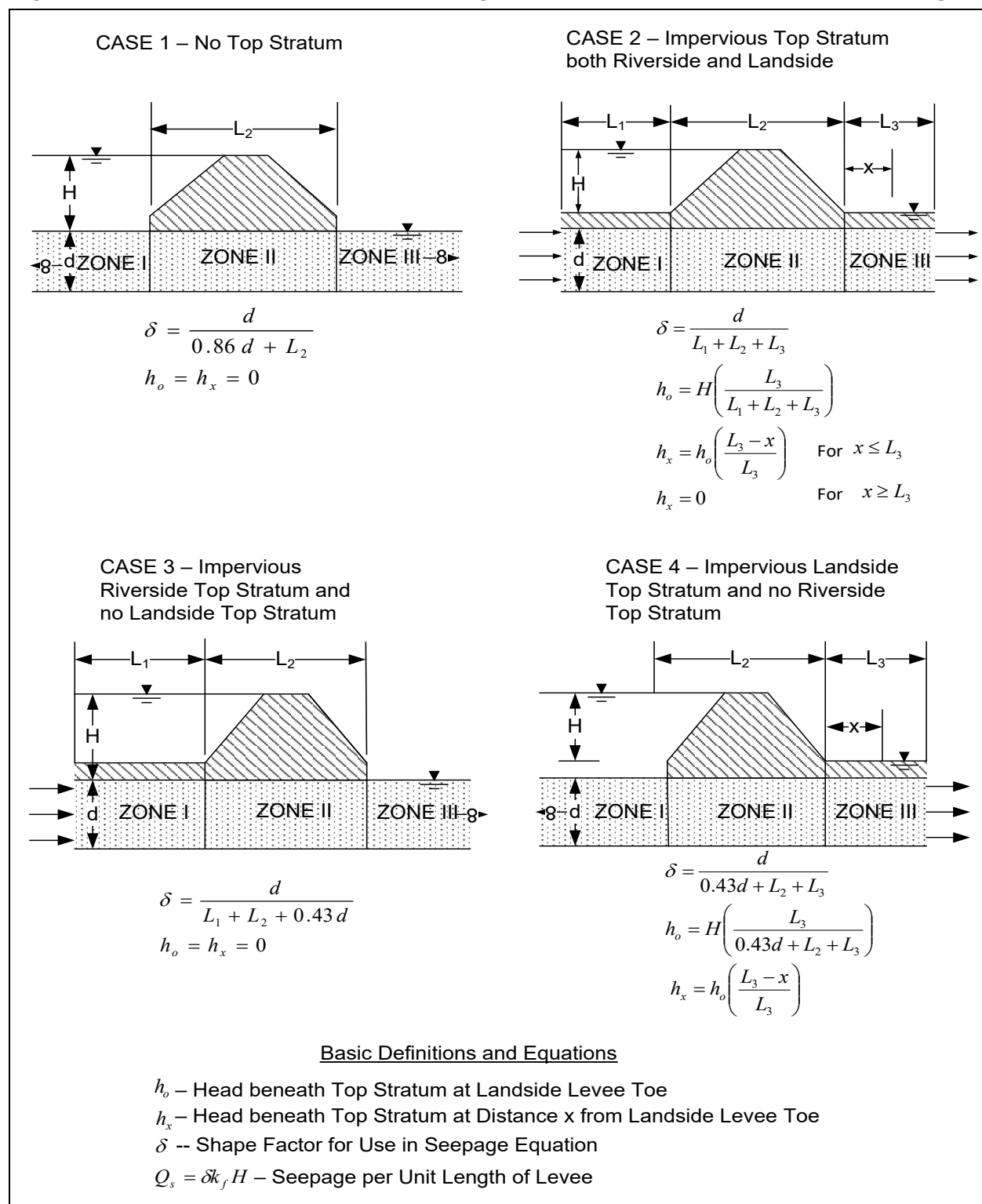
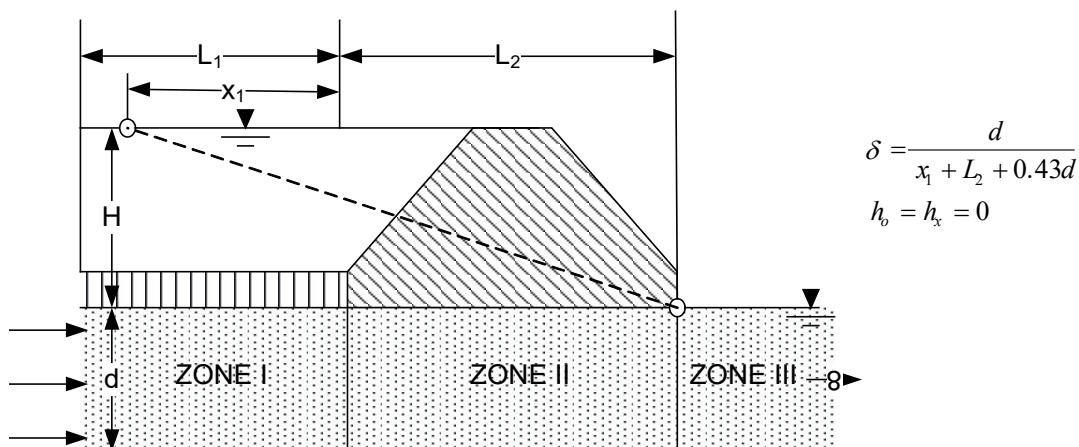
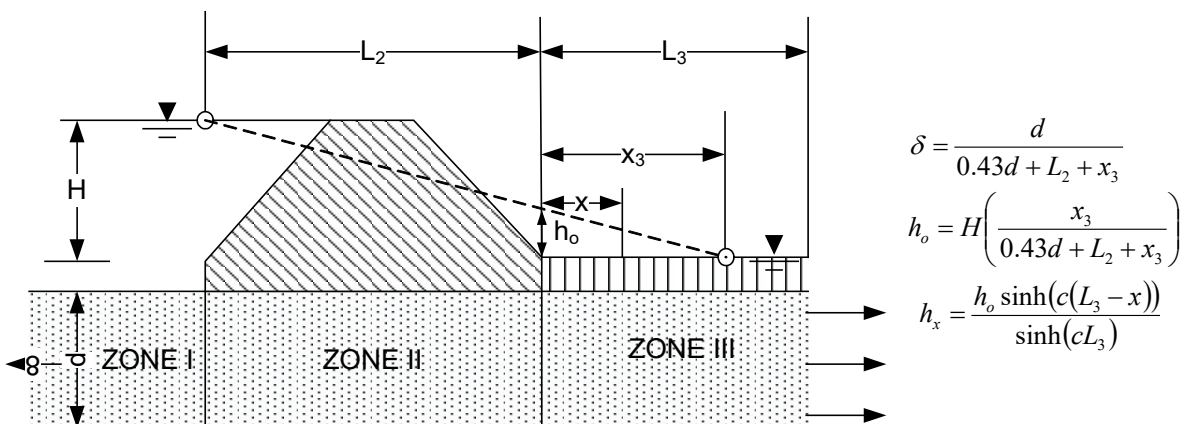


Figure 21. Equations for computation of underseepage flow and substratum pressures for Cases 5 and 6.

CASE 5 – Semipervious Riverside Top Stratum and No Landside Top Stratum



CASE 6 – Semipervious Landside Top Stratum and No Riverside Top Stratum

Basic Definitions and Equations

h_o – Head beneath Top Stratum at Landside Levee Toe

h_x – Head beneath Top Stratum at Distance x from Landside Levee Toe

δ -- Shape Factor for Use in Seepage Equation

$Q_s = \delta k_f H$ – Seepage per Unit Length of Levee

Figure 22. Equations for computation of underseepage flow and substratum pressures for Case 7.

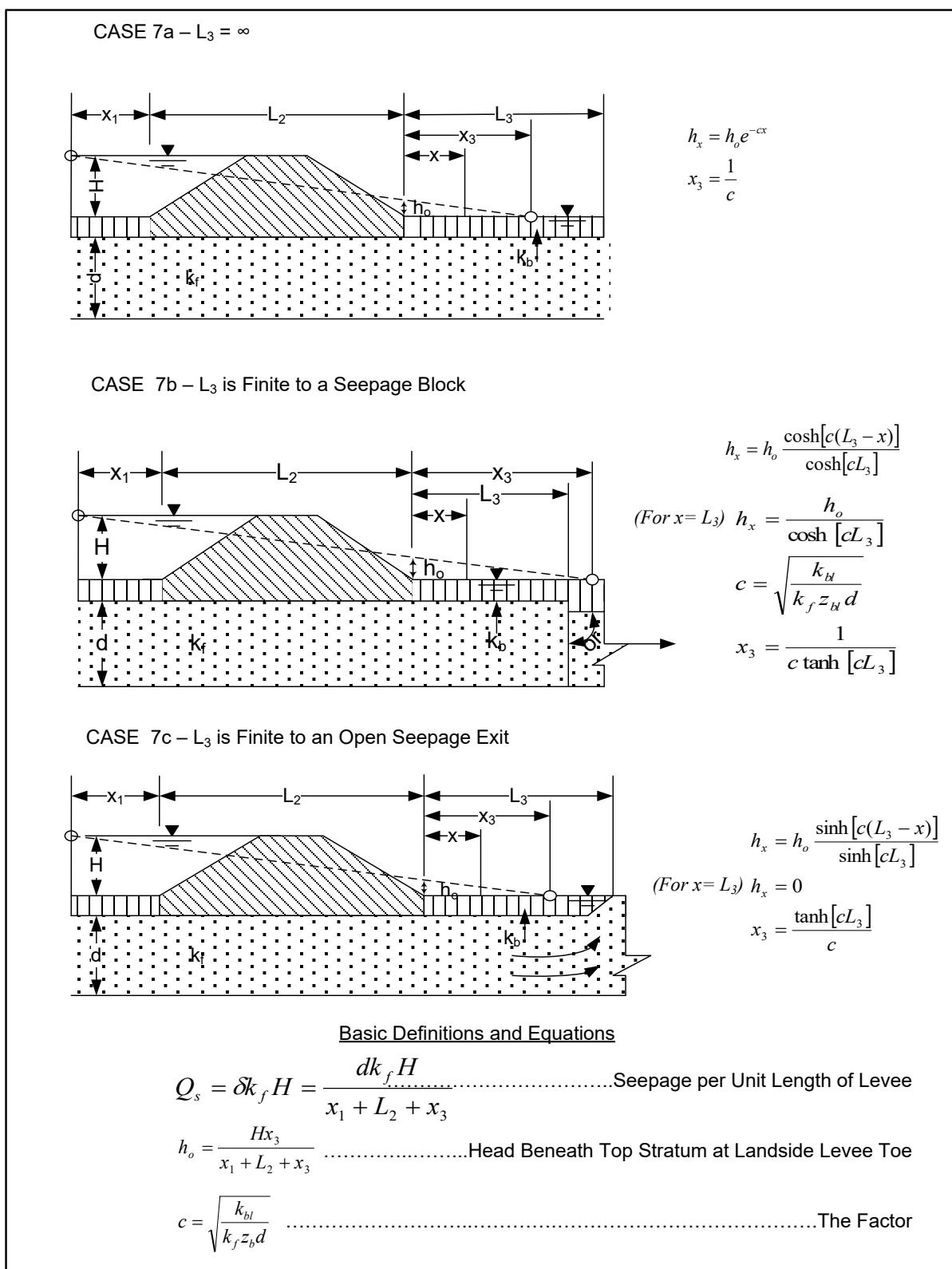
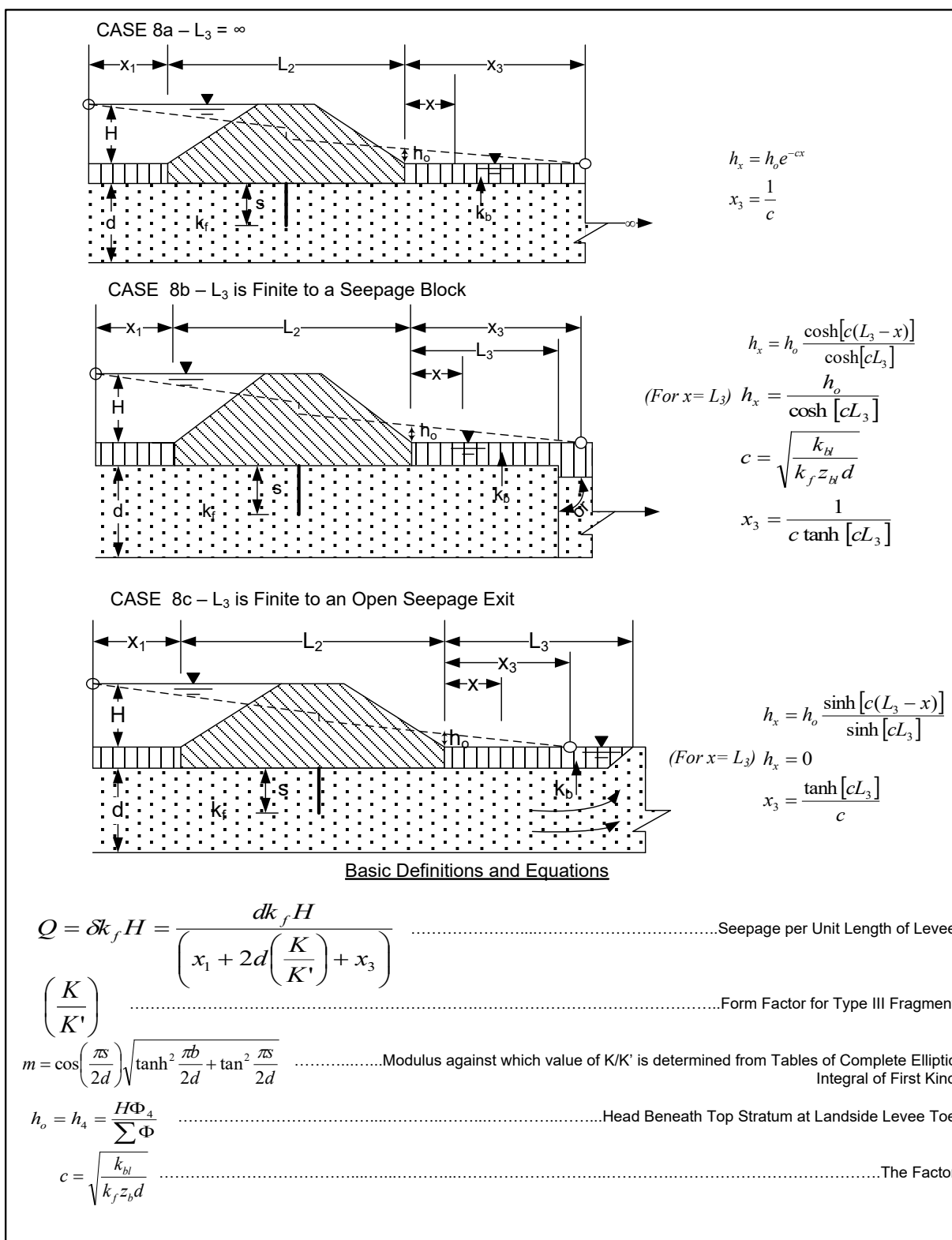


Figure 23. Equations for computation of underseepage flow and substratum pressures for Case 8.



The Blanket Theory equations are based on approximate values of permeabilities and thicknesses of the top and pervious strata. The permeability value for the pervious stratum should be the horizontal component of the permeability. The permeability value for the semi-pervious stratum should be the vertical component of the permeability. Also, it is prudent to use a range of permeability and thickness values to cover the range of variation of these parameters for field cases.

The concept of a transformed thickness of the top stratum is only applicable to semi-pervious top stratum cases and not for impervious top stratum cases. Of the impervious cases, the top blanket essentially has zero thickness and is only a factor when computing the uplift gradient. The equations presented in Appendix B of USACE (2000) are said to be derived from information contained in USACE (1956). However, the transformed permeability of the top stratum is defined differently in USACE (1956), in which a weighted average is taken to determine k_b . In Appendix B of USACE (2000), the permeability of the most impervious stratum is taken as the transformed permeability of the top stratum. An analysis of layered top stratum conditions using Blanket Theory and FEA is discussed in a later section of this report.

The constant $c = \sqrt{\frac{k_f z_b d}{k_b}}$ is defined only in terms of the landward stratum in Appendix B of the USACE (2000). However, it can also be stated in terms of riverward side to determine x_1 .

There are errors in the definition of the total head loss through the section (ΔH or H) in USACE (2000). The corrections for these errors are made in this report as shown in Figures 7, 8, 9, and 10 for Cases 3, 4, 5 and 6, respectively. Similarly, the head at the toe of the levee (h_o) is shown incorrectly in Figure B-7 of USACE (2000). Blanket Theory computes h_o as head above (or excess) the landside water surface. However, USACE (2000) incorrectly shows h_o as the head from the base of the top stratum.

3 Evaluation of Blanket Theory Solutions with Finite Elements Analyses

3.1 Introduction

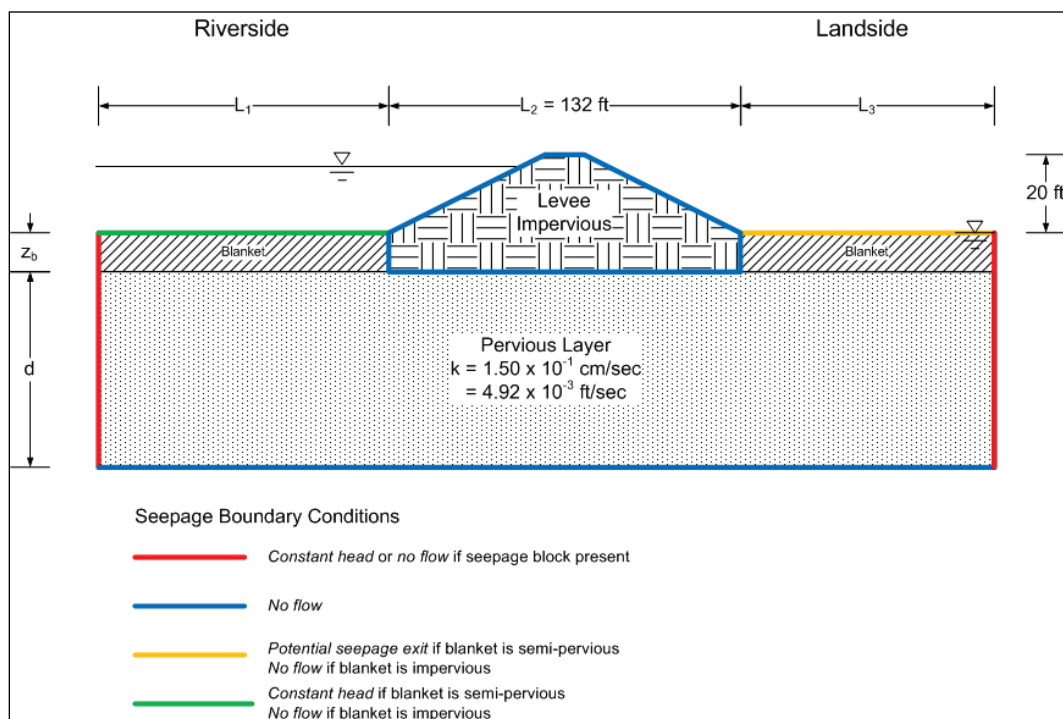
Finite element analyses were performed on 11 different seepage configurations in order to (1) verify the Blanket Theory solutions and (2) assess potential errors in the solutions when geometrical and soil property values are used outside of the recommended guidelines.

The finite element analyses were performed with SLIDE (Rocscience Version 6.0) for Case 1 through Case 8. A comparison of SLIDE and SEEP/W (Geo-Studio Version 7.13) was performed and is presented after all cases are discussed. The finite element analyses were performed using the same boundary conditions, layer thicknesses, and permeability values as used for the Blanket Theory solutions. Results are presented for volumetric flow rates per unit of levee length (Q_s) and for excess hydraulic head (h_o) under the toe of the levee (when applicable) using finite element analyses and closed-form solutions. The following cases were analyzed:

- Case 1 – No landside and riverside top stratum
- Case 2 – Impervious landside and riverside top stratum
- Case 3 – Impervious riverside top stratum and no landside top stratum
- Case 4 – Impervious landside top stratum and no riverside top stratum
- Case 5 – Semi-pervious riverside top stratum and no landside top stratum
- Case 6 – Semi-pervious landside top stratum and no riverside top stratum
- Case 7a – Semi-pervious landside and riverside top stratum (top stratum extends infinitely landward of the levee)
- Case 7b – Semi-pervious landside and riverside top stratum (seepage block in the pervious substratum located landward of the levee)
- Case 7c – Semi-pervious landside and riverside top stratum (seepage exit in the pervious substratum located landward of the levee)
- Case 8b – Semi-pervious landside and riverside top stratum (seepage block in the pervious substratum located landward of the levee) with cutoff
- Case 8c – Semi-pervious landside and riverside top stratum (seepage exit in the pervious substratum located landward of the levee) with cutoff

The general boundary conditions used in Case 1 through Case 8 are shown in Figure 24. In all analyses, the base of the levee (L_2) was assumed to be 132 ft. This is equivalent to a 20-ft-tall levee having 3:1 slopes and a crest width of 12 ft. However, because the levee is modeled as an impervious structure in the FEA and Blanket Theory analyses, the true dimensions are inconsequential.

Figure 24. Generalized geometry and boundary conditions used in finite element analysis.



The finite element analyses were conducted with a minimum of 1,500 elements. The elements used were six-noded triangles. This mesh appeared to provide accurate results with short execution times.

For Cases 1 through 4, the permeability of the pervious layer was 4.92×10^{-3} ft/sec (0.15 cm/sec). For these cases, the value of permeability is not important for comparing FEA to Blanket Theory. The flow calculated for both methods is directly proportional to the permeability, and the excess head at the downstream toe does not depend on the value of permeability. For Cases 5 through 8, the value of permeability is more important, and values are given during the discussion of each case.

Cases 2 through 4 have an impervious blanket, which is modeled in FEA as a *no-flow* nodal boundary conditions. Both in Blanket Theory and in FEA,

this has the same effect as a blanket of zero thickness. For Cases 5 through 8, which have different combinations of riverside and landside semi-pervious blankets, the thickness of the blanket is an important factor, particularly in the manner in which the total head loss is defined.

3.2 Case 1 – No landside and riverside top stratum

Figure 25 shows the basic geometry used for the FEA of Case 1. This analysis was done for three different thicknesses of the pervious layer (d) of 25 ft, 50 ft, and 100 ft. This analysis was performed considering both riverside and landside dimensions of 100 ft and 1,500 ft, respectively. For Blanket Theory analyses, the L_1 and L_3 dimensions are considered to be infinite. However, for FEA, these dimensions must be assigned finite lengths.¹

In the FEA, the riverside nodal boundary conditions (horizontal and vertical) were set to a constant head of 20 ft. The landside boundary conditions (horizontal and vertical) were set to a constant head of 0 ft.

As shown in Figure 26, the flow (Q_s) increases with increasing thickness of the pervious layer (d), as expected. Values of L_1 and L_3 do not appear to affect the finite element results. Essentially the same values of flow were calculated for L_1 and L_3 dimensions of 100 ft as for L_1 and L_3 dimensions of 1,500 ft, as shown in Figure 27.

There is close agreement between the FEA and Blanket Theory for this case. The difference between the two methods seems to increase with decreasing L_2/d ratio as shown in Figure 28. This supports the recommendations given in the first section that L_2/d ratio ≥ 1 for application of Blanket Theory, as it seems to underestimate the flow for smaller ratios.

¹ SEEP/W contains an infinite boundary condition function. This was used in some of the SEEP/W analyses.

Figure 25. Geometry for Case 1 - No landside and riverside top stratum.

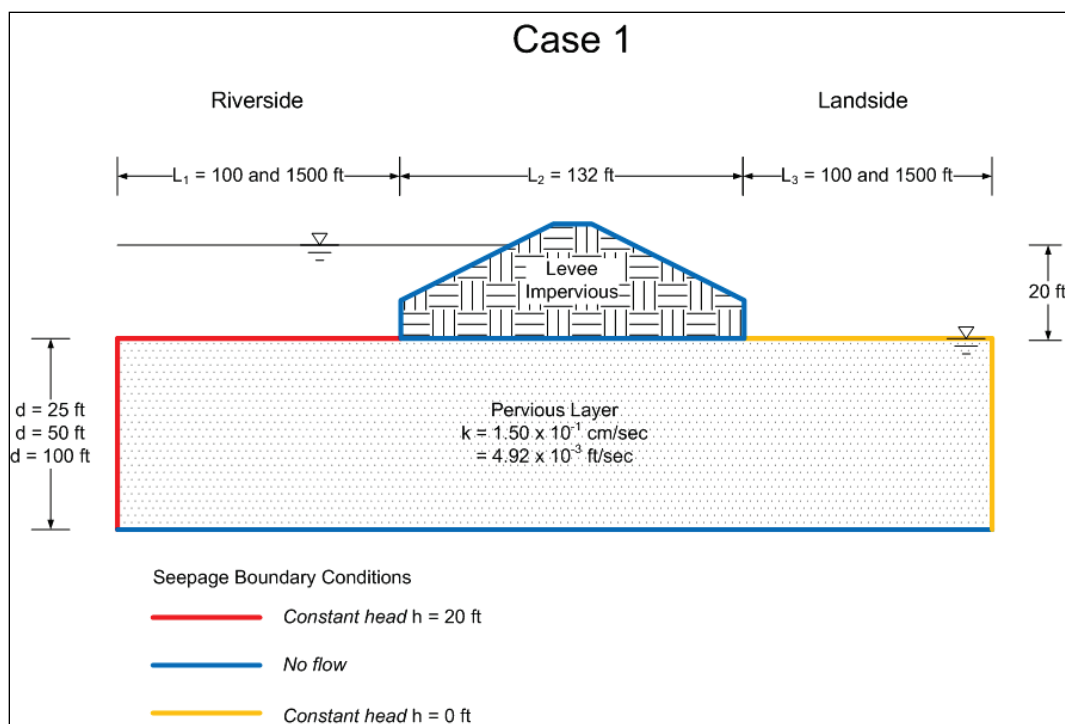
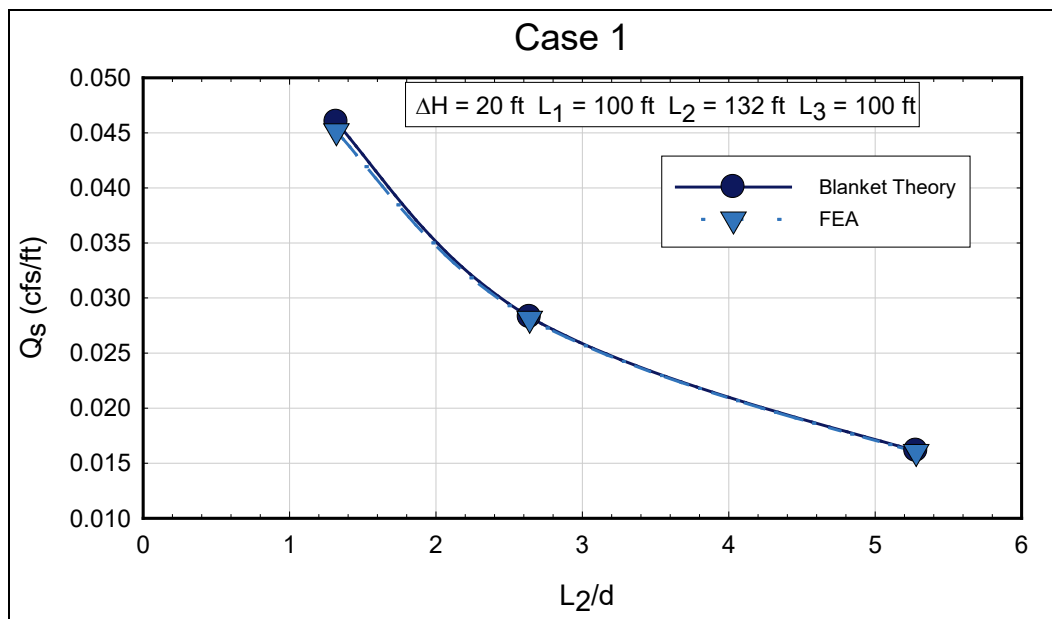
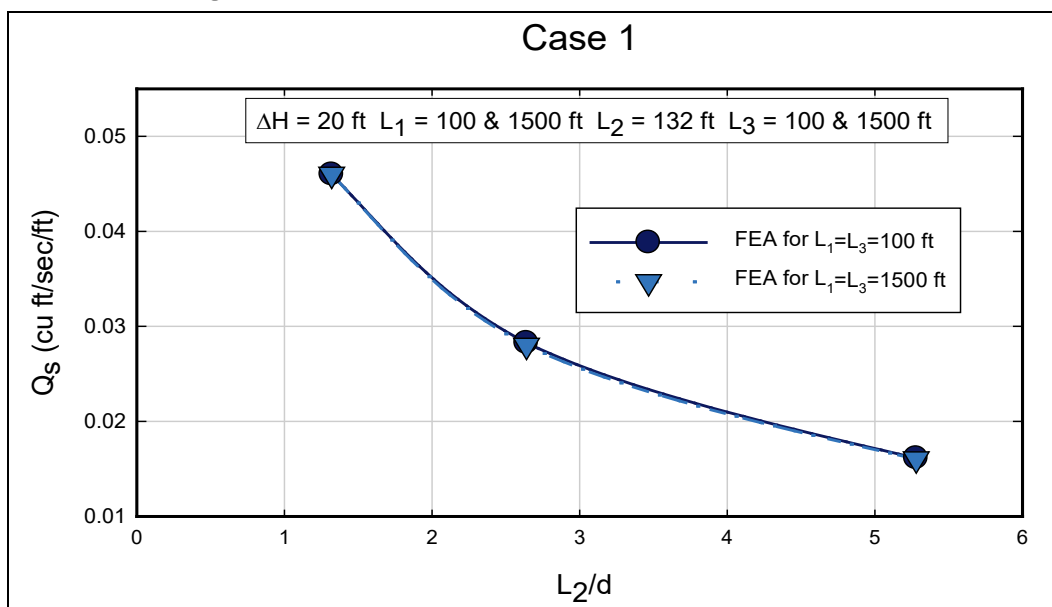
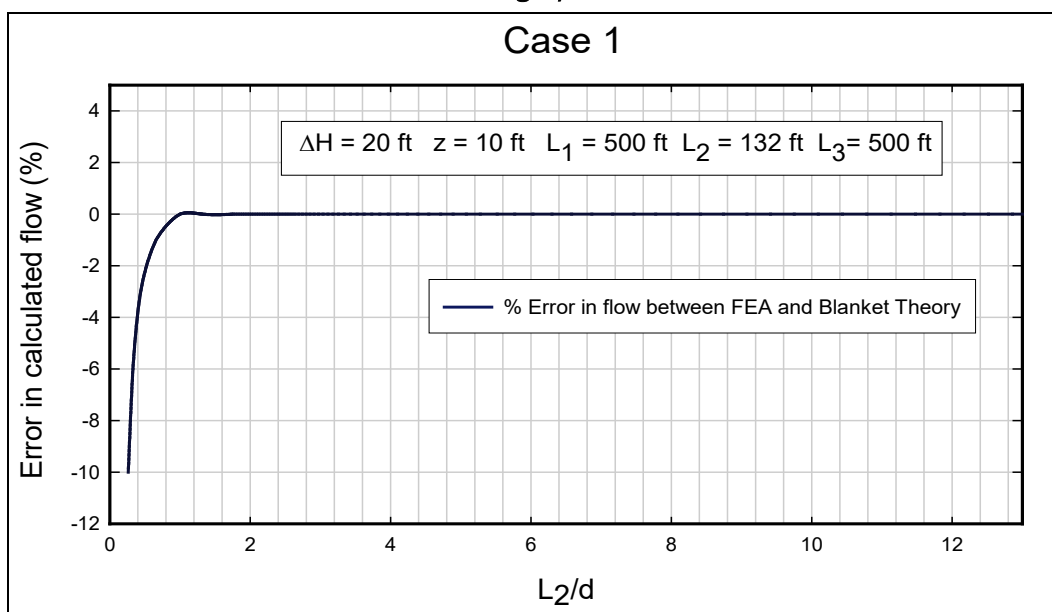
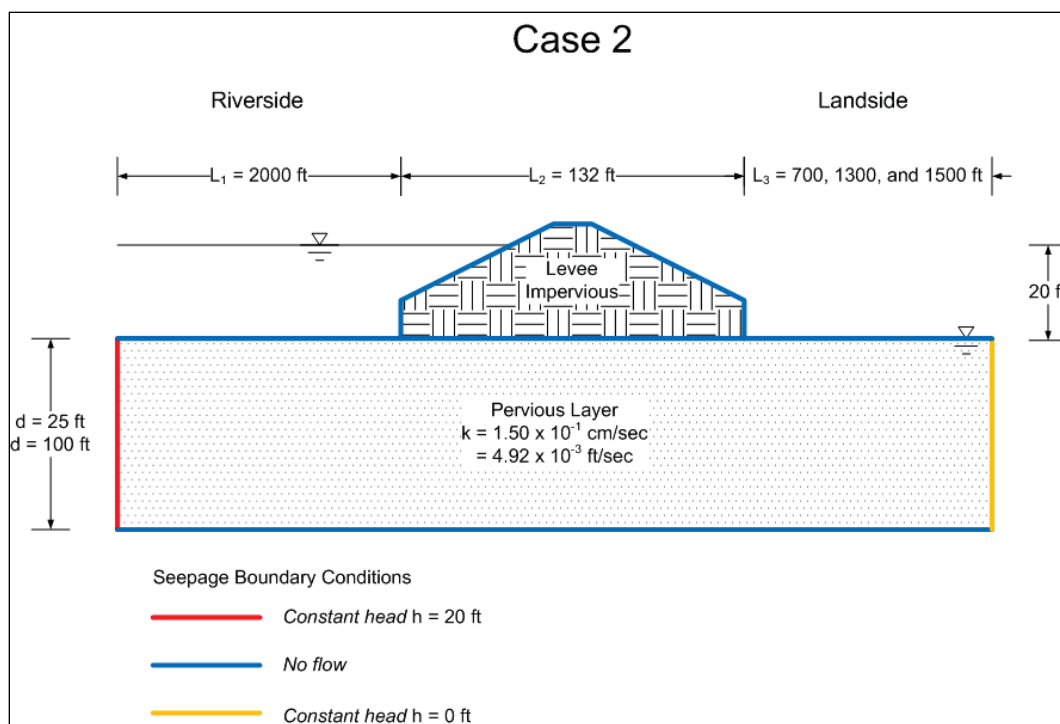
Figure 26. Calculated values of flow per unit length (Q_s) for different values of L_2/d for Case 1.

Figure 27. Comparison of different values of L_1 and L_3 for FEA.Figure 28. Percent error in calculated flow per unit length (Q_s) for Blanket Theory with increasing L_2/d ratios.

3.3 Case 2 – Impervious landside and riverside top stratum

Figure 29 shows the geometry used for Case 2. The boundary conditions were the same as for Case 1, except that the landside and riverside horizontal ground surfaces were assigned “no flow” boundary conditions to model an impervious top stratum. In this analysis, L_3 values of 700 ft, 1,300 ft, and 1,500 ft were used. A constant value of L_1 equal to 2,000 ft was used in all analyses.

Figure 29. Geometry for Case 2 - Impervious landside and riverside top stratum.



Analyses were done for values of d equal to 25 ft and 100 ft. The seepage per unit length beneath the levee (Q_s), and the pressure head at the toe of the levee were compared for the FEA and Blanket Theory solutions. For the geometry shown in Figure 29, the excess head at the toe (h_o) is equal to the pressure head at the toe because the far landside phreatic surface is at the ground surface.

Figure 30 shows the calculated values of Q_s for the different values of L_3 for both $d = 25 \text{ ft}$ and $d = 100 \text{ ft}$. The value of flow decreases with increasing L_3 and decreasing d . The values of flow calculated from FEA and Blanket Theory were essentially equal.

Figure 31 shows the variation of the pressure head (excess head) at the toe for different values of L_3 . The value of head plotted corresponds to the head at the node at the toe of the levee. The value of excess head determined using FEA and Blanket Theory is essentially the same, regardless of the value of the thickness of the pervious layer. As indicated in the theory portion of this report, the excess head beneath the blanket is not dependent on the thickness of the pervious substratum for Blanket Theory, and that result is substantiated by the FEA.

Figure 30. Calculated values of flow per unit length (Q_s) from Blanket Theory and finite element analysis for different values of L_3 for Case 2.

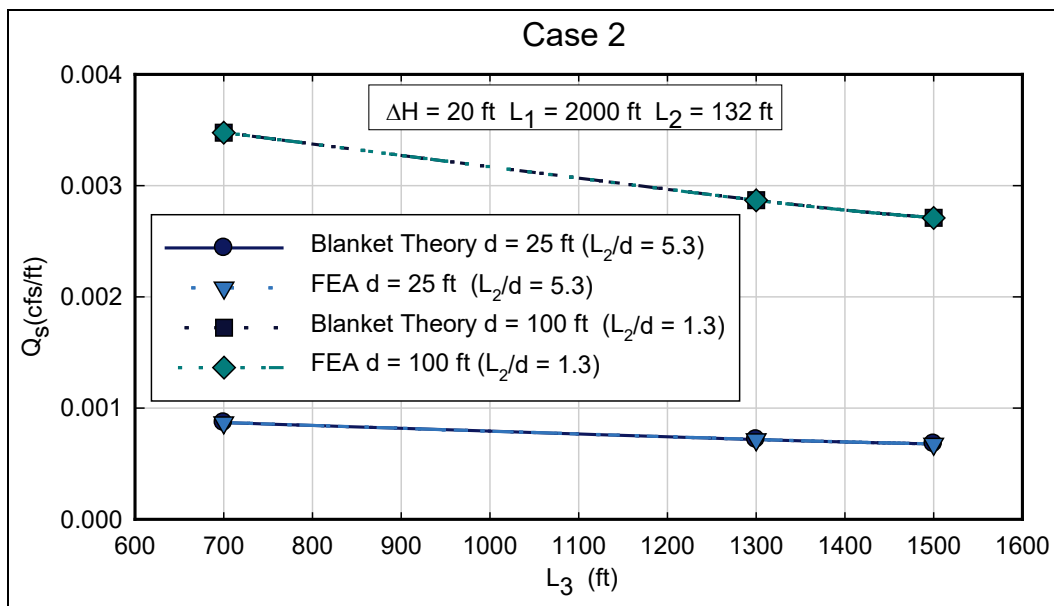
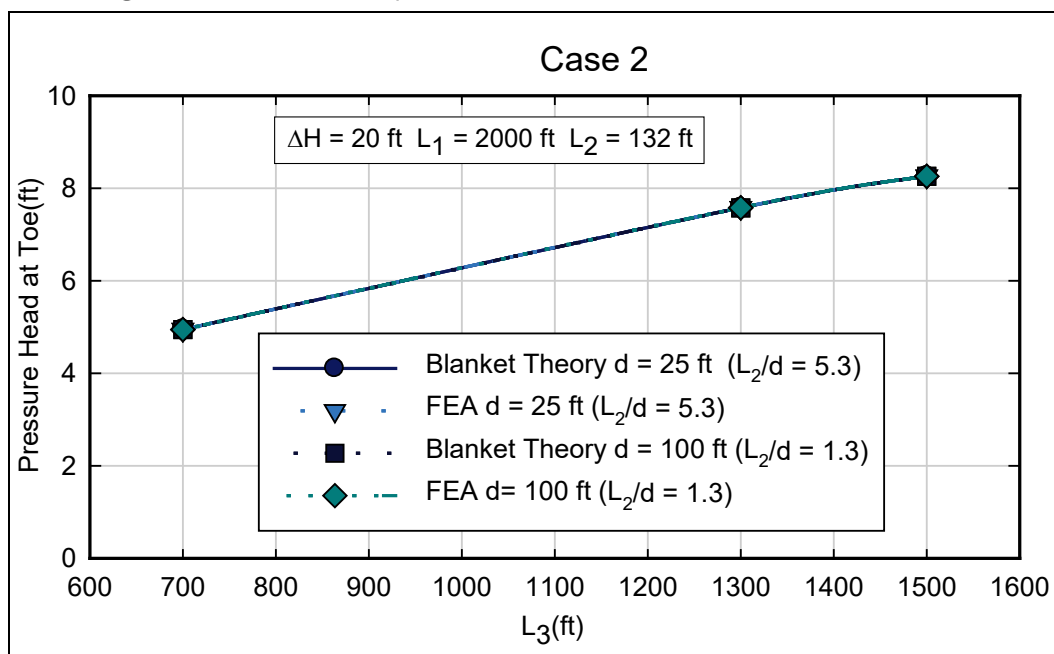


Figure 31. Excess head (h_o) or pressure head beneath blanket at toe for Case 2 calculated using FEA and Blanket Theory for different values of L_3 for $d = 25 \text{ ft}$ and $d = 100 \text{ ft}$.



3.4 Case 3 – Impervious riverside top stratum and no landside top stratum

The geometry and finite element boundary conditions for Case 3 (impervious riverside top stratum and no landside top stratum) are shown in Figure 32. The hydraulic boundary conditions are the same as for Case 1, except that *no-flow* nodal boundary conditions were assigned to the riverside ground surface to model an impermeable blanket. In the Blanket Theory derivation, the L_3 dimension is infinite. In order to approximate this with FEA, a value of L_3 equal to 1,500 ft was used in the analysis. Based on the results of Case 1, this is justified because the L_3 values of 100 ft to 1,500 ft produced the same calculated flows. L_1 values of 200 ft, 500 ft, and 1,000 ft were used in the FEA, and values of d equal to 25 ft and 100 ft were used.

Figure 32. Geometry for Case 3 - Impervious riverside top stratum and no landside top stratum.

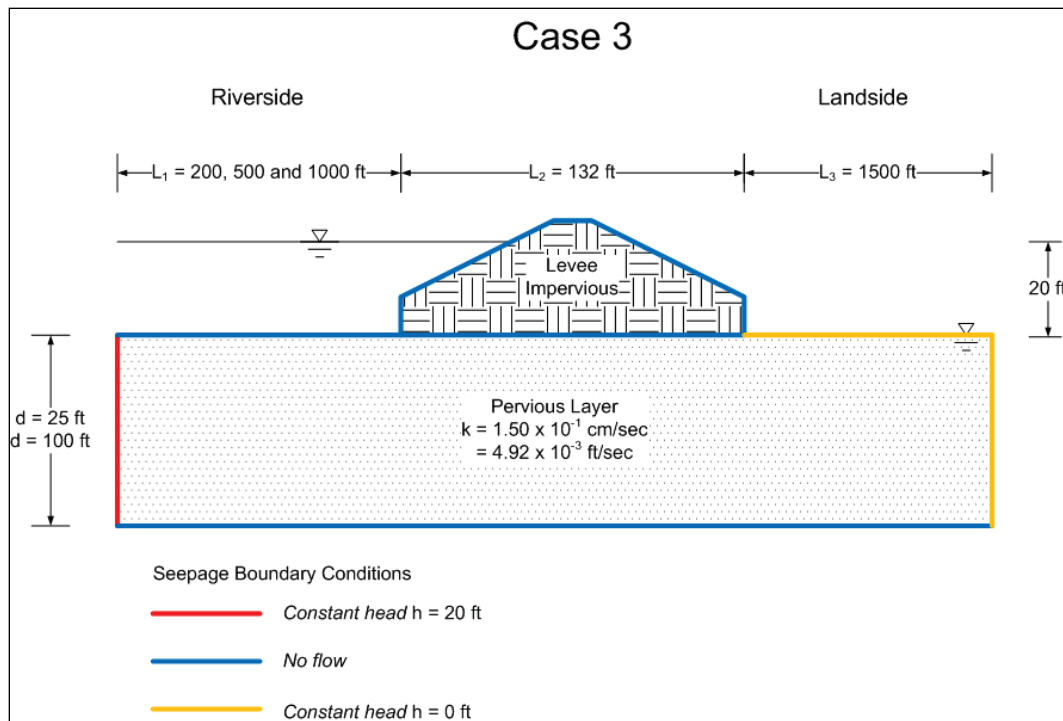
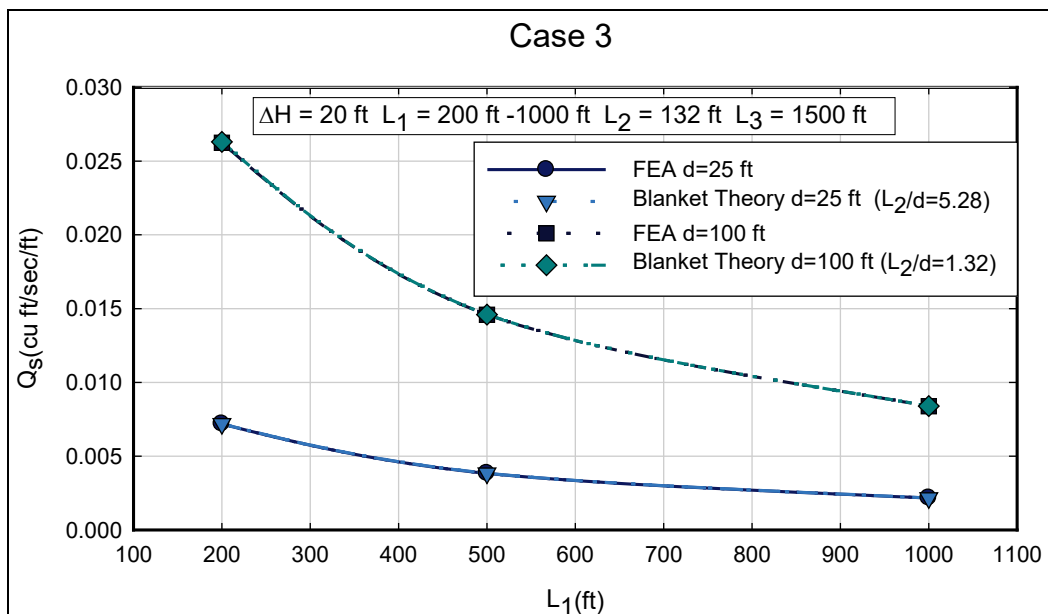


Figure 33 shows the calculated flow per unit length (Q_s) as a function of L_1 . The flow decreases, as expected, with increasing magnitude of L_1 and with decreasing magnitude of d . Again, the Blanket Theory results and the finite element results are in exact agreement.

Figure 33. Calculated values of flow per unit length (Q_s) from Blanket Theory and finite element analysis for different values of L_1 for Case 3.



3.5 Case 4 – Impervious landside top stratum and no riverside top stratum

The geometry for Case 4 (impervious landside top stratum and no riverside top stratum) is shown in Figure 34. The hydraulic boundary conditions are the same as for Case 1, except that *no-flow* nodal boundary conditions were assigned to the landside ground surface to model an impermeable blanket.

Similar to the previous example, in the Blanket Theory derivation, the L_1 dimension is infinite. In order to approximate this with FEA, a value of L_1 equal to 3,100 ft was used in the analysis. For the Case 4 analysis, L_3 values of 500 ft, 1,000 ft, and 1,600 ft were used and values of d equal to 25 ft and 100 ft were used.

Figure 35 shows the calculated flow per unit length (Q_s) beneath the levee for different values of L_3 . The results from FEA and Blanket Theory are essentially identical. Figure 36 shows the value of excess head (pressure head) at the toe of the levee for the same cases. Again, there is no difference between the values calculated using Blanket Theory and the values calculated using FEA.

Figure 34. Geometry for Case 4 - Impervious landside top stratum and no riverside top stratum.

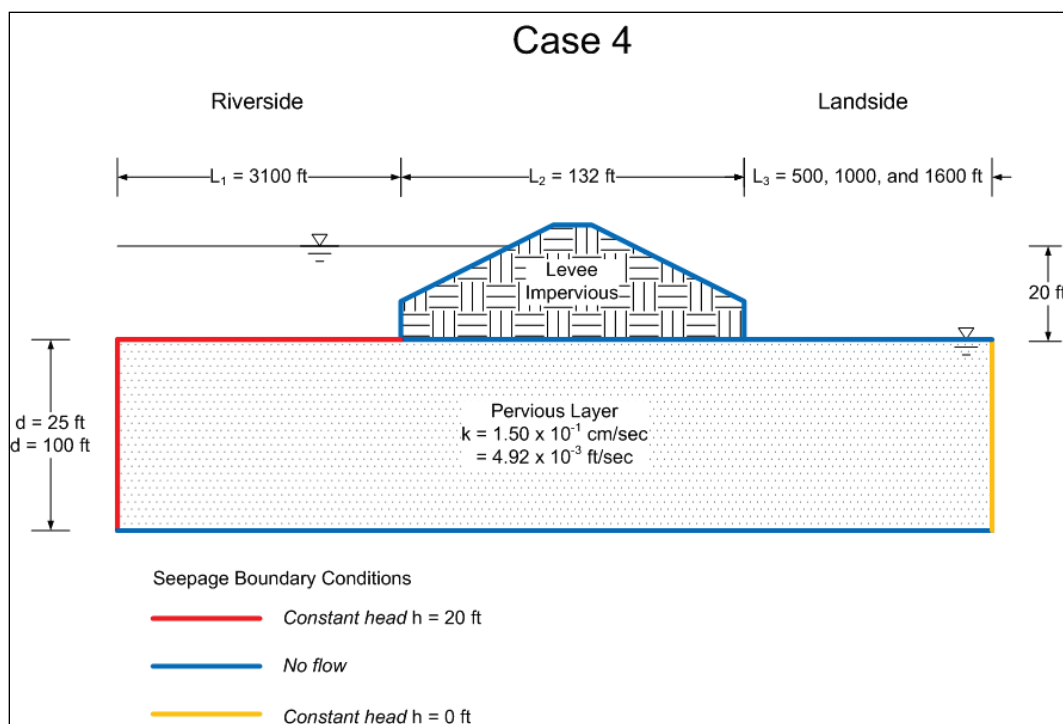
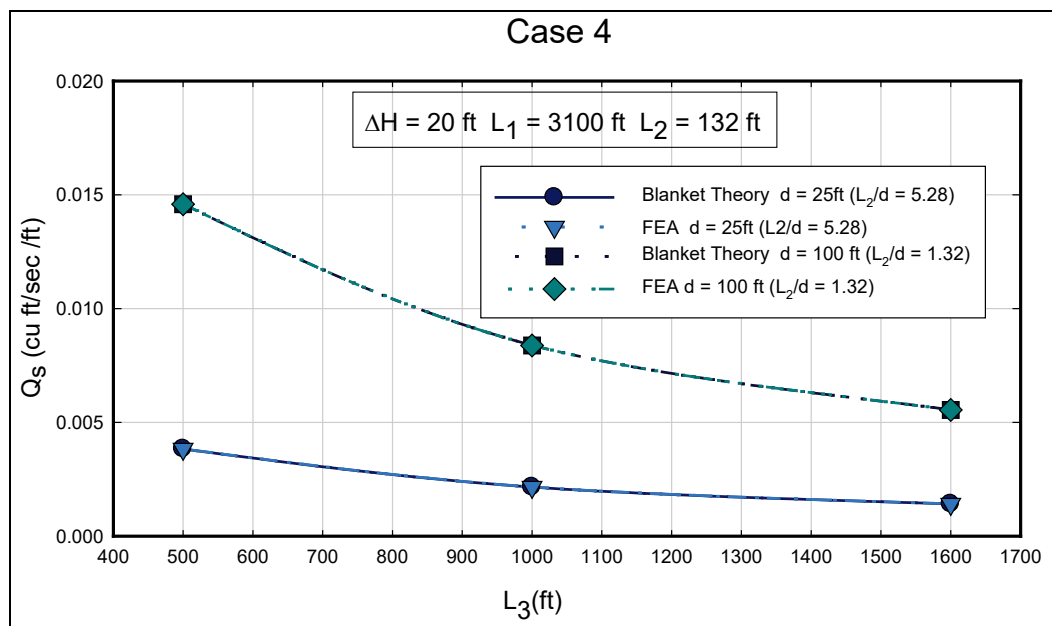
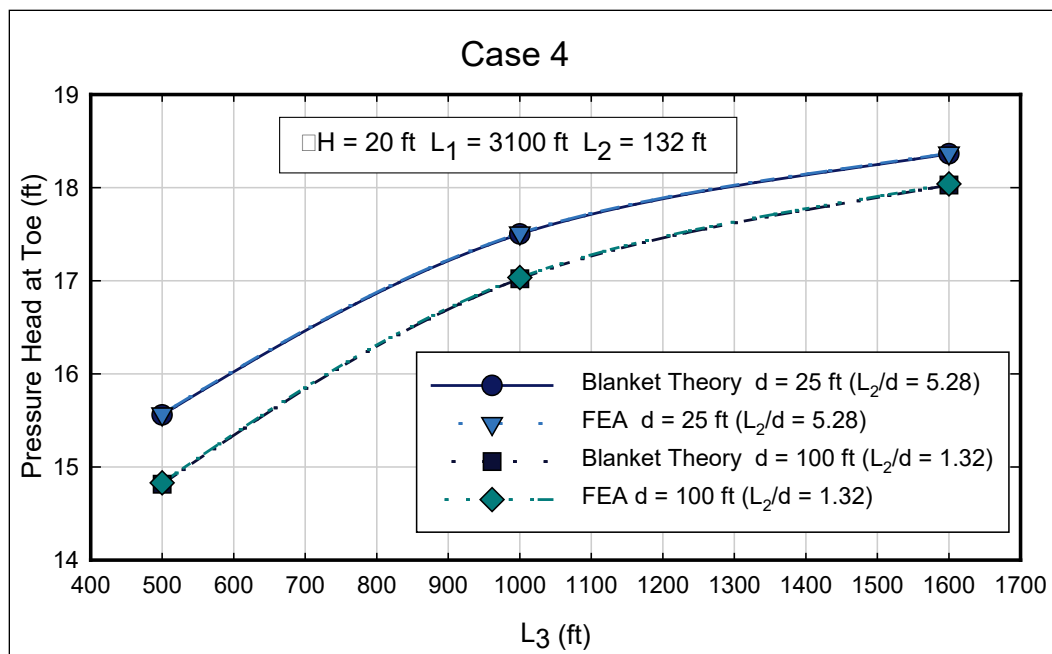
Figure 35. Calculated values of flow per unit length (Q_s) from Blanket Theory and finite element analysis for different values of L_3 for Case 4.

Figure 36. Excess head (h_o) or pressure head at toe calculated using FEA and Blanket Theory for different values of L_3 .



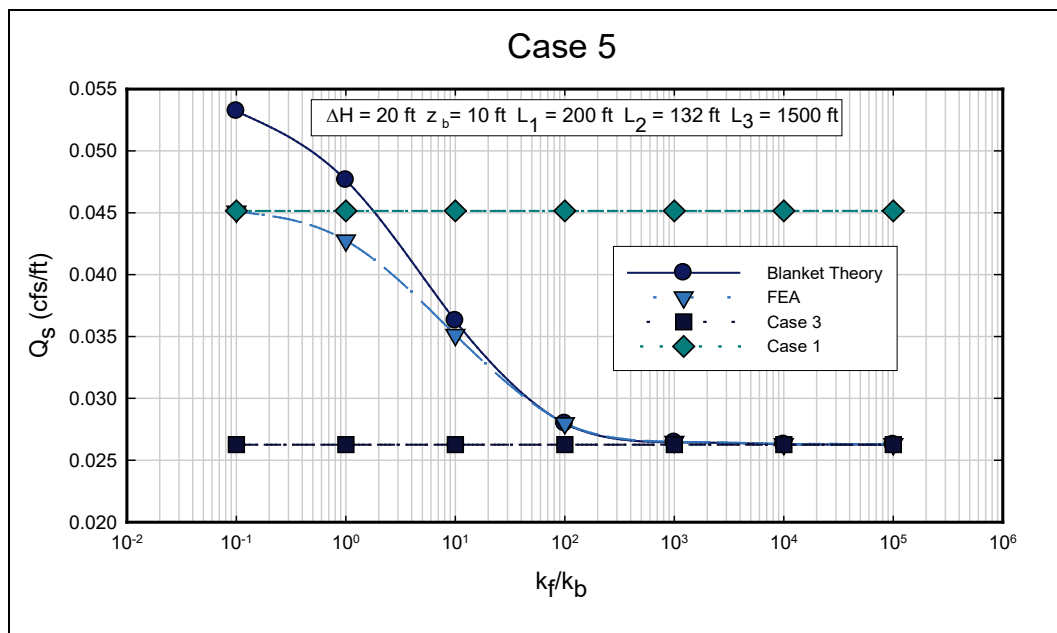
3.6 Case 5 – Semi-pervious riverside top stratum and no landside top stratum

Case 5 is the first case having a semi-pervious blanket. For cases similar to Case 5, the thickness and permeability of the semi-pervious blanket become important factors in the analyses. For the geometry shown in Figure 37, the thickness of the upstream blanket has an influence on the manner that the total head loss (H or ΔH) is defined. For the purpose of the FEA, ΔH is defined as the change in head from the river level to the ground surface elevation on the landside. This differs from the way the ΔH is shown for Case 5 in USACE (2000), where ΔH is defined as the distance from the top of the blanket to the river level.

Comparison of the cases having semi-pervious blankets with the impervious cases allows a determination of the threshold permeability values where a semi-pervious blanket becomes essentially impervious.

The semi-pervious cases require evaluation of more parameter combinations than Cases 1 through 4. The permeability of the pervious layer (k_f) was assigned a value of 4.92×10^{-3} ft/sec (0.15 cm/sec), which is the same value used in the previous analyses. The permeability of the semi-pervious blanket (k_b) was varied to be a multiple of the permeability of the pervious layer. Ratios of k_f to k_b from 0.1 to 100,000 were used in the analysis.

Figure 38. Calculated values of flow per unit length (Q_s) for various permeability ratios from Blanket Theory and finite element analysis for Case 5 for $z_b = 10$ ft and $L_1 = 200$ ft.



For a permeability ratio of about 50 and above, Blanket Theory and FEA are in excellent agreement. For permeability ratios less than 50, Blanket Theory predicts larger flow values than FEA. Although the FEA correctly converges to the Case 1 solution, the flows predicted by Blanket Theory exceed the Case 1 values for permeability ratios of about 2 and greater.

Shown in Figure 39 is a similar plot for all of the same boundary conditions, except that L_1 has been increased to 1,000 ft. As expected, the volume of flow is decreased. There appears to be closer agreement with the FEA and Blanket Theory results for this geometry.

Figure 40 shows the results of a similar analysis for a blanket thickness (z_b) equal to 20 ft and L_1 equal to 200 ft. This analysis shows a certain peculiarity of flow measurements using SLIDE. For this analysis, a vertical “flux section” was placed from the horizontal midpoint of the levee extending through the pervious layer. SLIDE calculates the flow perpendicular to this vertical section. For the case of $L_1 = 200$ ft, the flow lines are not exactly horizontal beneath the midpoint of the levee, and the flow calculated by SLIDE is slightly less than the total flow beneath the levee. This can be remedied by drawing the flux section parallel to the total head contours at this point beneath the levee.

Figure 39. Calculated values of flow per unit length (Q_s) for various permeability ratios from Blanket Theory and finite element analysis for Case 5 for $z_b = 10$ ft and $L_1 = 1,000$ ft.

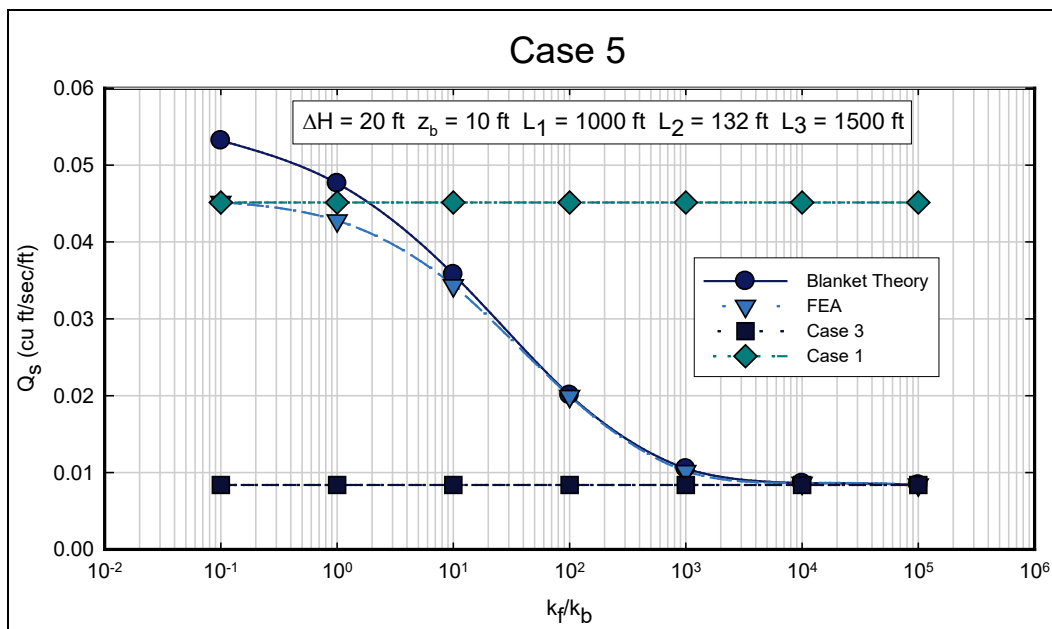
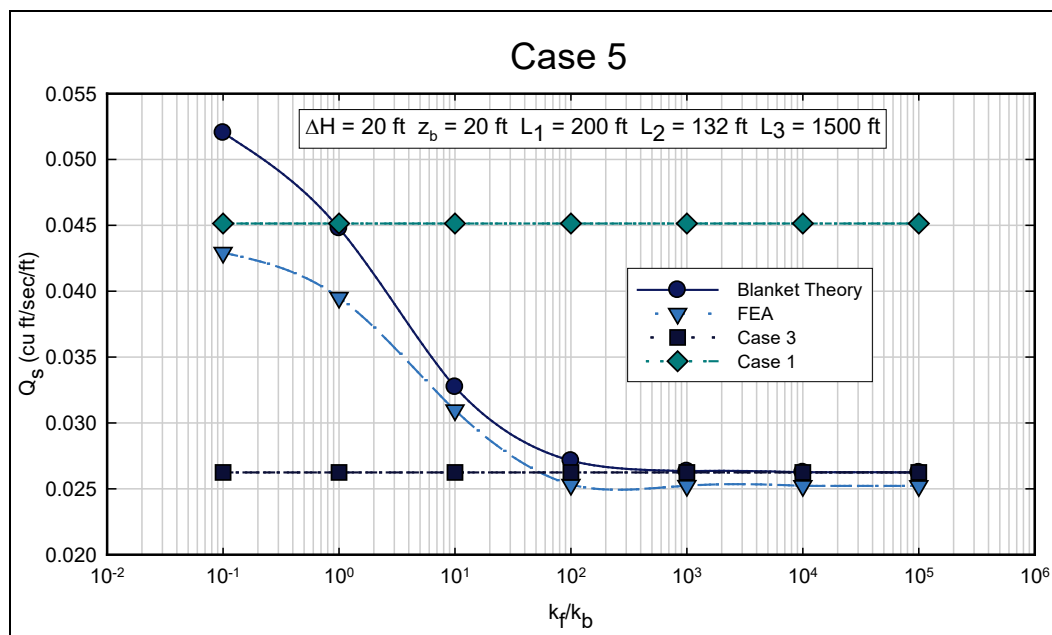


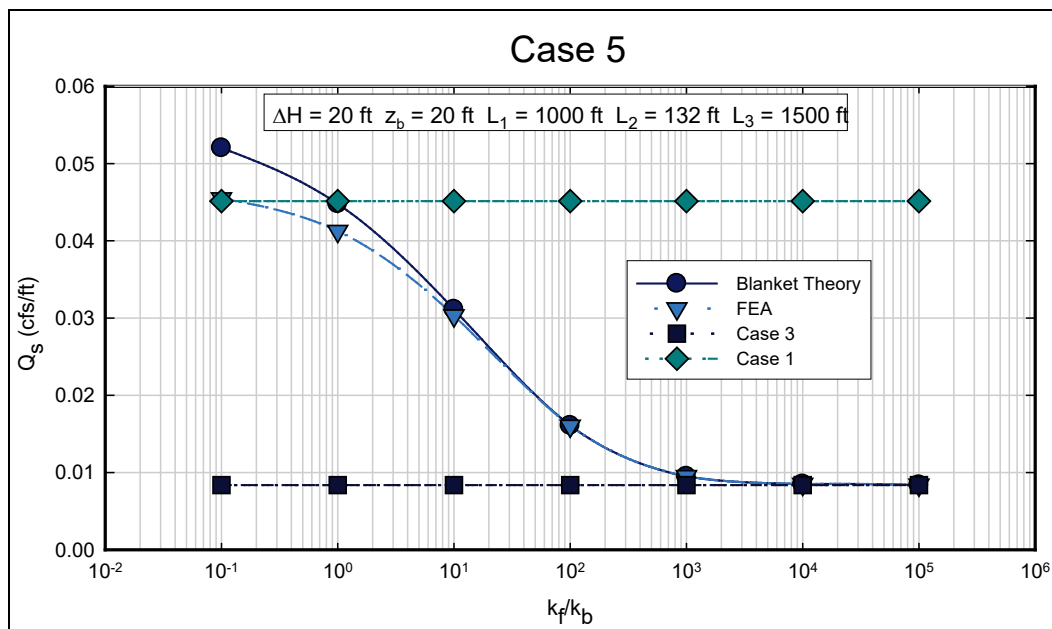
Figure 40. Calculated values of flow per unit length (Q_s) for various permeability ratios from Blanket Theory and finite element analysis for Case 5 for $z_b = 20$ ft and $L_1 = 200$ ft.



This artifact of SLIDE is further shown in Figure 41. These analyses were performed for the same boundary conditions as the previous figure, except that the length of the semi-pervious blanket has been increased to 1,000 ft. The net result of this is to decrease the flow, and the equipotential lines are vertical in the location of the flux section. This causes the calculated flow

to be the same as Blanket Theory for high permeability ratios. A comparison of the way that SLIDE and SEEP/W calculate flows is provided later in this report.

Figure 41. Calculated values of flow per unit length (Q_s) for various permeability ratios from Blanket Theory and finite element analysis for Case 5 for $z_b = 20$ ft and $L_1 = 1,000$ ft.

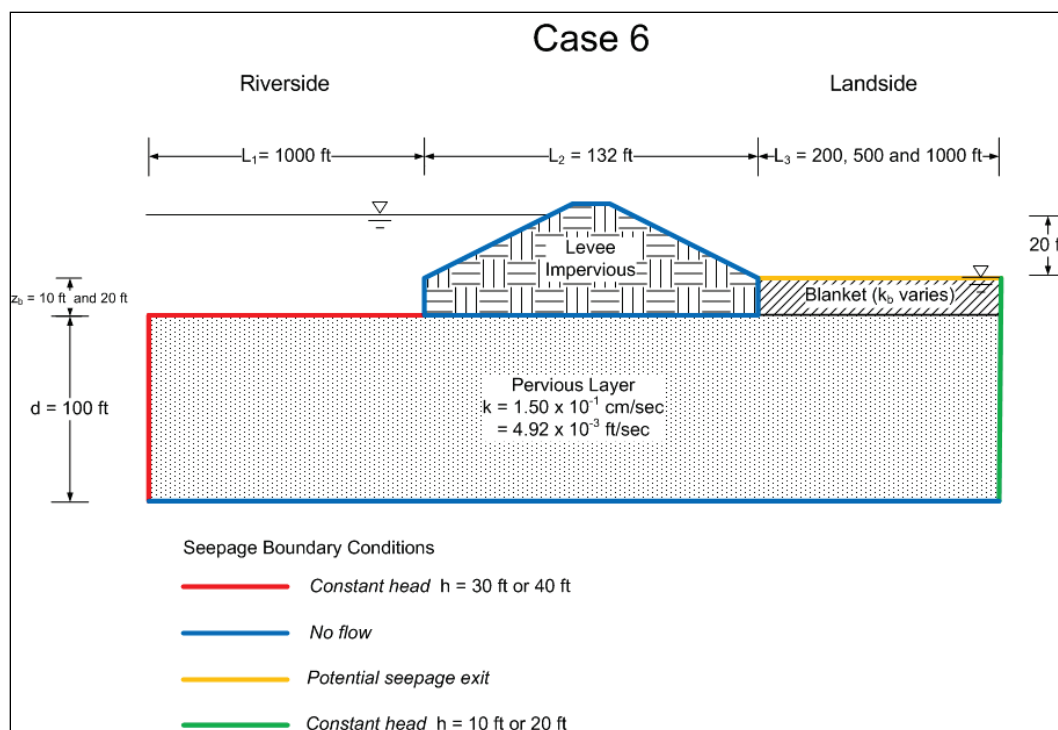


3.7 Case 6 – Semi-pervious landside top stratum and no riverside top stratum

The geometry and finite element boundary conditions for Case 6 are shown in Figure 42. This case has a L_1 dimension of infinity. A L_1 dimension of 1,000 ft was used in the finite element model because, as shown earlier, it provides results that correctly approximate those of an infinite boundary condition for cases where no blanket exists.

As indicated in Section 2 of this report, there is an inconsistency in USACE (2000) regarding the Case 6 solution. The head at a distance x cannot be calculated by assuming a linear head loss. The head is dependent on the landward side boundary conditions (i.e., infinite length of landside top stratum, open or blocked seepage exit). However, for this analysis, finite values of L_3 were used because an open seepage exit is shown in the Figure B6 of EM-1110-2-1913 (USACE 2000). The analyses were performed with L_3 values of 200 ft, 500 ft, and 1,000 ft. Blanket thicknesses of 10 ft and 20 ft were analyzed, and permeability ratios (k_f/k_b) from 0.1 to 100,000 were used.

Figure 42. Geometry for Case 6 - Semi-pervious landside top stratum and no riverside top stratum.



The phreatic surface on the landside was assigned to the ground surface at the far vertical boundary. This is different than that shown in USACE (2000) on Figure B6 on page B15. Based on the way that the change in head is defined, the phreatic surface on the landside would have to be at the interface between the blanket and the pervious layer. For the FEA, the phreatic surface was assigned to the ground surface such that only flow through saturated media would occur. If the phreatic surface was set at the interface between the pervious layer and the blanket, then the analysis would have been a free surface analysis, with the phreatic surface being within the landside blanket.

Shown in Figure 43 are the calculated volumetric flow rates (Q_s) for $L_3 = 1,000 \text{ ft}$ and $z_b = 10 \text{ ft}$. As was the case for Case 5, the finite element results are bracketed by the results for Case 1 (no blankets) and Case 4 (impervious landside blanket). At a permeability ratio of about 4,000, the landside blanket is effectively impervious, and the solution for Case 4 would apply.

Figure 43. Calculated values of flow per unit length (Q_s) for various permeability ratios from Blanket Theory and finite element analysis for Case 6 for $z_b = 10$ ft and $L_3 = 1,000$ ft.

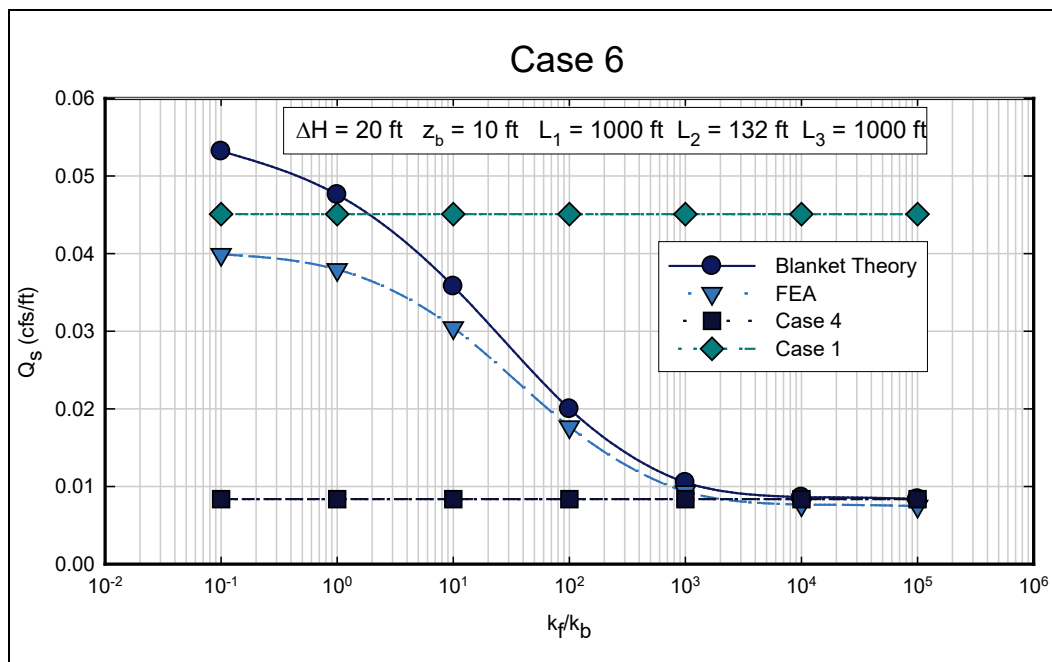


Figure 44 shows the results for a similar analysis with a blanket thickness of 20 ft. The results of all combinations of blanket thicknesses and L_3 dimensions produced reasonable results, with flow values decreasing with increasing values of z_b and L_3 .

For Case 6 and Case 7, the value of the excess head at the toe of the levee is perhaps the most important value calculated from a seepage analysis because this parameter affects the factor of safety for heave and for erosion. The head directly beneath the toe of the levee at the interface between the semi-pervious blanket and the pervious layer was calculated using FEA and Blanket Theory, and the results for $z_b = 10$ ft and $L_3 = 1,000$ ft are shown in Figure 45. As was the case with the calculated flows, the excess head at the toe is bracketed by the results of the Case 1 and Case 4 solutions.

The agreement between Blanket Theory and FEA for Case 6 is very close. The calculated heads are closer than the flow values presented earlier because the heads are not influenced by the specific technicalities of the flow calculations used in SLIDE. Figure 46 shows the calculated head values for the same boundary conditions, except the thickness of the blanket is increased to 20 ft. Again, the agreement between FEA and Blanket Theory is very good.

Figure 44. Calculated values of flow per unit length (Q_s) for various permeability ratios from Blanket Theory and finite element analysis for Case 6 for $z_b = 20$ ft and $L_3 = 1,000$ ft.

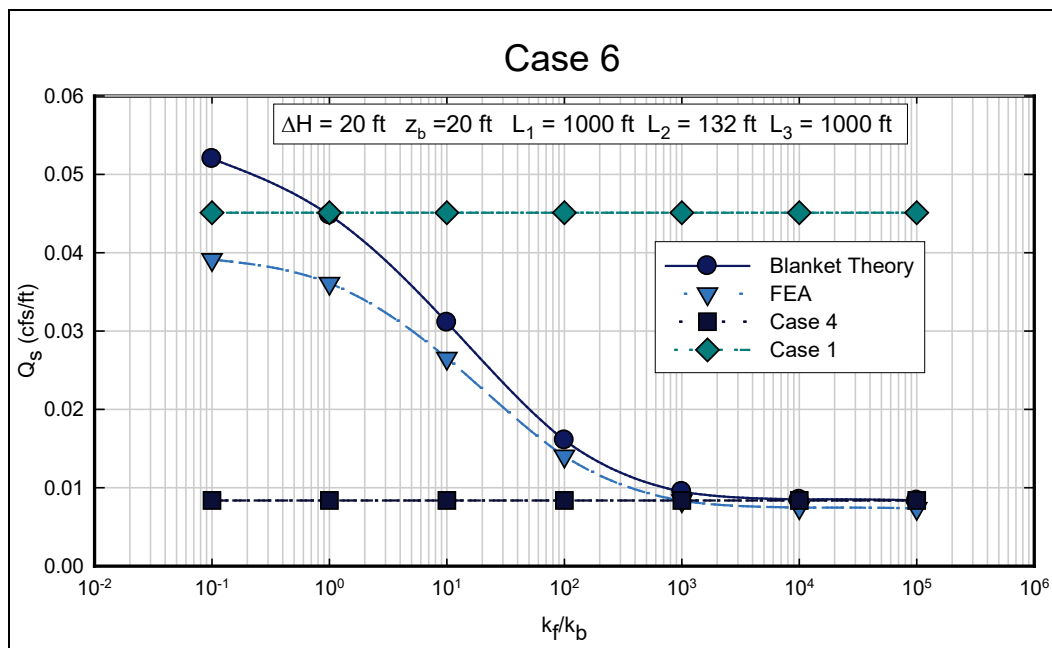


Figure 45. Excess head (h_b) or pressure head beneath blanket at toe for Case 6 calculated using finite element analysis and Blanket Theory for different permeability ratios for $z_b = 10$ ft and $L_3 = 1,000$ ft.

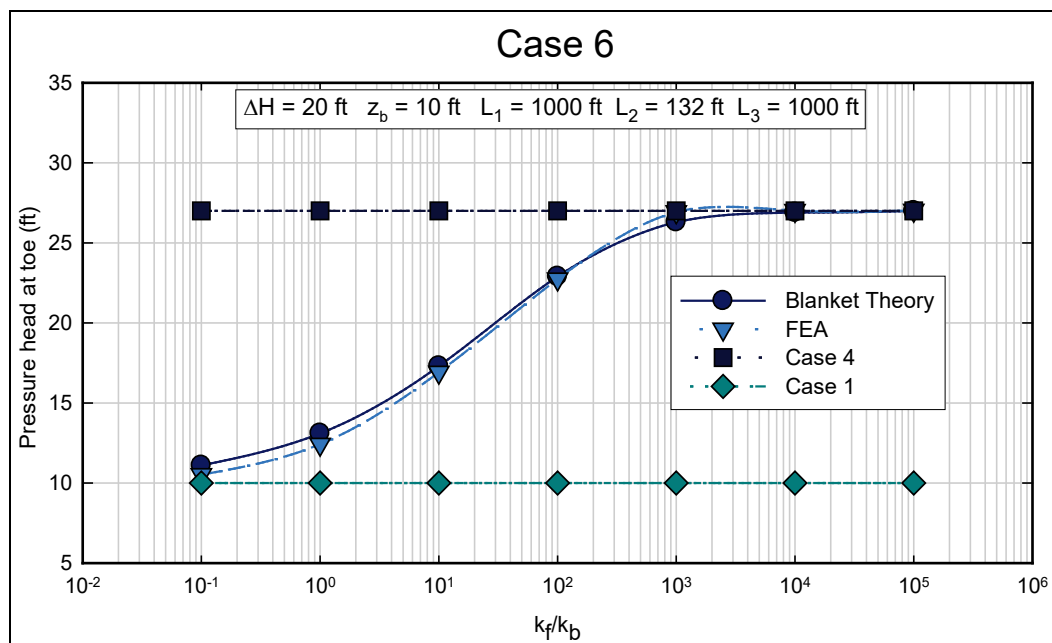
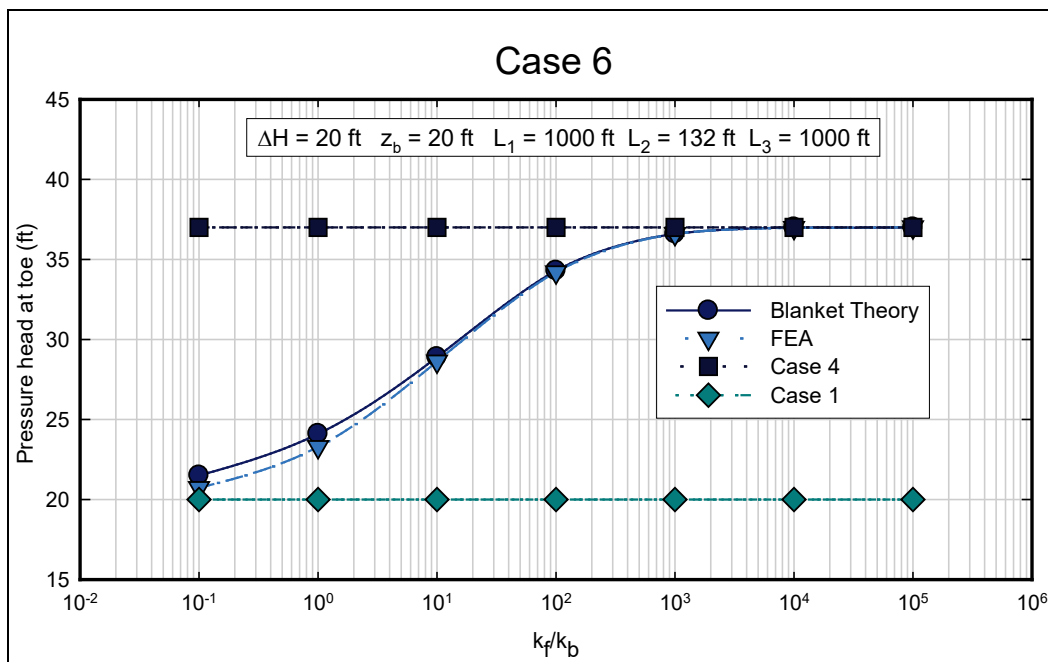


Figure 46. Pressure head beneath blanket at toe for Case 6 calculated using finite element analysis and Blanket Theory for different permeability ratios for $z_b = 20$ ft and $L_3 = 1,000$ ft.

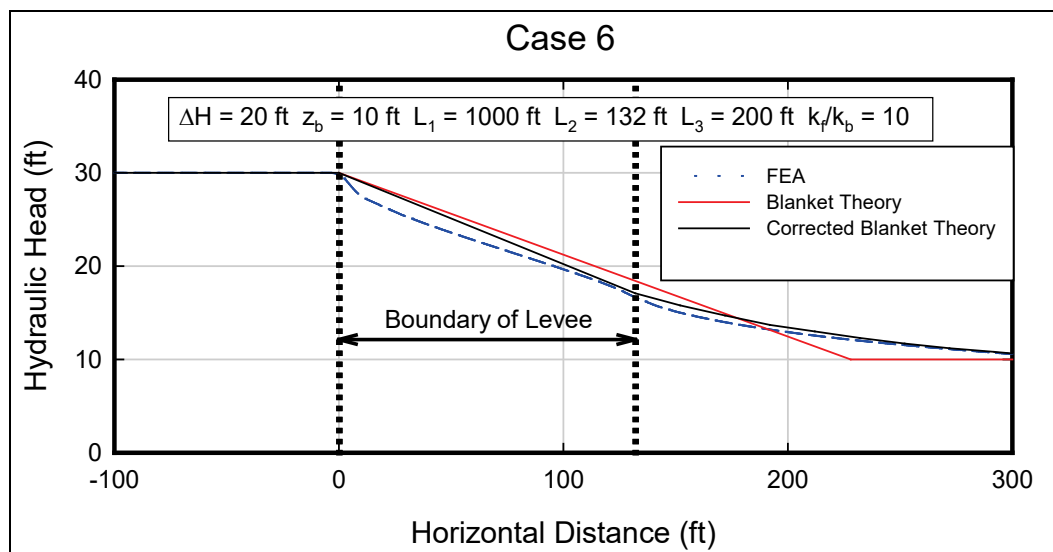


The results of the Case 6 analysis indicate that if the geometry of the problem is similar to that assumed in the Blanket Theory derivations, correct values of excess head at the toe and the associated factors of safety for erosion and heave, would be the same for FEA and Blanket Theory for the same hydraulic boundary conditions. When the permeability of the blanket is about 4,000 times less than the pervious layer, the blanket is essentially impervious, and the Case 4 equations can be used.

The FEA can further be compared to Blanket Theory for Case 6 by examining the values of x_3 . The value of x_3 is defined as the horizontal distance from the landside toe of the levee to the location, where the head at the bottom of the blanket is equal to the landside phreatic surface. This value is important because x_3 would be used as a coordinate for the piezometric grade line (PGL) to model the pore pressures in the pervious layer for a slope stability analysis. Instead of comparing only the value of x_3 , it is convenient to compare Blanket Theory with FEA by plotting the hydraulic head at the interface between the pervious layer and blanket. For Case 6, this would be a linear relationship for Blanket Theory (based on current equation present in USACE [2000]) from a value of $\Delta H + z_b$ at the riverside toe of the levee to a head value of z_b at the x_3 distance. However, if we use the equation similar to Case 7c for Case 6 to determine head at distance x as explained in Section 2 portion of the report, this would no

longer be linear due to the vertical flow occurring through semi-pervious top stratum. Hence, two separate lines are plotted in Figures 47 through 49 to indicate these two scenarios. The line labeled “Blanket Theory” is based on the current equation present in USACE (2000), while the line labeled “Corrected Blanket Theory” is based on the equation calculating head in a similar manner as Case 7c. Similarly, the line labeled as “FEA” shows the head values for the nodes at the interface and will also be non-linear.

Figure 47. Piezometric grade line for Case 6 where $L_3 = 200$ ft, $z_b = 10$ ft, and $k_f/k_b = 10$.



Shown in Figure 47 is the PGL for Case 6 where $L_3 = 200$ ft, $z_b = 10$ ft, and $k_f/k_b = 10$. Beneath the levee, the PGL for Blanket Theory is above that determined from FEA. At a point about 60 ft landward from the levee toe, the head predicted by Blanket Theory is less than that predicted by FEA. In general, the PGL predicted using Blanket Theory appears to be a conservative approximation of the true PGL. This would mean that the pore pressures calculated using the Blanket Theory PGL would be greater than those determined by FEA, and lower factors of safety would result from slope stability analyses. However, the PGL predicted by the corrected Blanket Theory is closer to FEA than by Blanket Theory and becomes equal to FEA at about 120 ft landward of the levee toe and beyond.

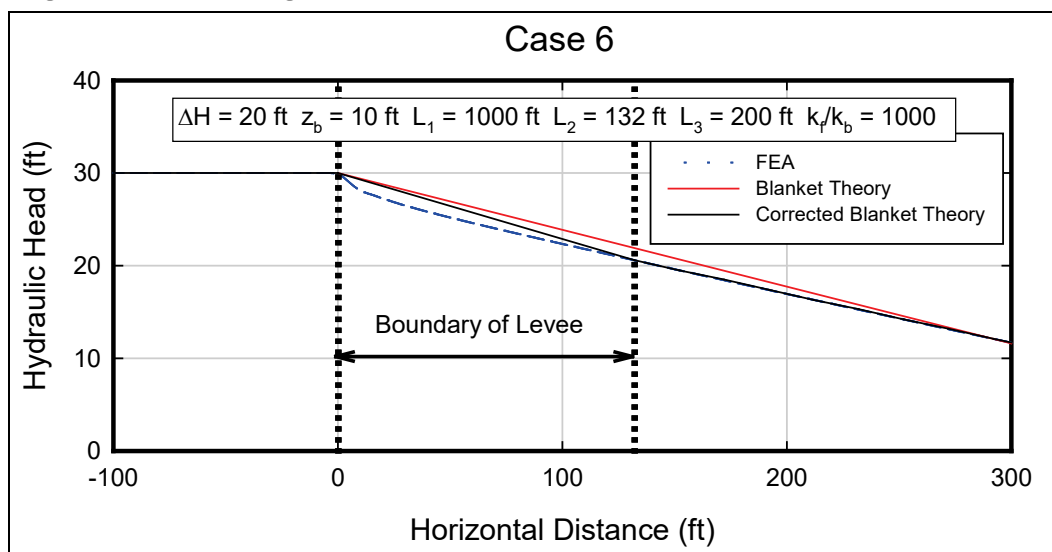
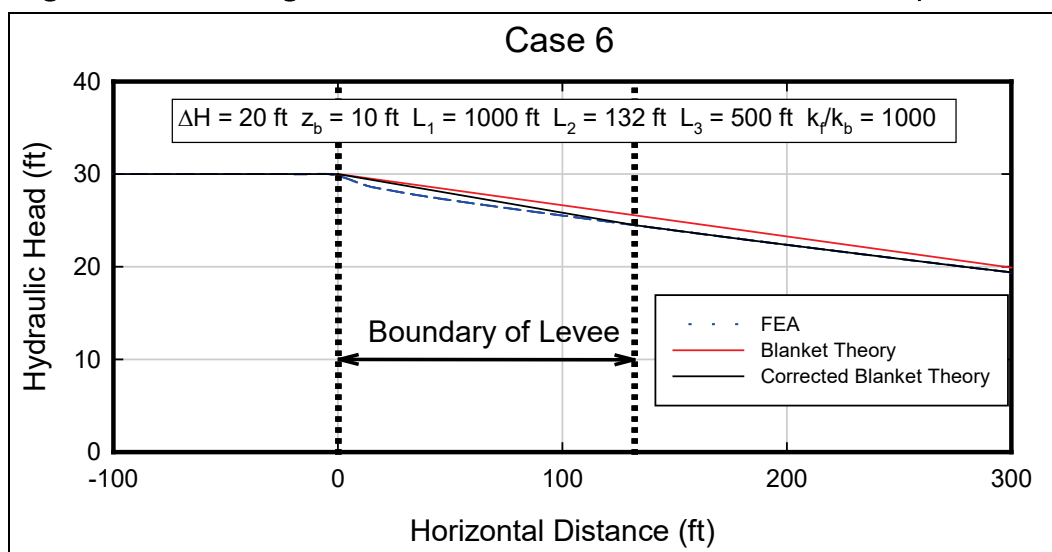
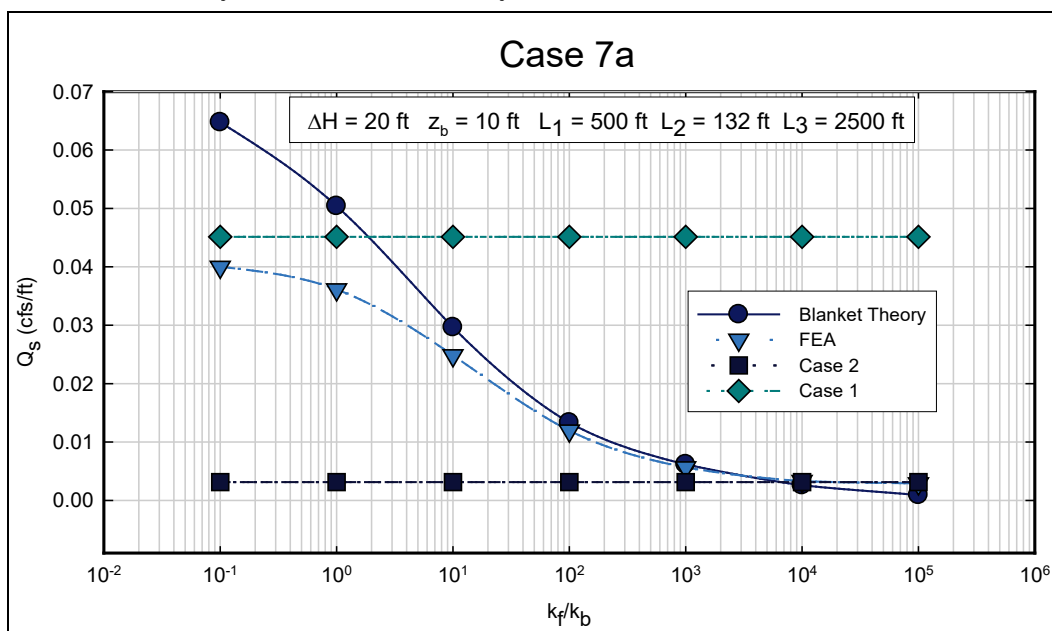
Figure 48. Piezometric grade line for Case 6 where $L_3 = 200$ ft, $z_b = 10$ ft, and $k_f/k_b = 1000$.Figure 49. Piezometric grade line for Case 6 where $L_3 = 500$ ft, $z_b = 10$ ft, and $k_f/k_b = 1000$.

Figure 48 shows a similar plot, except that the permeability ratio is equal to 1,000. As the permeability ratio increases, the value of x_3 increases, and the point where the PGL from Blanket Theory exceeds the PGL from FEA increases. For these boundary conditions, the PGLs cross at about 170 ft landward from the toe of the levee. As was the case for the previous example, the PGL determined using Blanket Theory appears to be a conservative approximation of the true piezometric surface. Figure 49 shows the results from the same analysis, except that L_3 was increased to 500 ft. Increasing the value of L_3 also serves to increase the distance where the PGL predicted by Blanket Theory and FEA are equivalent.

The phreatic surface was assumed to be at the ground surface on the landside. A constant head, equal to the ground surface elevation, was assigned to the far landside vertical boundary. The nodes on the horizontal landside ground surface were assigned *potential seepage exit* conditions. The riverside nodes, both on the horizontal ground surface and at the vertical domain boundary, were assigned constant heads equal to the landside head plus 20 ft, so that $\Delta H = 20$ ft for the analysis.

The calculated volumetric flow rate per unit length (Q_s) is plotted in Figure 51 for both the finite element and Blanket Theory solutions as a function of permeability ratio. The FEA results are bracketed by both the Case 1 and Case 2 results. The flows calculated by the Blanket Theory exceed the Case 1 results at a permeability ratio of about 2. The Case 2 results shown on the figure were calculated assuming a $L_3 = 2,500$ ft to be consistent with the FEA.

Figure 51. Calculated values of flow per unit length (Q_s) for various permeability ratios from Blanket Theory and finite element analysis for Case 7a for $z_b = 10$ ft and $L_1 = 500$ ft.



Blanket Theory agrees well with the FEA results for permeability ratios greater than about 100. For permeability ratios less than 100, the flows calculated by Blanket Theory are greater than calculated by the FEA but that could be partially due to the way that SLIDE calculates flow values.

Shown in Figure 52 is an analysis identical to the previous one, but the thicknesses of both the riverside and landside blankets have been

increased to 20 ft. The results are similar to that obtained for a blanket thickness of 10 ft, except that the Case 5 Blanket Theory intersects the Case 2 results at a permeability ratio of 1. Again, good agreement is obtained between Blanket Theory and FEA.

Figure 52. Calculated values of flow per unit length (Q_s) for various permeability ratios from Blanket Theory and finite element analysis for Case 7a for $z_b = 20$ ft and $L_1 = 500$ ft.

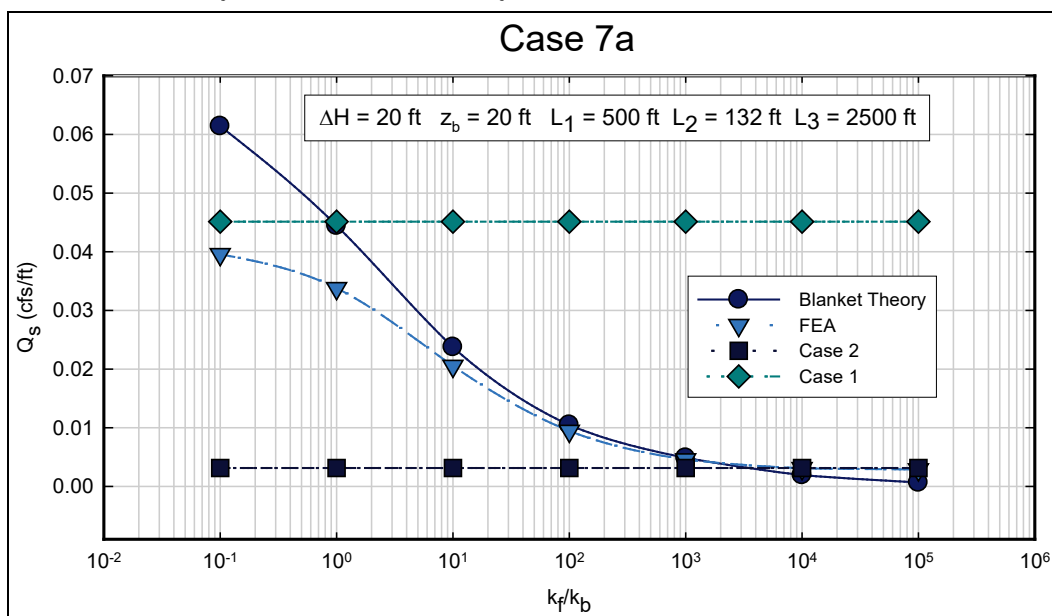


Figure 53 shows the calculated pressure head beneath the toe of the levee at the top of the pervious layer for a blanket thickness of 10 ft. There is generally good agreement between Blanket Theory and FEA. The difference above permeability ratios of about 10,000 may be due to the fact that a $L_3 = 2,500$ ft may not have been large enough to model infinity. However, this permeability ratio is outside of the range that Case 7a would be applicable. Overall, these results indicated that equivalent exit gradients would be obtained using either Blanket Theory or FEA.

Figure 53. Excess head (h_e) or pressure head beneath blanket at toe for Case 7a calculated using FEA and Blanket Theory for different permeability ratios for $z_b = 10$ ft and $L_1 = 500$ ft.

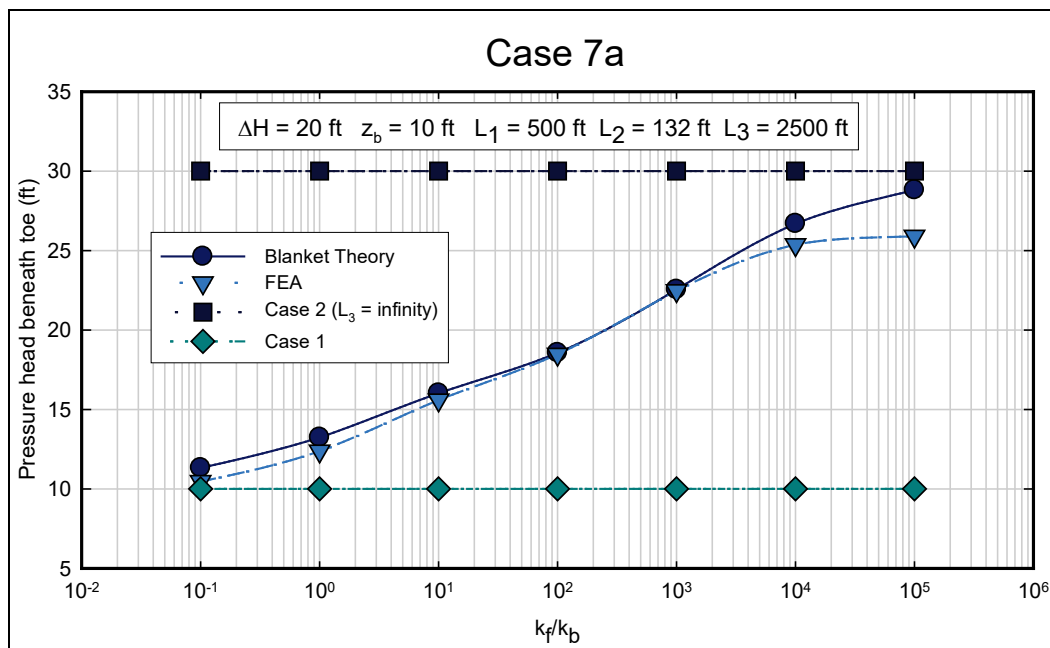
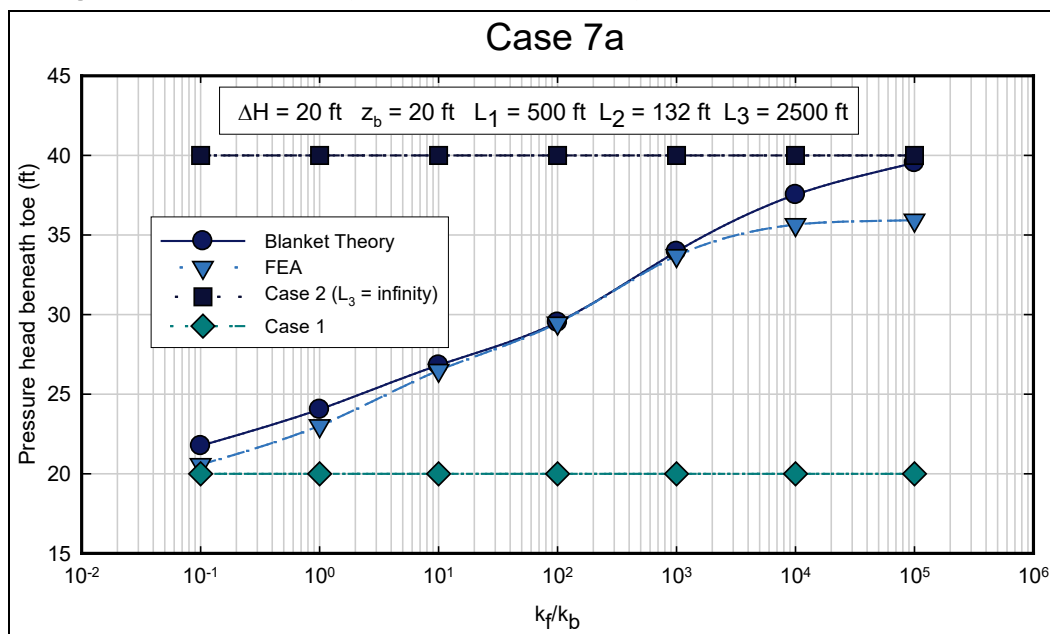


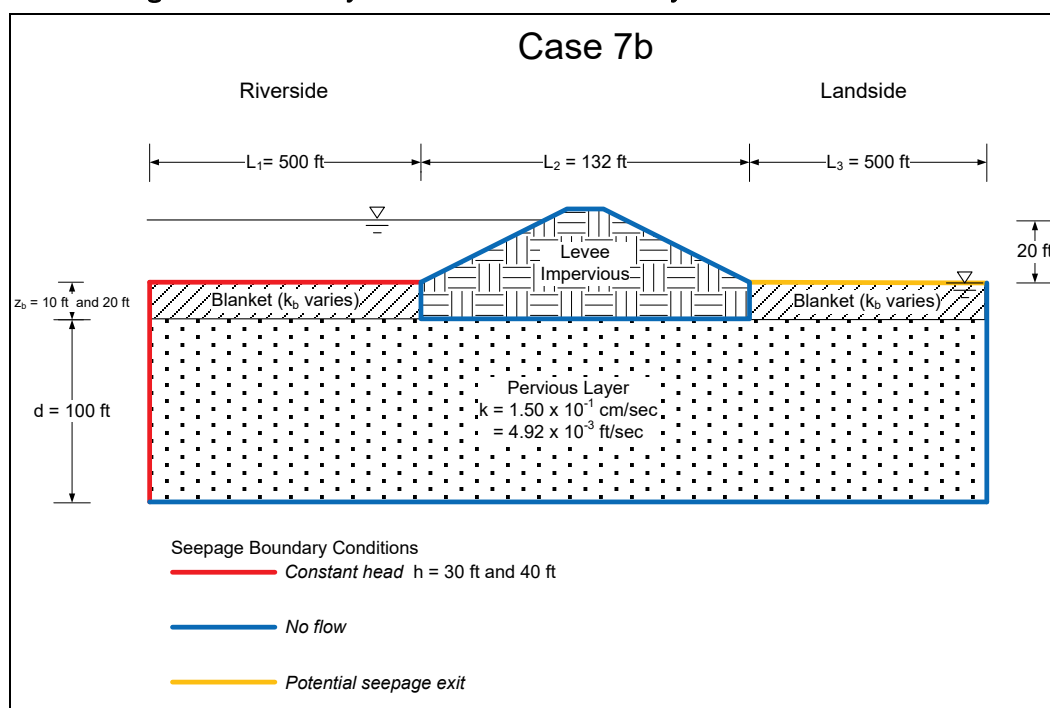
Figure 54 shows essentially the same results for a blanket thickness of 20 ft. Again, there is good agreement between Blanket Theory and FEA for the boundary conditions used.

Figure 54. Excess head (h_e) or pressure head beneath blanket at toe for Case 7a calculated using FEA and Blanket Theory for different permeability ratios for $z_b = 20$ ft and $L_1 = 500$ ft.



3.8.2 Case 7b – Semi-pervious landside and riverside top stratum (seepage block in the pervious substratum located landward of the levee)

Figure 55. Geometry and finite element boundary conditions for Case 7b.



A L_1 value of 500 ft and a L_3 value of 500 ft were used in all analyses. The thickness of the pervious layer (d) was 100 ft. The main parameter varied in these analyses was the permeability of the semi-pervious blankets. Permeability ratios (k_f/k_b) ranging from 0.1 to 100,000 were used. The same permeability was applied to both the upstream and downstream blankets.

The calculated volumetric flow rate per unit length (Q_s) is plotted in Figure 56 for both the finite element and Blanket Theory solutions as a function of permeability ratio. The FEA results reach an approximate asymptote at the Case 1 solution. However, similar to what was found for Case 7a, the flows calculated by the Blanket Theory exceed the Case 1 results at a permeability ratio of about 2. For permeability ratios less than about 100, Blanket Theory produces larger flows than FEA. For permeability ratios greater than this, the calculated flow is approximately the same.

Figure 56. Calculated values of flow per unit length (Q_s) for various permeability ratios from Blanket Theory and finite element analysis for Case 7b for $z_b = 10$ ft and $L_1 = 500$ ft and $L_3 = 500$ ft.

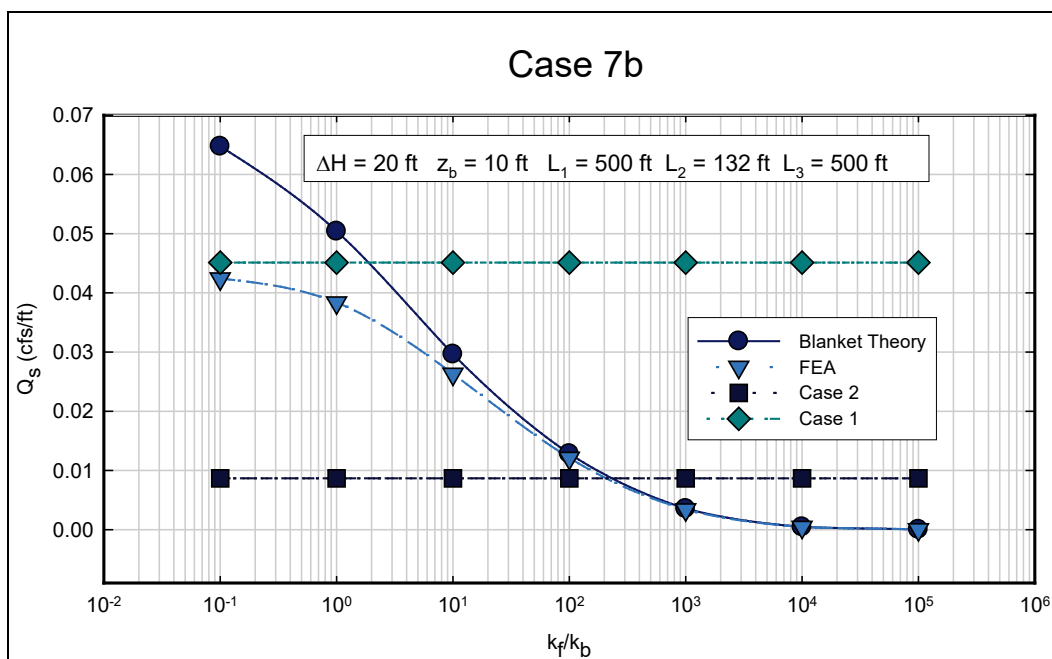


Figure 57 shows the same general analysis but with the thickness of the riverside and landside blanket increased to 20 ft. The agreement between the Blanket Theory and FEA flow values is generally very good for permeability ratios greater than about 100.

Figure 57. Calculated values of flow per unit length (Q_s) for various permeability ratios from Blanket Theory and finite element analysis for Case 7b for $z_b = 20$ ft and $L_1 = 500$ ft and $L_3 = 500$ ft.

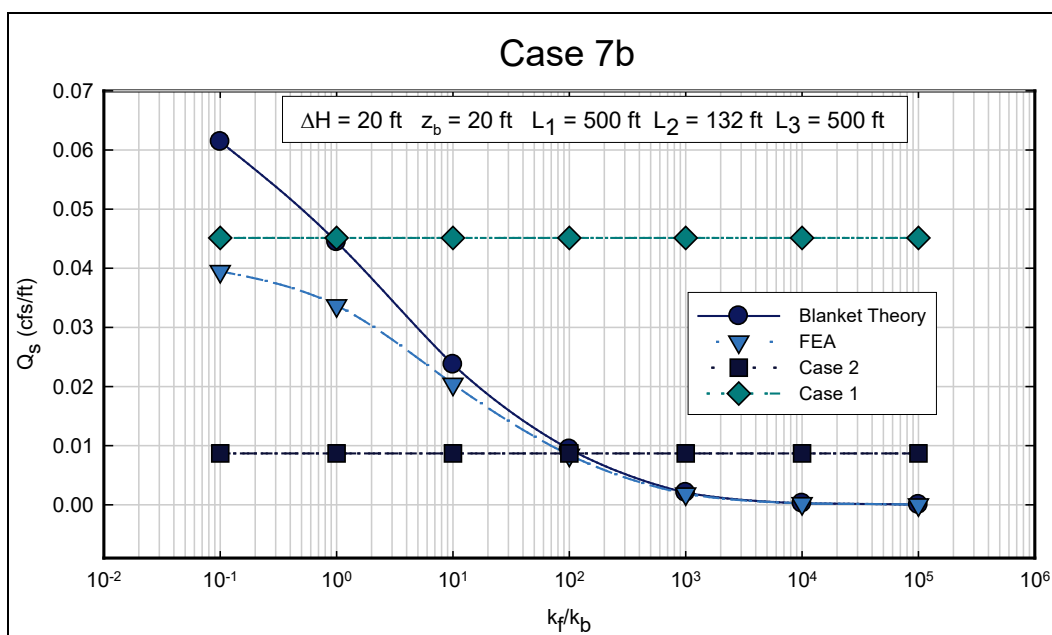


Figure 58 shows the heads beneath the toe of the levee for Blanket Theory and FEA for a blanket thickness of 10 ft. As can be seen, the head values agree very well. Figure 59 shows the results for the same boundary conditions for a blanket thickness of 20 ft. Again, there is generally a good agreement between the pressure heads calculated using Blanket Theory and FEA.

Figure 58. Excess head (h_b) or pressure head beneath blanket at toe for Case 7b calculated using FEA and Blanket Theory for different permeability ratios for $z_b = 10$ ft, $L_1 = 500$ ft, and $L_3 = 500$ ft.

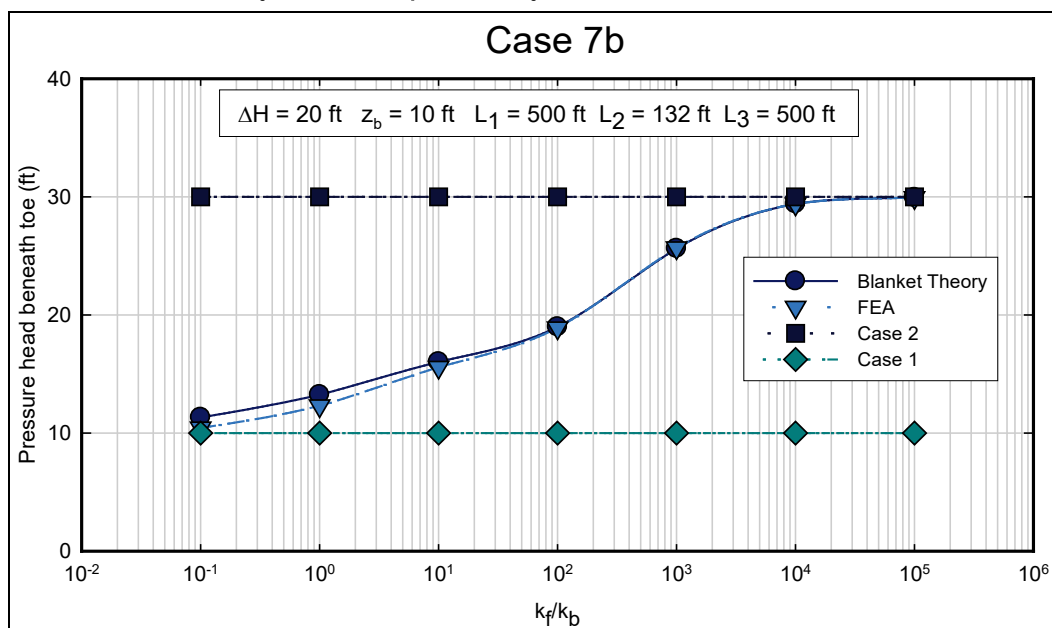
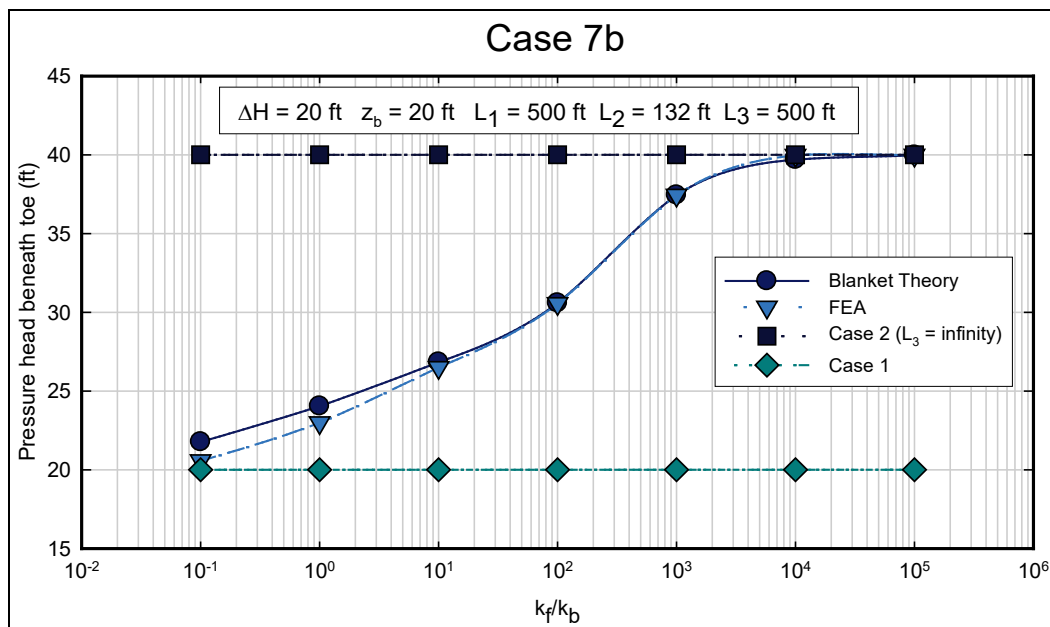


Figure 59. Excess head (h_0) or pressure head beneath blanket at toe for Case 7b calculated using FEA and Blanket Theory for different permeability ratios for $z_b = 20$ ft, $L_1 = 500$ ft, and $L_3 = 500$ ft.



3.8.3 Case 7c – Semi-pervious landside and riverside top stratum (seepage exit in the pervious substratum located landward of the levee)

The geometry and finite element boundary conditions for Case 7c are shown in Figure 60. This case is essentially the same as Case 7a, except that a finite value of L_3 is used. The general boundary conditions are the same for Case 7c as for Case 7a.

For Case 7c, a L_1 value of 500 ft and a L_3 value of 500 ft were used in the analysis. The thickness of the pervious layer (d) was 100 ft, and the thicknesses of the blanket (z_b) were 10 ft and 20 ft. The permeability of the blanket was varied in the analysis, and permeability ratios ranging from 0.1 to 100,000 were used.

Shown in Figure 61 are the volumetric flow rates calculated using Blanket Theory and FEA for the range of permeability ratios. There is excellent agreement between Blanket Theory and FEA for permeability ratios greater than 100, and both methods converge to the Case 2 solution (impervious blanket). The difference between Blanket Theory and FEA increases as the permeability of the blanket becomes closer to the permeability of the pervious layer. The FEA approximately converges to the Case 1 solution, but the Blanket Theory predicts higher flows than the Case 1 solution for permeability ratios less than 2.

Figure 60. Geometry and boundary conditions for Case 7c.

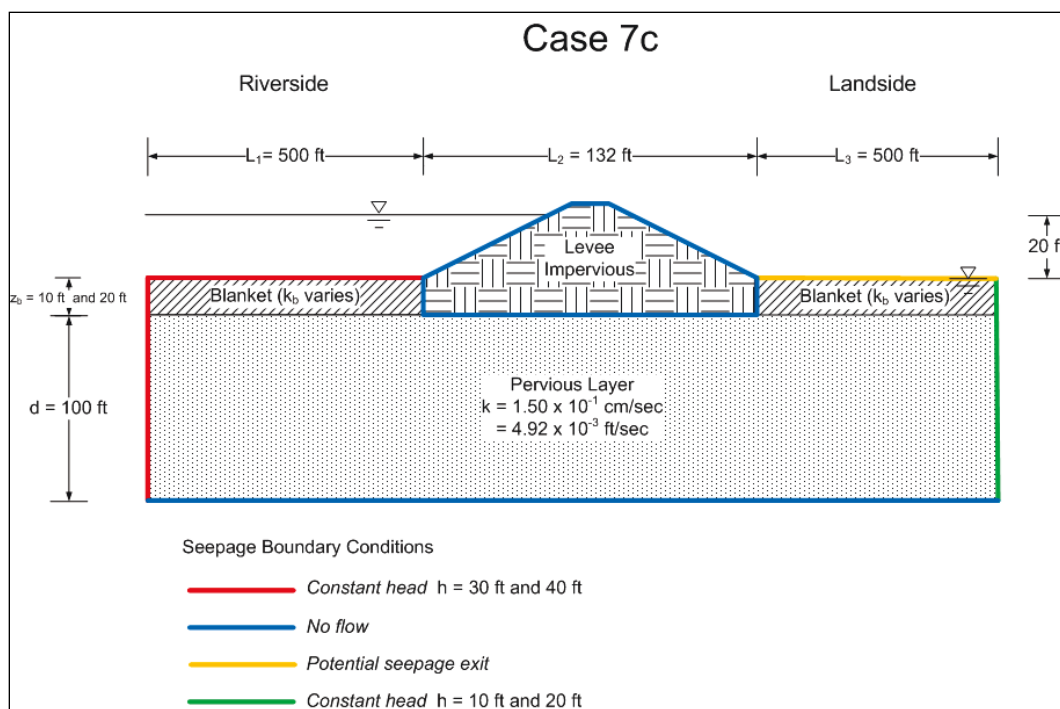
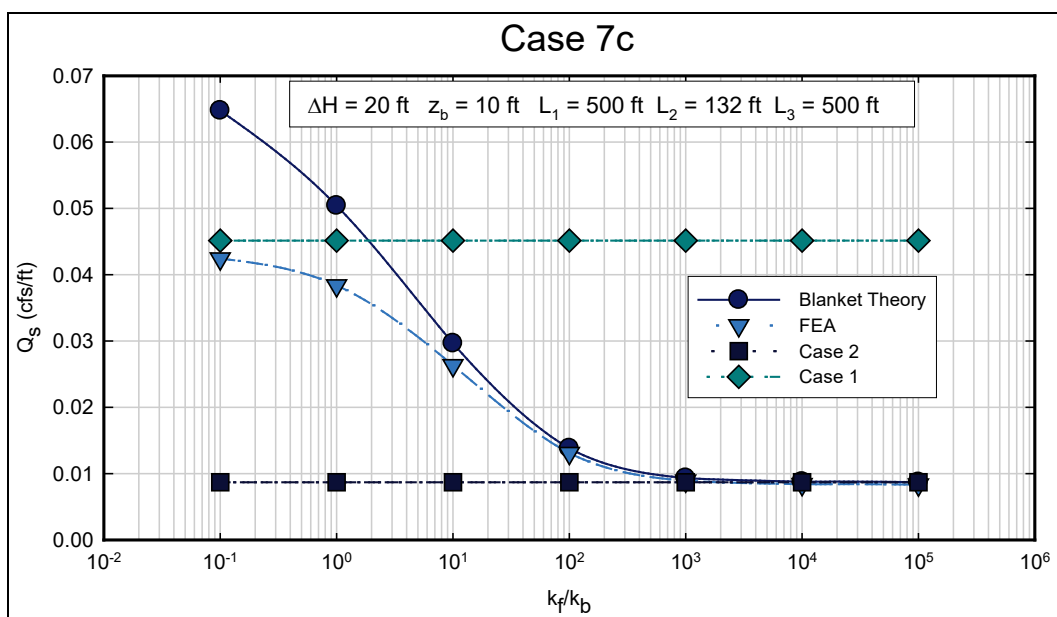
Figure 61. Calculated values of flow per unit length (Q_s) for various permeability ratios from Blanket Theory and finite element analysis for Case 7c for $z_b = 10 \text{ ft}$ and $L_1 = 500 \text{ ft}$ and $L_3 = 500 \text{ ft}$.

Figure 62 shows a plot for the results using the same boundary conditions as the previous analysis, except that the thickness of the semi-pervious blanket was increased to 20 ft. As in previous cases, the Blanket Theory predicts higher flows for low permeability ratios. The value of permeability ratio where the Case 7c and Case 2 analyses are equal is about unity.

Figure 63 shows the pressure head beneath the toe of the levee at the top of the pervious layer for different permeability ratios. Again, the heads calculated with Blanket Theory and FEA are in close agreement for permeability ratios greater than 100, and the difference increases for smaller values of permeability ratio. The exit gradients calculated using Blanket Theory would be generally greater than or equal to those calculated by FEA. Figure 64 shows the results for the same conditions, except the thickness of the blanket is 20 ft. The same general trends are evident.

Figure 62. Calculated values of flow per unit length (Q_s) for various permeability ratios from Blanket Theory and finite element analysis for Case 7c for $z_b = 20$ ft and $L_1 = 500$ ft and $L_3 = 500$ ft.

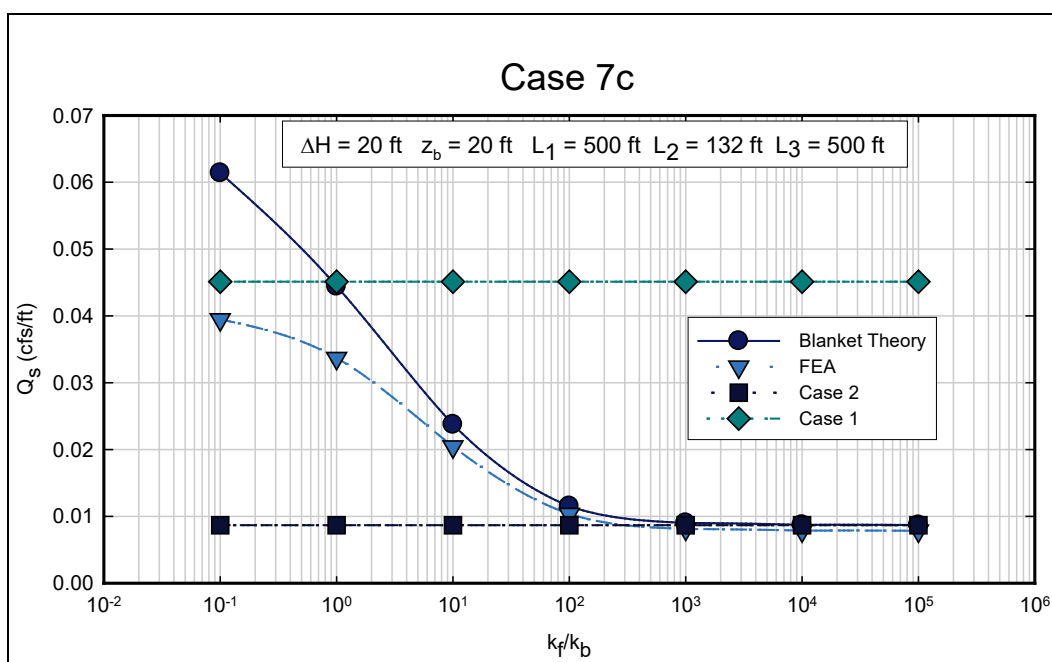


Figure 63. Excess head (h_e) or pressure head beneath blanket at toe for Case 7c calculated using FEA and Blanket Theory for different permeability ratios for $z_b = 10$ ft, $L_1 = 500$ ft, and $L_3 = 500$ ft.

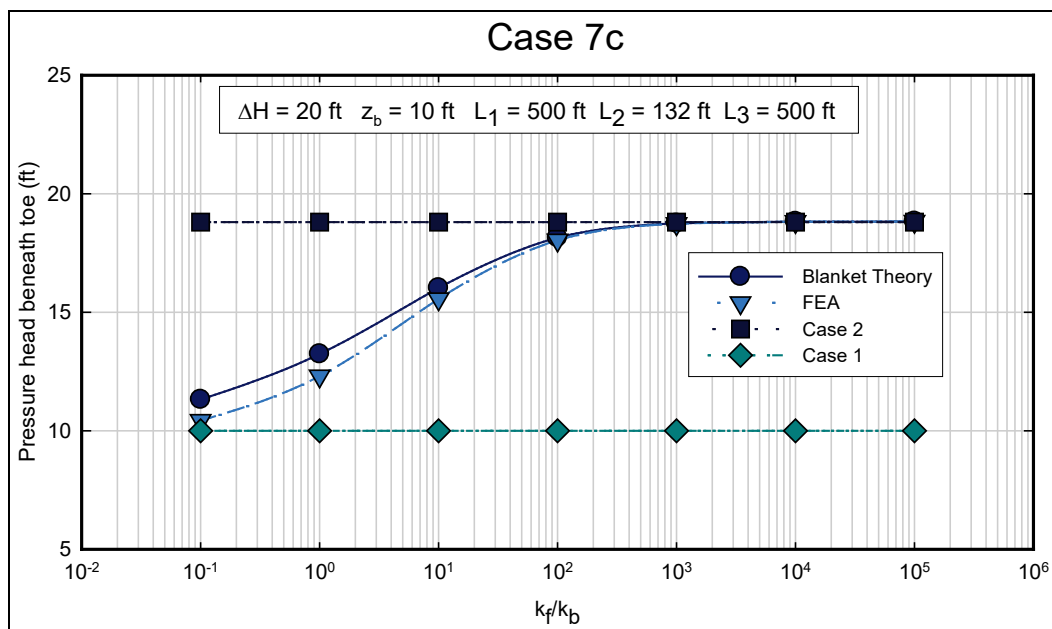


Figure 64. Excess head (h_e) or pressure head beneath blanket at toe for Case 7c calculated using FEA and Blanket Theory for different permeability ratios for $z_b = 20$ ft, $L_1 = 500$ ft, and $L_3 = 500$ ft.

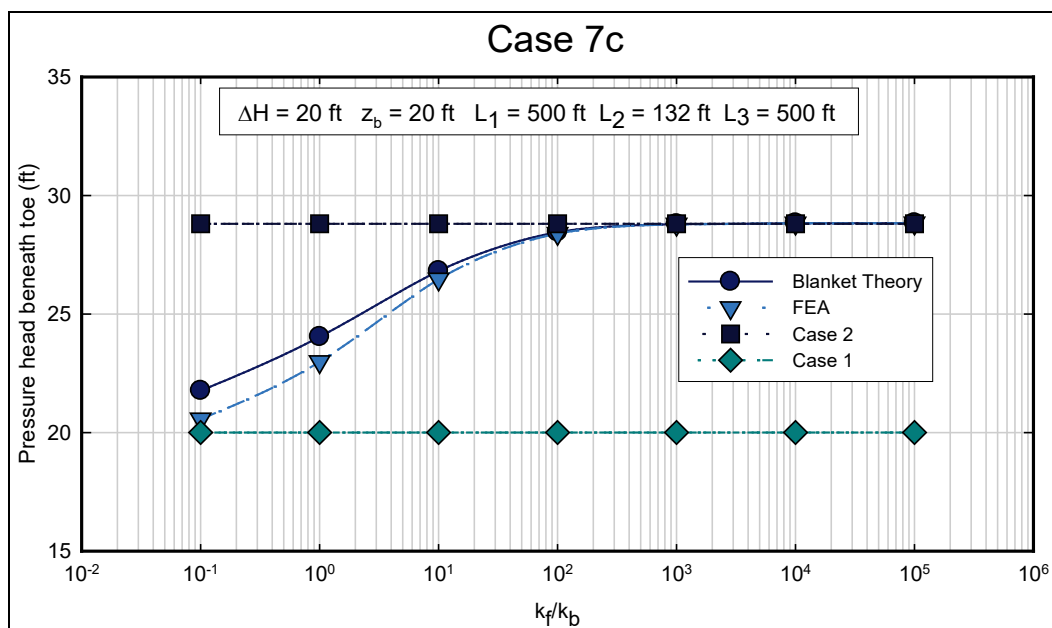


Figure 65 shows the pressure head as a function of horizontal distance at the blanket/pervious layer interface calculated using Blanket Theory and FEA. The agreement between the two methods is excellent underneath the levee and for a distance of about 50 ft from the toe of the levee. At horizontal distances greater than 50 ft from the toe, the solutions diverge. Toward the riverside, Blanket Theory provides higher heads than FEA. Toward the landside, FEA provides higher pressure heads than Blanket Theory.

The agreement between Blanket Theory and FEA is still better with increasing permeability ratio. Shown in Figure 66 are the results for the same boundary condition, except that the semi-pervious blanket is 1,000 times less permeable than the pervious layer. For the range of horizontal distances plotted in the figure, the agreement is exact.

Figure 65. Pressure head at the top of the pervious layer for Case 7c calculated with finite element analysis and Blanket Theory for $z_b = 10$ ft and $k_f/k_b = 10$.

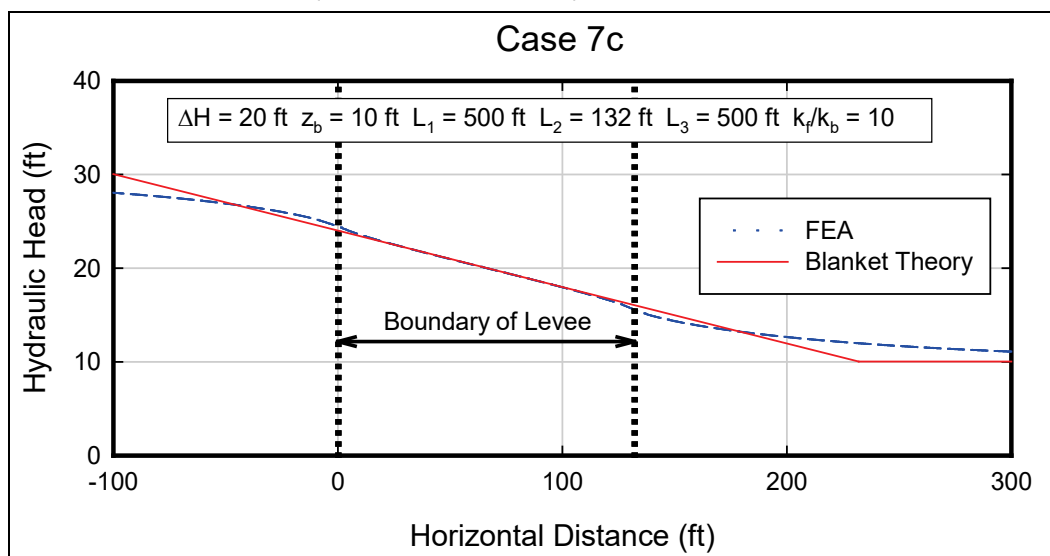
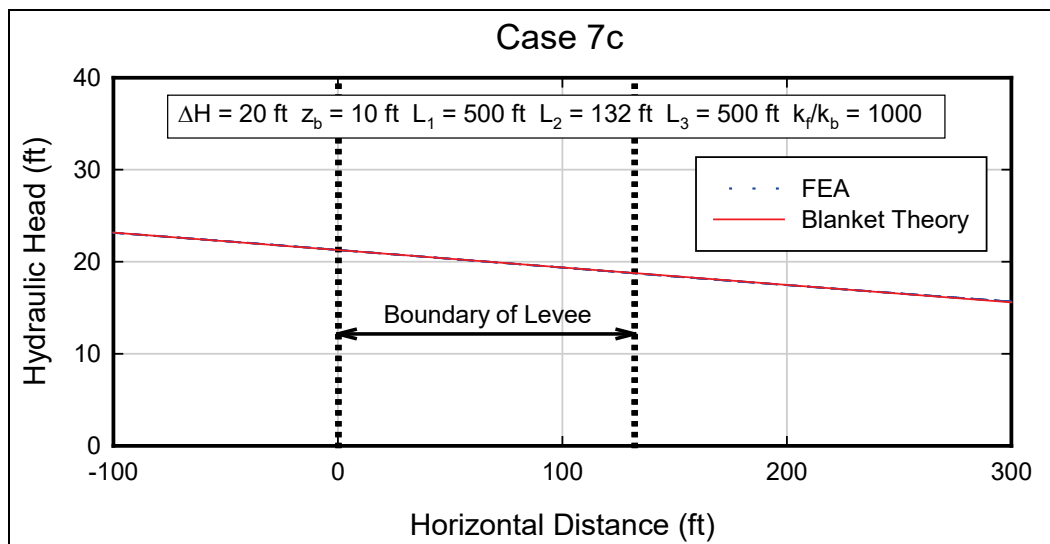


Figure 66. Pressure head at the top of the pervious layer for Case 7c calculated with finite element analysis and Blanket Theory for $z_b = 10$ ft and $k_f/k_b = 1000$.



3.9 Case 8 – Semi-pervious top strata on riverside and landside

Case 8 was developed as part of this study to increase the accuracy of seepage calculations for cases where sheet-pile cutoffs are employed. Case 8 is basically Case 7 with the sheet pile cutoff added. Both have a semi-pervious layer on the riverside and the landside. Similar to Case 7, Case 8 has been subdivided into 8a (infinite landside dimension), 8b (seepage block at L_3), and 8c (finite L_3 dimension). The equations can be developed for different sheet pile penetrations into the pervious layer. The examples presented are for 50 percent penetration.

Because the difference between Cases 8a and Case 8c is the length of L_3 , Case 8a will be omitted from the discussion. Cases 8b and 8c were analyzed with similar geometry. The differences in the analysis are the landside boundary conditions at the edge of the domain. All analyses were conducted with L_1 and L_3 equal to 500 ft. The thickness of the pervious layer (d) was 100 ft, and the thickness of the semi-pervious blanket was 10 ft. The permeability of the blanket was varied in the analysis, and permeability ratios ranging from 0.1 to 10,000 were used.

Comparisons of FEA and Blanket Theory were made based on calculated flows beneath the levee and pressure heads at the landside toe of the levee. A comparison of PGLs for FEA and Blanket Theory was not made for Case 8 because of the non-linearity of the PGL resulting from the inclusion of the cutoff wall.

3.9.1 Case 8b – Semi-pervious landside and riverside top stratum (seepage block in the pervious substratum located landward of the levee) with cutoff wall

Shown in Figure 67 are the geometry and boundary conditions for Case 8b. To model a seepage block, the landslide vertical boundary was assigned no-flow nodal boundary conditions.

Figure 68 shows the calculated flow underneath the levee as a function of permeability ratio. In general, the FEA results in lower flow rates than Blanket Theory, as has been the case for other sections as well. Figure 69 shows the pressure head beneath the landside toe of the levee. There is excellent agreement between FEA and Blanket Theory, and both analysis methods would result in the same hydraulic gradient.

Figure 67. Geometry and boundary conditions for Case 8b.

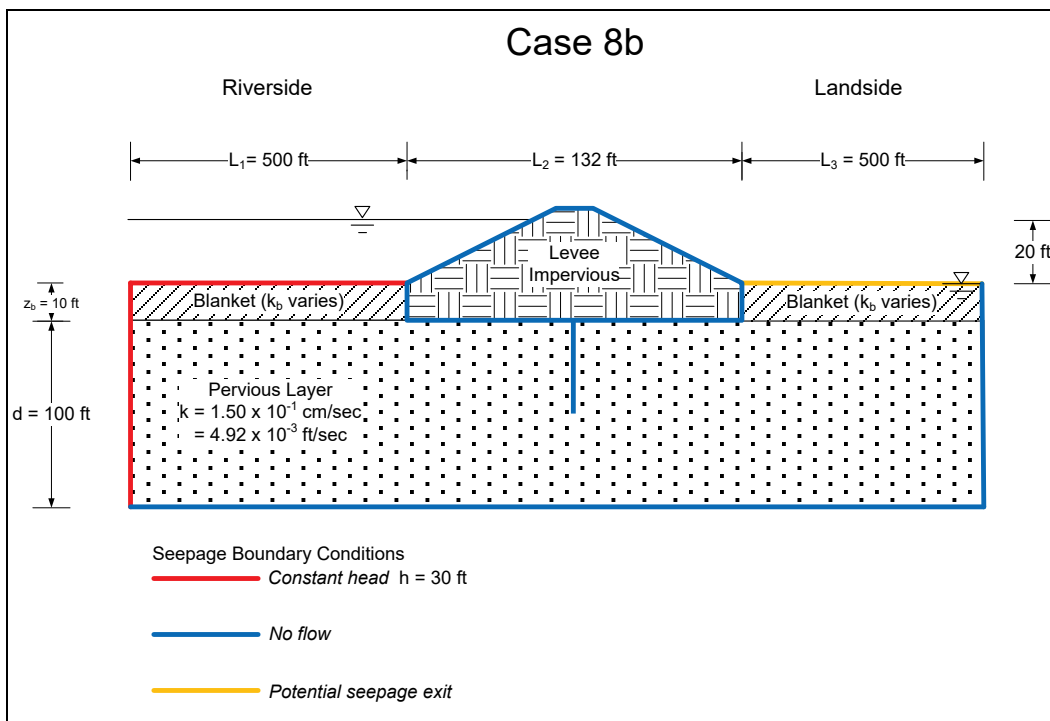


Figure 68. Calculated values of flow per unit length (Q_s) for various permeability ratios from Blanket Theory and finite element analysis for Case 8b for $z_b = 10$ ft and $L_1 = 500$ ft and $L_3 = 500$ ft.

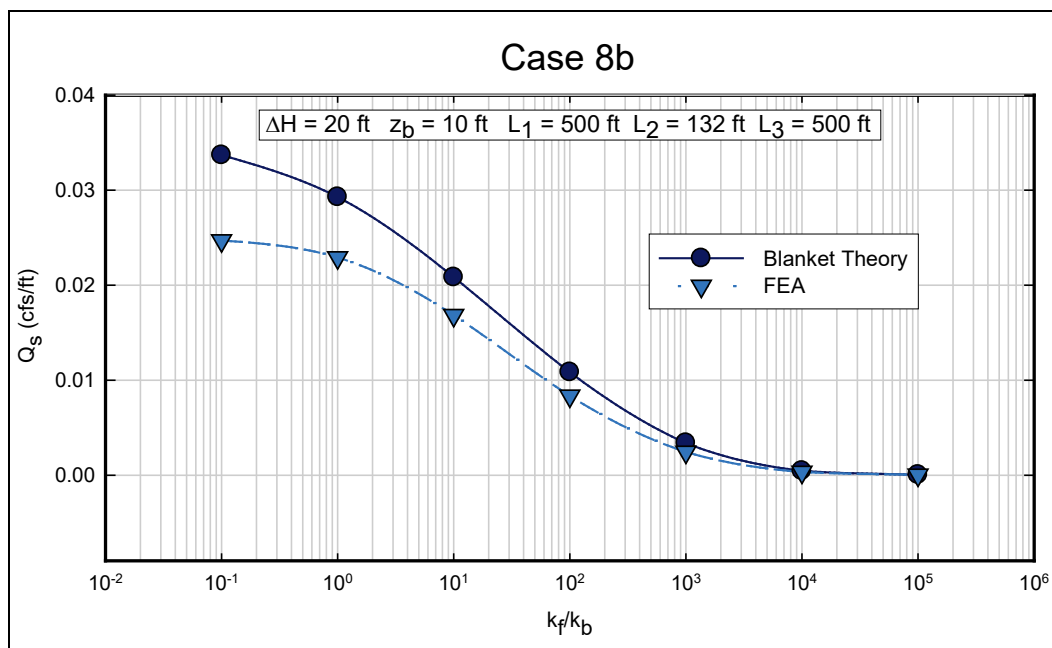
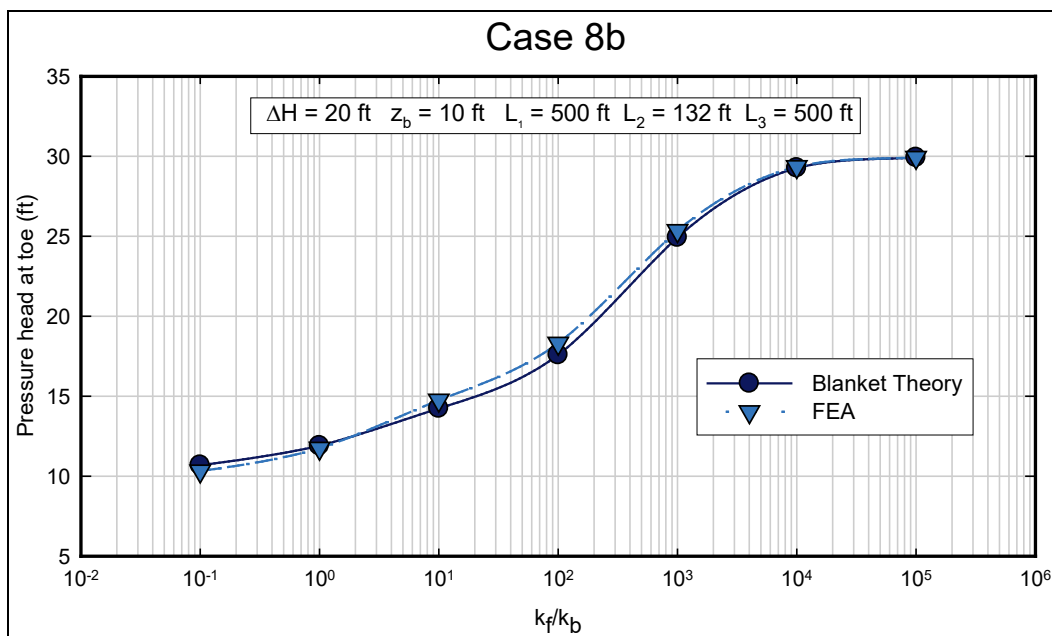


Figure 69. Pressure head beneath blanket at toe for Case 8b calculated using FEA and Blanket Theory for different permeability ratios for $z_b = 10$ ft, $L_1 = 500$ ft, and $L_3 = 500$ ft.



3.9.2 Case 8c – Semi-pervious landside and riverside top stratum (seepage exit in the pervious substratum located landward of the levee) with cutoff wall

The geometry and boundary conditions for Case 8c are shown in Figure 70. The boundary conditions are the same as for Case 7c, except that no-flow boundary conditions are assigned to the cutoff wall.

Figure 70. Geometry and boundary conditions for Case 8c.

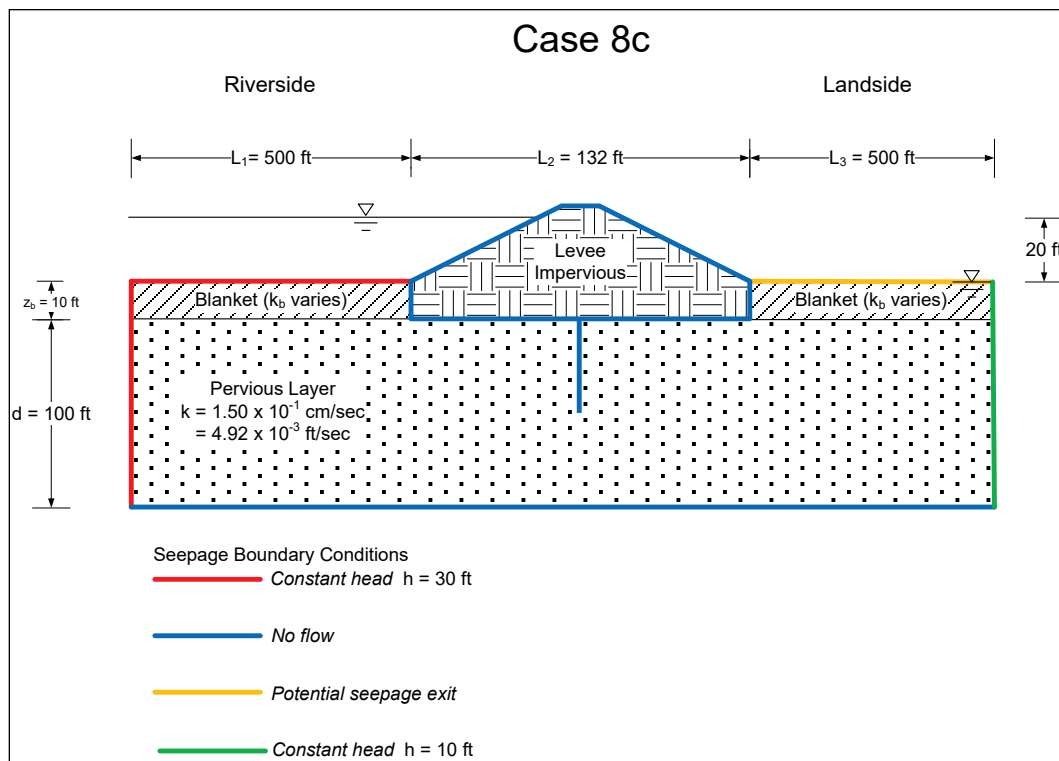


Figure 71 shows flow underneath the levee calculated by FEA and Blanket Theory. The FEA predicts less flow than Blanket Theory for every permeability ratio. This may possibly be due to the manner in which SLIDE calculates flow as being the flow perpendicular to a flux boundary. The agreement between Blanket Theory and pressure head beneath the landside toe of the levee was better (Figure 72).

The new Blanket Theory Case 8 shows good agreement with results of FEA and indicates the versatility of Blanket Theory in accommodating sheet-pile cutoffs. However, the Blanket Theory equations should not be generalized, as the effect of penetration depth of the sheet pile cutoff on discharge and excess head has not been investigated.

Figure 71. Calculated values of flow per unit length (Q_s) for various permeability ratios from Blanket Theory and finite element analysis for Case 8c for $z_b = 10$ ft and $L_1 = 500$ ft and $L_3 = 500$ ft.

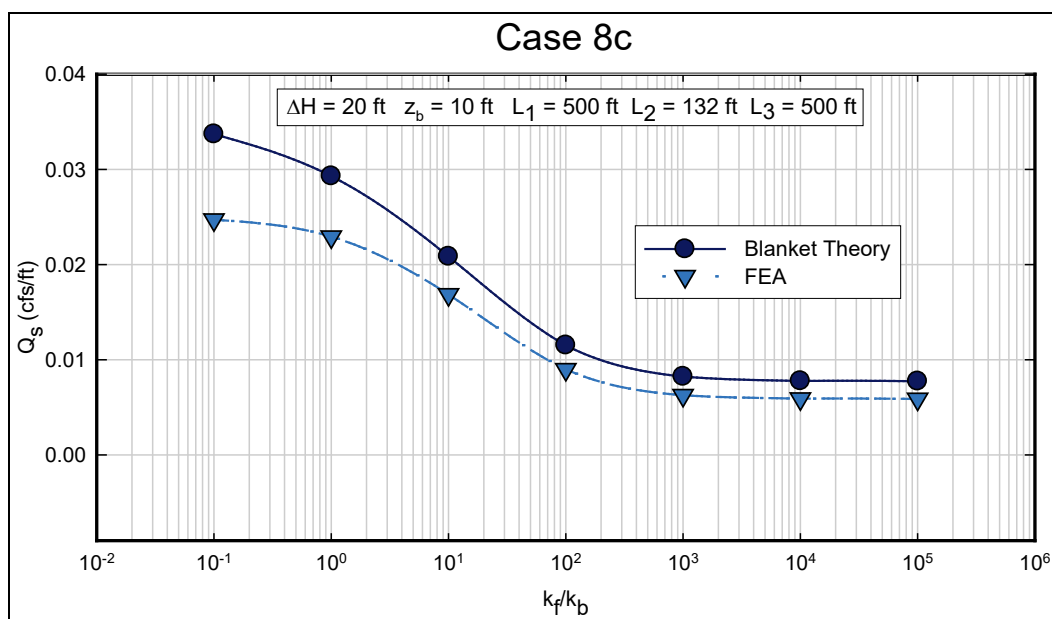
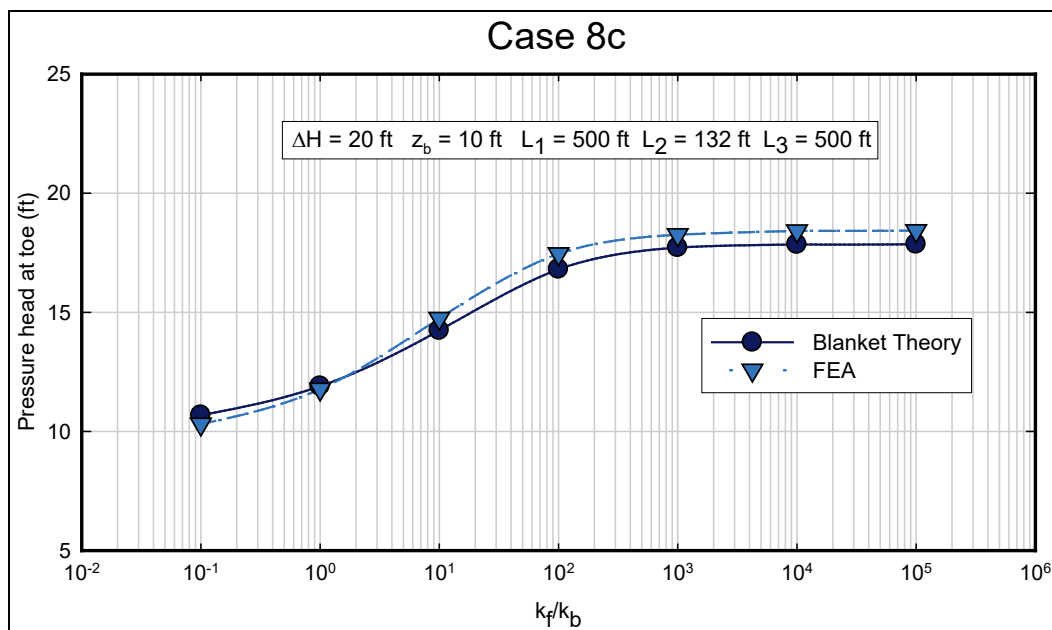


Figure 72. Pressure head beneath blanket at toe for Case 8c calculated using FEA and Blanket Theory for different permeability ratios for $z_b = 10$ ft, $L_1 = 500$ ft, and $L_3 = 500$ ft.



4 Comparison of SLIDE with SEEP/W

A comparison of the results from the finite element programs SLIDE and SEEP/W was made for all cases. For cases with finite boundaries (L_1 and L_3 dimensions), SLIDE and SEEP/W provided equivalent results. As an example, shown in Figures 73 and 74 are the results from Case 7c for the flow underneath the levee and the pressure head at the toe of the levee. There is a slight difference in the reported values of flow for the two programs due to the way that flow is reported by SLIDE and SEEP/W. For SLIDE, flow is reported as the flow perpendicular to a line drawn from the horizontal midpoint of the levee down to the bottom of the pervious layer. For SEEP/W, the total flow across the same interface is reported. The difference in flow is the greatest for cases where the blanket has a relatively high permeability, because the flow lines would not be completely horizontal, and some flow may be occurring at an angle to the interface. This would cause SLIDE to report a smaller flow than SEEP/W. For cases where the permeability of the blanket is low, the flow lines are virtually horizontal, and both programs report the same flow. The values of the pressure head at the toe of the levee (Figure 74) are the same.

Figure 73. Calculated flows for SLIDE and SEEP/W for Case 7c.

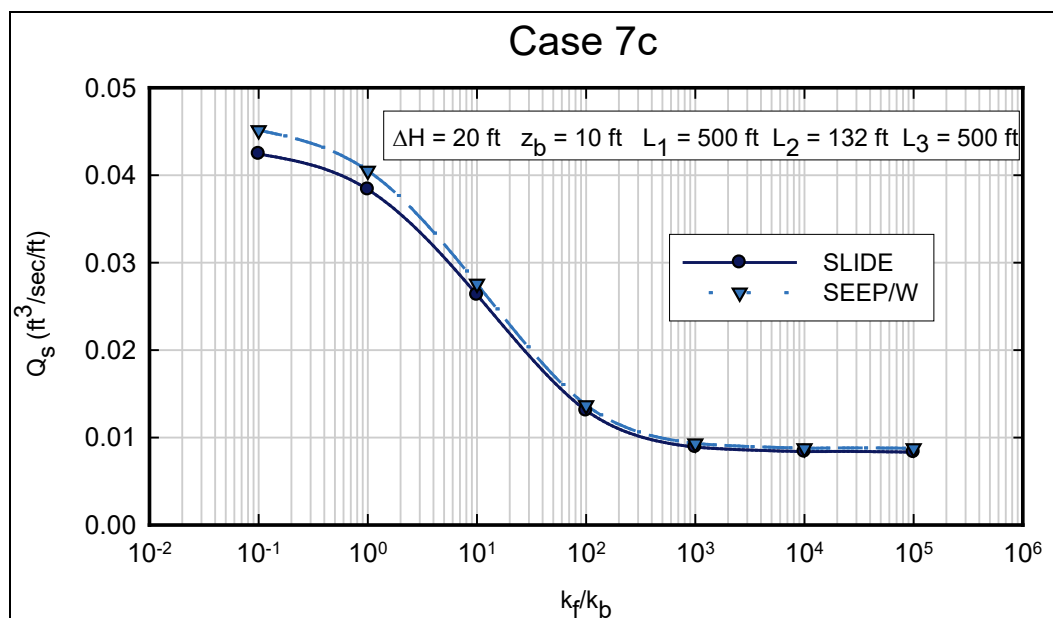
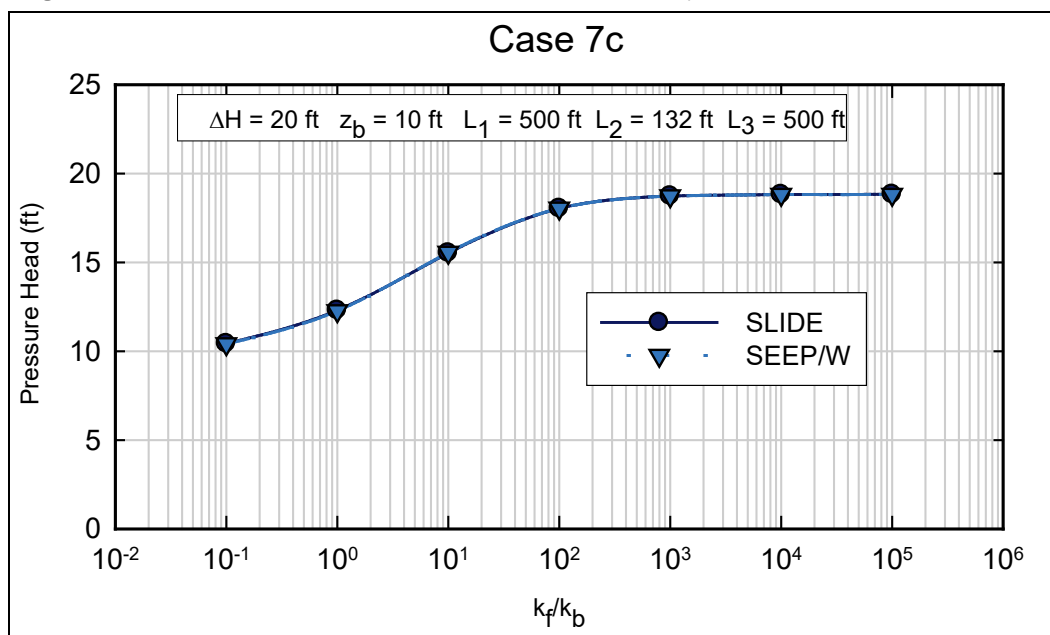


Figure 74. Pressure head at the toe of the levee calculated by SLIDE and SEEP/W for Case 7c.

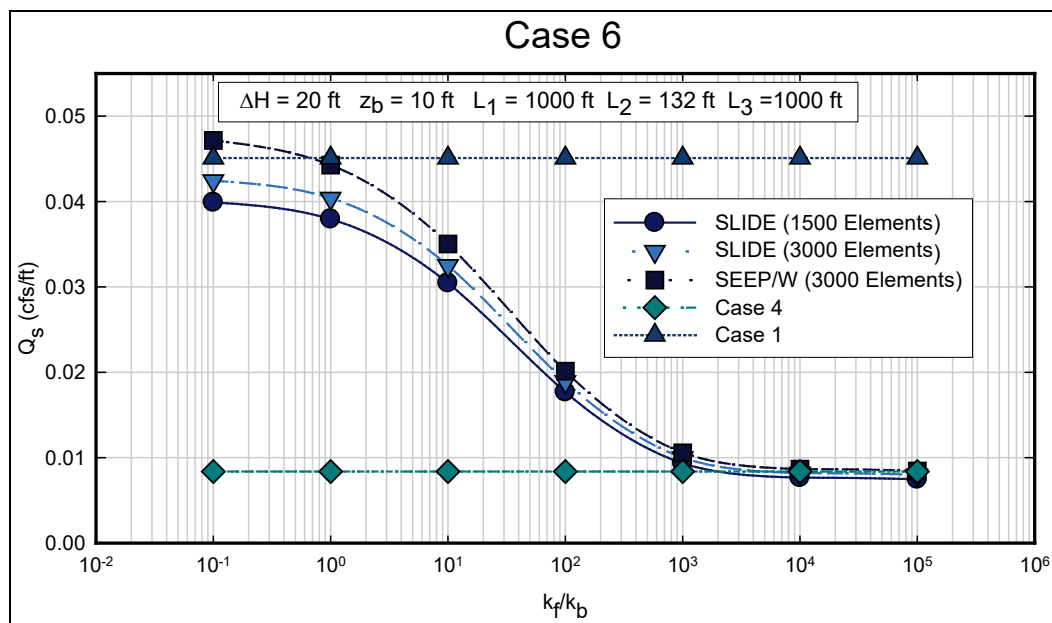


SEEP/W has a special boundary condition that allows an infinite horizontal distance to be simulated using a decay function. This boundary condition was used in SEEP/W analyses for Cases 1, 3, 4, 5, 6, and 7a. Reasonable results were obtained for cases where only one material and boundary condition were present at the vertical boundary (Cases 1, 3, 4, 5, and 6). Use of this boundary condition did not provide reasonable results for Case 7a.

5 Issues with Numbers of Elements

Both SLIDE and SEEP/W often produce poor results when less than 1,500 elements are used in the analysis. This may be due to the fact that the domain is relatively shallow compared to the length. Shown in Figure 75 is an example from the Case 6 analyses that shows the difference in the flow calculated by SLIDE and SEEP/W. For SLIDE, the flow increases with increasing number of elements. A sensitivity study was not conducted for SEEP/W.

Figure 75. Calculated flows for Case 6 showing the effect of number of elements.



This sensitivity to the number of elements for SLIDE seems to be only for the calculated flow values. The head values were essentially the same for 1,500 and 3,000 elements.

Both programs have a default number of elements of about 1,500. It may be prudent for the user to increase the number to about 3,000. The larger mesh only requires marginally greater computation time, and there does not seem to be any other distinct disadvantages to using a larger number of elements.

6 General Guidelines for Finite Element Analysis

Based on the results presented in the previous section, it seems that finite element seepage analysis can be conducted using the same boundary conditions used for Blanket Theory, and virtually identical results will be obtained for identical conditions. The finite element method has the additional advantage that geometry more complex than that assumed in Blanket Theory can be easily accommodated.

This section will provide guidance for setting boundary conditions for finite element seepage analysis for the separate seepage cases as defined in USACE (2000). In addition, suggestions for boundary conditions for modeling other cases, such as outfall canals, are given.

7 Boundary Conditions for Blanket Theory Cases

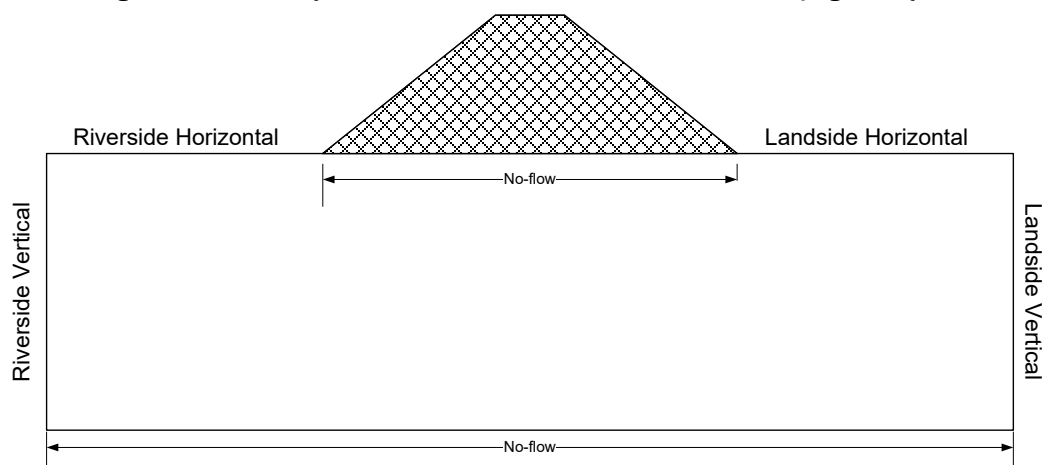
The type of boundary conditions needed, as defined in SLIDE, SEEP/W, Groundwater Modeling System (GMS), and other FEA programs are as follows:

- Constant head boundary with head set to riverside maximum water elevation
- Constant head boundary with head set to landside ground surface elevation
- No-flow ($q = 0$) boundary condition
- Potential seepage face or “unknown” boundary condition

Because the levee is considered to be impermeable in Blanket Theory, the levee does not need to be included in the finite element mesh, and the nodes at the base of the levee are assigned as a no-flow boundary condition. The nodes at the base of the domain (mesh) are also set as a no-flow boundary condition.

For each of the eight seepage cases presented in the previous section, the boundary conditions will be specified for the riverside horizontal and vertical surfaces and the landside horizontal and vertical surfaces as shown in Figure 76 below. The dimensions as defined in Blanket Theory (L_1 , L_2 , and L_3) should be the same in the finite element model as would be used in Blanket Theory.

Figure 76. Boundary conditions to be set for finite element seepage analysis.



Case 1 – No top stratum

Riverside horizontal	Constant head with head assigned to riverside water elevation
Riverside vertical	Constant head with head assigned to riverside water elevation
Landside horizontal	Constant head with head assigned to landside ground elevation
Landside vertical	Constant head with head assigned to landside ground elevation

Case 2 – Impervious top stratum both riverside and landside

Riverside horizontal	No-flow
Riverside vertical	Constant head with head assigned to riverside water elevation
Landside horizontal	No-flow
Landside vertical	Constant head with head assigned to landside ground elevation

Case 3 – Impervious riverside top stratum and no landside top stratum

Riverside horizontal	No-flow
Riverside vertical	Constant head with head assigned to riverside water elevation
Landside horizontal	Constant head with head assigned to landside ground elevation
Landside vertical	Constant head with head assigned to landside ground elevation

Case 4 – Impervious landside top stratum and no riverside top stratum

Riverside horizontal	Constant head with head assigned to riverside water elevation
Riverside vertical	Constant head with head assigned to riverside water elevation
Landside horizontal	No-flow
Landside vertical	Constant head with head assigned to landside ground elevation

Case 5 – Semi-pervious riverside top stratum and no landside top stratum

Riverside horizontal	Constant head with head assigned to riverside water elevation
Riverside vertical	Constant head with head assigned to riverside water elevation
Landside horizontal	Constant head with head assigned to landside ground elevation
Landside vertical	Constant head with head assigned to landside ground elevation

Case 6 – Semi-pervious landside top stratum and no riverside top stratum

Riverside horizontal	Constant head with head assigned to riverside water elevation
Riverside vertical	Constant head with head assigned to riverside water elevation
Landside horizontal	Potential seepage face
Landside vertical	Constant head with head assigned to landside ground elevation

Case 7a – Semi-pervious landside top strata both riverside and landside with $L_3 = \infty$

Riverside horizontal	Constant head with head assigned to riverside water elevation
Riverside vertical	Constant head with head assigned to riverside water elevation
Landside horizontal	Potential seepage face
Landside vertical	Constant head with head assigned to landside ground elevation

Note: When L_3 is infinite, then the landside vertical boundary should be sufficiently far from the levee such that an infinite landside blanket is simulated in the finite element seepage analysis. Results presented in the previous section indicate that a landside vertical boundary of greater than 500 ft from the levee toe gives an approximate infinite landside blanket condition in the finite element seepage analysis, if no blanket is present. If a blanket is present, then a value of about 3,000 ft should be used. Ideally, this dimension could logically be expressed as a factor of d or L_2 , and that will be investigated in subsequent phases of this research. In addition, SEEP/W has an “infinite” region that possibly can be used for the landside vertical boundary, but the authors did not have success in using it on this project.

Case 7b – Semi-pervious landside top strata both riverside and landside with L_3 finite to a seepage block.

Riverside horizontal	Constant head with head assigned to riverside water elevation
Riverside vertical	Constant head with head assigned to riverside water elevation
Landside horizontal	Potential seepage face
Landside vertical	No-flow

Case 7c – Semi-pervious landside top strata both riverside and landside with L_3 finite to an open seepage exit.

Riverside horizontal	Constant head with head assigned to riverside water elevation
Riverside vertical	Constant head with head assigned to riverside water elevation
Landside horizontal	Potential seepage face
Landside vertical	Constant head with head assigned to landside ground elevation

The results presented in the previous section indicate that the transition between semi-pervious and impervious blanket behavior occurs at a ratio of pervious layer permeability to blanket permeability between 1,000 and 4,000. At permeability ratios in the range of these values, the semi-pervious solutions (Cases 5, 6, and 7) produce essentially the same values of heads and flows as the impervious solutions, and the results of Blanket Theory agree closely with FEA.

Similarly, the transformation from a fully pervious to a semi-pervious blanket occurs at a ratio of pervious layer permeability to blanket permeability of about 2. In other words, the use of the semi-pervious equations will produce a more accurate determination of the flow and the excess head for permeability ratios equal to or greater than 2 as compared to solutions considering the blanket as fully pervious (non-existent). For

permeability ratios less than 2, the presence of the blanket may be ignored, and the solutions for cases having no blanket will generally provide more accurate results than the solutions for the semi-pervious cases.

Case 8 was added in this study to extend the conventional Blanket Theory analyses to cross sections that contain a partially penetrating sheet-pile cutoff. The boundary conditions for FEA of Case 8 solutions is essentially the same as for Case 7, except that no-flow boundary conditions are assigned to the nodes at the exterior of the sheet pile, or the sheet pile can be modeled as an impervious material (i.e., no material type in SEEP/W).

8 Layered Top Strata

Blanket Theory transforms the top strata into one layer of uniform thickness and permeability. The comparison of the Blanket Theory with the finite element analyses presented in this report is also for the transformed parameters. However, it is useful to study the effect of this transformation on seepage under the structure and heads at the toe of the levee. Therefore, as a next step, a two-layered top stratum is modeled in FEA and output parameters are compared with Blanket Theory solutions, which will consider the transformed thickness and permeability.

The analyses are conducted for the thickness of top stratum as 20 ft. However, the top stratum is further divided into two layers as shown in Figure 77, where k_1 and z_1 are the permeability and thickness of the top layer, respectively, while k_2 and z_2 are the permeability and thickness of the bottom layer of the blanket, respectively. The method shown in USACE (2000) was used to transform the top stratum to a single layer of uniform thickness and permeability. Note that this transformation is only used in the Blanket Theory calculations of seepage pressures and seepage flow. Different transformation is used when computing uplift gradients and factors of safety for underseepage. The transformed permeability (k_b) of the layer is determined as the vertical permeability of the least pervious layer in the top stratum. The transformed thickness of the layer (z_b) is determined by the following equation:

$$z_b = z_1 \frac{k_b}{k_1} + z_2 \frac{k_b}{k_2} \quad (139)$$

Figure 77. General configuration of top strata used in the analyses.

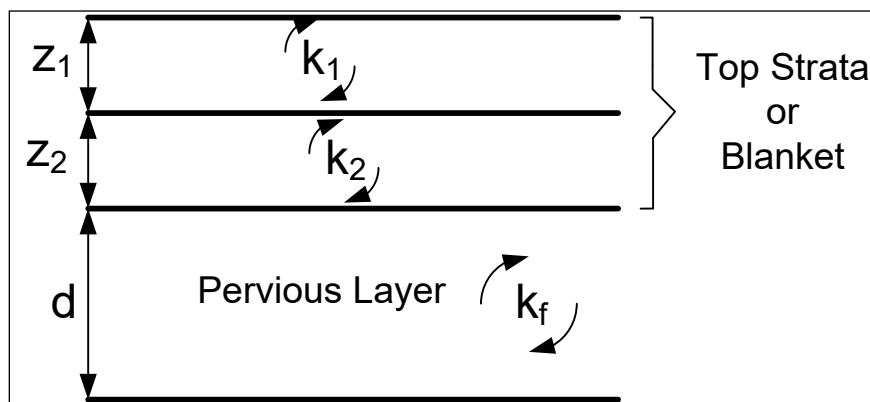


Table 1 summarizes the permeabilities of different combinations used in the analyses of layered top strata having two layers of equal thicknesses of 10 ft. Combinations 1 to 6 have the permeability of bottom layer as 4.92×10^{-5} ft/sec, while the permeability of the top layer is varied from 4.92×10^{-3} ft/sec to 4.92×10^{-8} ft/sec. Similarly, the order of permeabilities is reversed for combinations 7 to 12 with top layer having the permeability as 4.92×10^{-5} ft/sec and permeability is varied for the bottom layer. Combinations 13 to 17 have the permeability of the bottom layer fixed at a very low value of 4.92×10^{-8} ft/sec, and the permeability is varied from 4.92×10^{-4} ft/sec to 4.92×10^{-8} ft/sec for the top layer. Combinations 18 to 22 indicate the permeability of the bottom layer fixed at the value of 4.92×10^{-4} ft/sec (one order of magnitude lower than the pervious layer), and the permeability is again varied from 4.92×10^{-4} ft/sec to 4.92×10^{-8} ft/sec for the top layer. Similarly, Tables 2 and 3 indicate the same information for different thicknesses of two layers comprising the top strata. Table 2 is for the thicknesses of both the top and bottom layers of the blanket as 5 and 15 ft, respectively. The thicknesses of the blanket layers are reversed in Table 3. The combinations are repeated if the permeability of the top layer is same as the permeability of the bottom layer, although the layer thicknesses may be different and are shown just for completeness.

The boundary conditions and other hydraulic properties are considered the same as explained earlier in the discussion. The analysis is conducted for Case 6, which has top stratum on landward side and no riverside top stratum. The permeability of the pervious layer (k_f) was assigned a value of 4.92×10^{-3} ft/sec (0.15 cm/sec), which is the same value used in the previous analyses. The value of both L_1 and L_3 is 1,000 ft, and the net head (H) on the levee is 20 ft for the analysis. Similarly, thickness of the pervious layer (d) is 100 ft. The finite element analyses were conducted in the similar manner as before for all the cases shown in Tables 1, 2, and 3. The Blanket Theory solutions were also computed, and the transformed thicknesses and permeabilities used in the analyses are listed in Tables 1, 2, and 3. The volumetric flow rates per unit of levee length (Q_s) and excess hydraulic head (h_o) under the toe of the levee were compared from both the analyses.

Table 1. Summary of parameters for combinations 1 to 22 used in the analyses of top strata having $z_1 = z_2 = 10$ ft.

Case no.	Permeability		Thickness		Case no.	Permeability		Thickness	
	Original	Transformed	Original	Transformed		Original	Transformed	Original	Transformed
	(ft/sec)	k_b (ft/sec)	(ft)	z_b (ft)		(ft/sec)	k_b (ft/sec)	(ft)	z_b (ft)
1	$k_1 = 4.92 \times 10^{-3}$	4.92×10^{-5}	$z_1 = 10$	10.1	12	$k_1 = 4.92 \times 10^{-5}$	4.92×10^{-8}	$z_1 = 10$	10.01
	$k_2 = 4.92 \times 10^{-5}$		$z_2 = 10$			$k_2 = 4.92 \times 10^{-8}$		$z_2 = 10$	
2	$k_1 = 4.92 \times 10^{-4}$	4.92×10^{-5}	$z_1 = 10$	11	13	$k_1 = 4.92 \times 10^{-4}$	4.92×10^{-8}	$z_1 = 10$	10.001
	$k_2 = 4.92 \times 10^{-5}$		$z_2 = 10$			$k_2 = 4.92 \times 10^{-8}$		$z_2 = 10$	
3	$k_1 = 4.92 \times 10^{-5}$	4.92×10^{-5}	$z_1 = 10$	20	14	$k_1 = 4.92 \times 10^{-5}$	4.92×10^{-8}	$z_1 = 10$	10.01
	$k_2 = 4.92 \times 10^{-5}$		$z_2 = 10$			$k_2 = 4.92 \times 10^{-8}$		$z_2 = 10$	
4	$k_1 = 4.92 \times 10^{-6}$	4.92×10^{-6}	$z_1 = 10$	11	15	$k_1 = 4.92 \times 10^{-6}$	4.92×10^{-8}	$z_1 = 10$	10.1
	$k_2 = 4.92 \times 10^{-5}$		$z_2 = 10$			$k_2 = 4.92 \times 10^{-8}$		$z_2 = 10$	
5	$k_1 = 4.92 \times 10^{-7}$	4.92×10^{-7}	$z_1 = 10$	10.1	16	$k_1 = 4.92 \times 10^{-7}$	4.92×10^{-8}	$z_1 = 10$	11
	$k_2 = 4.92 \times 10^{-5}$		$z_2 = 10$			$k_2 = 4.92 \times 10^{-8}$		$z_2 = 10$	
6	$k_1 = 4.92 \times 10^{-8}$	4.92×10^{-8}	$z_1 = 10$	10.01	17	$k_1 = 4.92 \times 10^{-8}$	4.92×10^{-8}	$z_1 = 10$	20
	$k_2 = 4.92 \times 10^{-5}$		$z_2 = 10$			$k_2 = 4.92 \times 10^{-8}$		$z_2 = 10$	
7	$k_1 = 4.92 \times 10^{-5}$	4.92×10^{-5}	$z_1 = 10$	10.1	18	$k_1 = 4.92 \times 10^{-4}$	4.92×10^{-4}	$z_1 = 10$	20
	$k_2 = 4.92 \times 10^{-3}$		$z_2 = 10$			$k_2 = 4.92 \times 10^{-4}$		$z_2 = 10$	
8	$k_1 = 4.92 \times 10^{-5}$	4.92×10^{-5}	$z_1 = 10$	11	19	$k_1 = 4.92 \times 10^{-5}$	4.92×10^{-5}	$z_1 = 10$	11
	$k_2 = 4.92 \times 10^{-4}$		$z_2 = 10$			$k_2 = 4.92 \times 10^{-4}$		$z_2 = 10$	
9	$k_1 = 4.92 \times 10^{-5}$	4.92×10^{-5}	$z_1 = 10$	20	20	$k_1 = 4.92 \times 10^{-6}$	4.92×10^{-6}	$z_1 = 10$	10.1
	$k_2 = 4.92 \times 10^{-5}$		$z_2 = 10$			$k_2 = 4.92 \times 10^{-4}$		$z_2 = 10$	
10	$k_1 = 4.92 \times 10^{-5}$	4.92×10^{-6}	$z_1 = 10$	11	21	$k_1 = 4.92 \times 10^{-7}$	4.92×10^{-7}	$z_1 = 10$	10.01
	$k_2 = 4.92 \times 10^{-6}$		$z_2 = 10$			$k_2 = 4.92 \times 10^{-4}$		$z_2 = 10$	
11	$k_1 = 4.92 \times 10^{-5}$	4.92×10^{-7}	$z_1 = 10$	10.1	22	$k_1 = 4.92 \times 10^{-8}$	4.92×10^{-8}	$z_1 = 10$	10.001
	$k_2 = 4.92 \times 10^{-7}$		$z_2 = 10$			$k_2 = 4.92 \times 10^{-4}$		$z_2 = 10$	

Table 2. Summary of parameters for combinations 23 to 44 used in the analyses of top strata having $z_1 = 5$ ft and $z_2 = 15$ ft.

Case no.	Permeability		Thickness		Case no.	Permeability		Thickness	
	Original (ft/sec)	Transformed k_b (ft/sec)	Original (ft)	Transformed z_b (ft)		Original (ft/sec)	Transformed k_b (ft/sec)	Original (ft)	Transformed z_b (ft)
23	$k_1 = 4.92 \times 10^{-3}$	4.92×10^{-5}	$z_1 = 5$	15.05	34	$k_1 = 4.92 \times 10^{-5}$	4.92×10^{-8}	$z_1 = 5$	15.005
	$k_2 = 4.92 \times 10^{-5}$		$z_2 = 15$			$k_2 = 4.92 \times 10^{-8}$		$z_2 = 15$	
24	$k_1 = 4.92 \times 10^{-4}$	4.92×10^{-5}	$z_1 = 5$	15.5	35	$k_1 = 4.92 \times 10^{-4}$	4.92×10^{-8}	$z_1 = 5$	15.0005
	$k_2 = 4.92 \times 10^{-5}$		$z_2 = 15$			$k_2 = 4.92 \times 10^{-8}$		$z_2 = 15$	
25	$k_1 = 4.92 \times 10^{-5}$	4.92×10^{-5}	$z_1 = 5$	20	36	$k_1 = 4.92 \times 10^{-5}$	4.92×10^{-8}	$z_1 = 5$	15.005
	$k_2 = 4.92 \times 10^{-5}$		$z_2 = 15$			$k_2 = 4.92 \times 10^{-8}$		$z_2 = 15$	
26	$k_1 = 4.92 \times 10^{-6}$	4.92×10^{-6}	$z_1 = 5$	6.5	37	$k_1 = 4.92 \times 10^{-6}$	4.92×10^{-8}	$z_1 = 5$	15.05
	$k_2 = 4.92 \times 10^{-5}$		$z_2 = 15$			$k_2 = 4.92 \times 10^{-8}$		$z_2 = 15$	
27	$k_1 = 4.92 \times 10^{-7}$	4.92×10^{-7}	$z_1 = 5$	5.15	38	$k_1 = 4.92 \times 10^{-7}$	4.92×10^{-8}	$z_1 = 5$	15.5
	$k_2 = 4.92 \times 10^{-5}$		$z_2 = 15$			$k_2 = 4.92 \times 10^{-8}$		$z_2 = 15$	
28	$k_1 = 4.92 \times 10^{-8}$	4.92×10^{-8}	$z_1 = 5$	5.015	39	$k_1 = 4.92 \times 10^{-8}$	4.92×10^{-8}	$z_1 = 5$	20
	$k_2 = 4.92 \times 10^{-5}$		$z_2 = 15$			$k_2 = 4.92 \times 10^{-8}$		$z_2 = 15$	
29	$k_1 = 4.92 \times 10^{-5}$	4.92×10^{-5}	$z_1 = 5$	5.15	40	$k_1 = 4.92 \times 10^{-4}$	4.92×10^{-4}	$z_1 = 5$	20
	$k_2 = 4.92 \times 10^{-3}$		$z_2 = 15$			$k_2 = 4.92 \times 10^{-4}$		$z_2 = 15$	
30	$k_1 = 4.92 \times 10^{-5}$	4.92×10^{-5}	$z_1 = 5$	6.5	41	$k_1 = 4.92 \times 10^{-5}$	4.92×10^{-5}	$z_1 = 5$	6.5
	$k_2 = 4.92 \times 10^{-4}$		$z_2 = 15$			$k_2 = 4.92 \times 10^{-4}$		$z_2 = 15$	
31	$k_1 = 4.92 \times 10^{-5}$	4.92×10^{-5}	$z_1 = 5$	20	42	$k_1 = 4.92 \times 10^{-6}$	4.92×10^{-6}	$z_1 = 5$	5.15
	$k_2 = 4.92 \times 10^{-5}$		$z_2 = 15$			$k_2 = 4.92 \times 10^{-4}$		$z_2 = 15$	
32	$k_1 = 4.92 \times 10^{-5}$	4.92×10^{-6}	$z_1 = 5$	15.5	43	$k_1 = 4.92 \times 10^{-7}$	4.92×10^{-7}	$z_1 = 5$	5.015
	$k_2 = 4.92 \times 10^{-6}$		$z_2 = 15$			$k_2 = 4.92 \times 10^{-4}$		$z_2 = 15$	
33	$k_1 = 4.92 \times 10^{-5}$	4.92×10^{-7}	$z_1 = 5$	15.05	44	$k_1 = 4.92 \times 10^{-8}$	4.92×10^{-8}	$z_1 = 5$	5.0015
	$k_2 = 4.92 \times 10^{-7}$		$z_2 = 15$			$k_2 = 4.92 \times 10^{-4}$		$z_2 = 15$	

Table 3. Summary of parameters for combinations 45 to 66 used in the analyses of top strata having $z_1 = 15$ ft and $z_2 = 5$ ft.

Case no.	Permeability		Thickness		Case no.	Permeability		Thickness	
	Original (ft/sec)	Transformed k_b (ft/sec)	Original (ft)	Transformed z_b (ft)		Original (ft/sec)	Transformed k_b (ft/sec)	Original (ft)	Transformed z_b (ft)
45	$k_1 = 4.92 \times 10^{-3}$	4.92×10^{-5}	$z_1 = 15$	5.15	56	$k_1 = 4.92 \times 10^{-5}$	4.92×10^{-8}	$z_1 = 15$	5.015
	$k_2 = 4.92 \times 10^{-5}$		$z_2 = 5$			$k_2 = 4.92 \times 10^{-8}$		$z_2 = 5$	
46	$k_1 = 4.92 \times 10^{-4}$	4.92×10^{-5}	$z_1 = 15$	6.5	57	$k_1 = 4.92 \times 10^{-4}$	4.92×10^{-8}	$z_1 = 15$	5.0015
	$k_2 = 4.92 \times 10^{-5}$		$z_2 = 5$			$k_2 = 4.92 \times 10^{-8}$		$z_2 = 5$	
47	$k_1 = 4.92 \times 10^{-5}$	4.92×10^{-5}	$z_1 = 15$	20	58	$k_1 = 4.92 \times 10^{-5}$	4.92×10^{-8}	$z_1 = 15$	5.015
	$k_2 = 4.92 \times 10^{-5}$		$z_2 = 5$			$k_2 = 4.92 \times 10^{-8}$		$z_2 = 5$	
48	$k_1 = 4.92 \times 10^{-6}$	4.92×10^{-6}	$z_1 = 15$	15.5	59	$k_1 = 4.92 \times 10^{-6}$	4.92×10^{-8}	$z_1 = 15$	5.15
	$k_2 = 4.92 \times 10^{-5}$		$z_2 = 5$			$k_2 = 4.92 \times 10^{-8}$		$z_2 = 5$	
49	$k_1 = 4.92 \times 10^{-7}$	4.92×10^{-7}	$z_1 = 15$	15.05	60	$k_1 = 4.92 \times 10^{-7}$	4.92×10^{-8}	$z_1 = 15$	6.5
	$k_2 = 4.92 \times 10^{-5}$		$z_2 = 5$			$k_2 = 4.92 \times 10^{-8}$		$z_2 = 5$	
50	$k_1 = 4.92 \times 10^{-8}$	4.92×10^{-8}	$z_1 = 15$	15.005	61	$k_1 = 4.92 \times 10^{-8}$	4.92×10^{-8}	$z_1 = 15$	20
	$k_2 = 4.92 \times 10^{-5}$		$z_2 = 5$			$k_2 = 4.92 \times 10^{-8}$		$z_2 = 5$	
51	$k_1 = 4.92 \times 10^{-5}$	4.92×10^{-5}	$z_1 = 15$	15.05	62	$k_1 = 4.92 \times 10^{-4}$	4.92×10^{-4}	$z_1 = 15$	20
	$k_2 = 4.92 \times 10^{-3}$		$z_2 = 5$			$k_2 = 4.92 \times 10^{-4}$		$z_2 = 5$	
52	$k_1 = 4.92 \times 10^{-5}$	4.92×10^{-5}	$z_1 = 15$	15.5	63	$k_1 = 4.92 \times 10^{-5}$	4.92×10^{-5}	$z_1 = 15$	15.5
	$k_2 = 4.92 \times 10^{-4}$		$z_2 = 5$			$k_2 = 4.92 \times 10^{-4}$		$z_2 = 5$	
53	$k_1 = 4.92 \times 10^{-5}$	4.92×10^{-5}	$z_1 = 15$	20	64	$k_1 = 4.92 \times 10^{-6}$	4.92×10^{-6}	$z_1 = 15$	15.05
	$k_2 = 4.92 \times 10^{-5}$		$z_2 = 5$			$k_2 = 4.92 \times 10^{-4}$		$z_2 = 5$	
54	$k_1 = 4.92 \times 10^{-5}$	4.92×10^{-6}	$z_1 = 15$	6.5	65	$k_1 = 4.92 \times 10^{-7}$	4.92×10^{-7}	$z_1 = 15$	15.005
	$k_2 = 4.92 \times 10^{-6}$		$z_2 = 5$			$k_2 = 4.92 \times 10^{-4}$		$z_2 = 5$	
55	$k_1 = 4.92 \times 10^{-5}$	4.92×10^{-7}	$z_1 = 15$	5.15	66	$k_1 = 4.92 \times 10^{-8}$	4.92×10^{-8}	$z_1 = 15$	15.0005
	$k_2 = 4.92 \times 10^{-7}$		$z_2 = 5$			$k_2 = 4.92 \times 10^{-4}$		$z_2 = 5$	

The comparison of volumetric flow values calculated from FEA and Blanket Theory for combinations 1 to 22 is shown in Figure 78. The Blanket Theory analysis provides close results with FEA; the greatest difference is obtained for combination 18 that has the same permeability value for top and bottom layers as 4.92×10^{-4} ft/sec. This gives the ratio of k_f to k_b as 10, which is exactly the borderline of the applicability of the Blanket Theory. Better agreement of results is obtained for higher ratios of k_f to k_b . Similarly, excellent agreement is obtained for the pressure head (excess head) beneath the toe from the two methods as shown in Figure 79 for combinations 1 to 22. Figures 80, 81, 82, and 83 show similar plots for combinations 23 through 66. Same trends are observed for the different thicknesses of top stratum and combination; having a k_f to k_b ratio of 10 shows the largest variation for volumetric flow per unit length. Again, the Blanket Theory results and the finite element results for pressure beneath the toe are in close agreement.

The analysis is controlled by the least pervious layer in Blanket Theory solutions, which also becomes true for FEA if permeability of one of the layers of the blanket is very small as compared to the other layer. The analyses conducted indicate that the Blanket Theory provides reliable results for layered problems especially if the assumptions of the theory are not violated. However, this class of problems is better addressed in FEA, which can easily incorporate the complex geometries and properties. In addition, if more than two layers are present for the blanket, FEA may be more appropriate for such cases.

Figure 78. Calculated values of flow per unit length (Q_s) from Blanket Theory and finite element analysis for combinations 1 to 22 for Case 6.

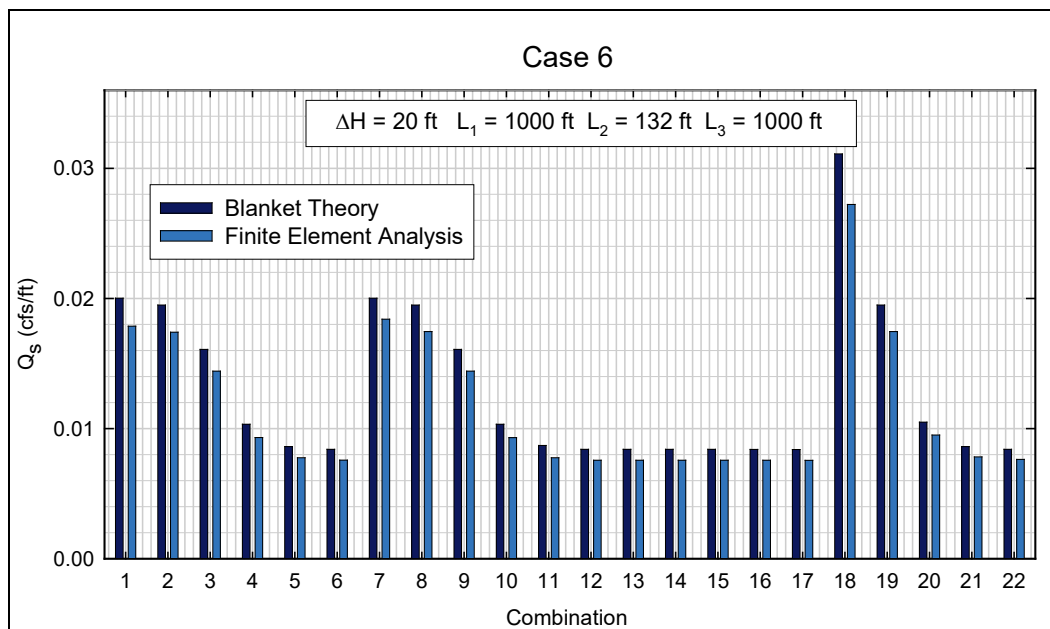


Figure 79. Excess head (h_b) or pressure head beneath blanket at toe for Case 6 calculated using FEA and Blanket Theory for combinations 1 to 22.

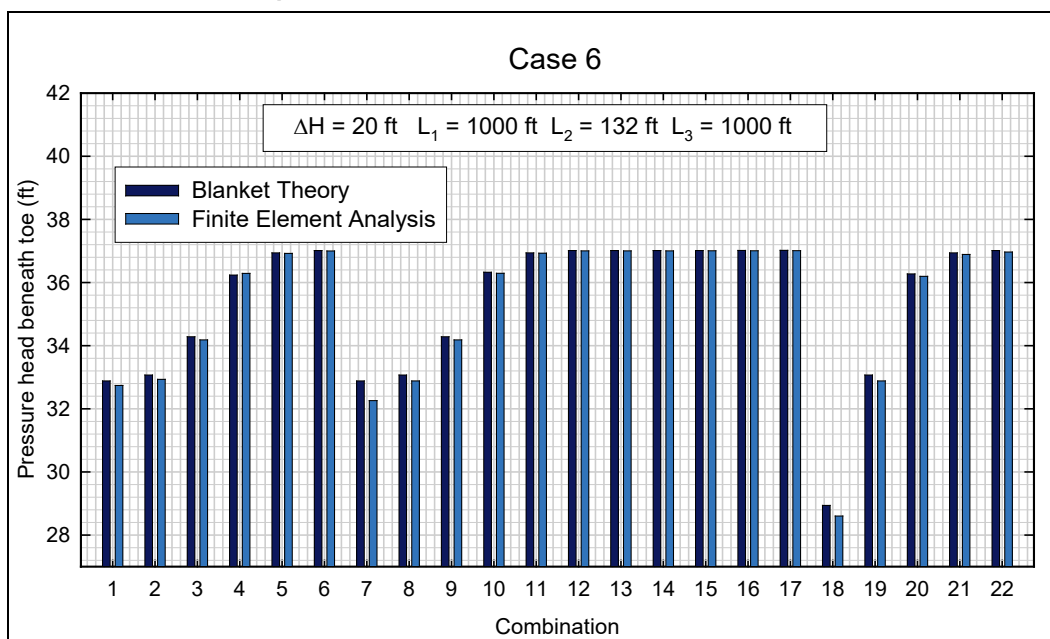


Figure 80. Calculated values of flow per unit length (Q_s) from Blanket Theory and finite element analysis for combinations 23 to 44 for Case 6.

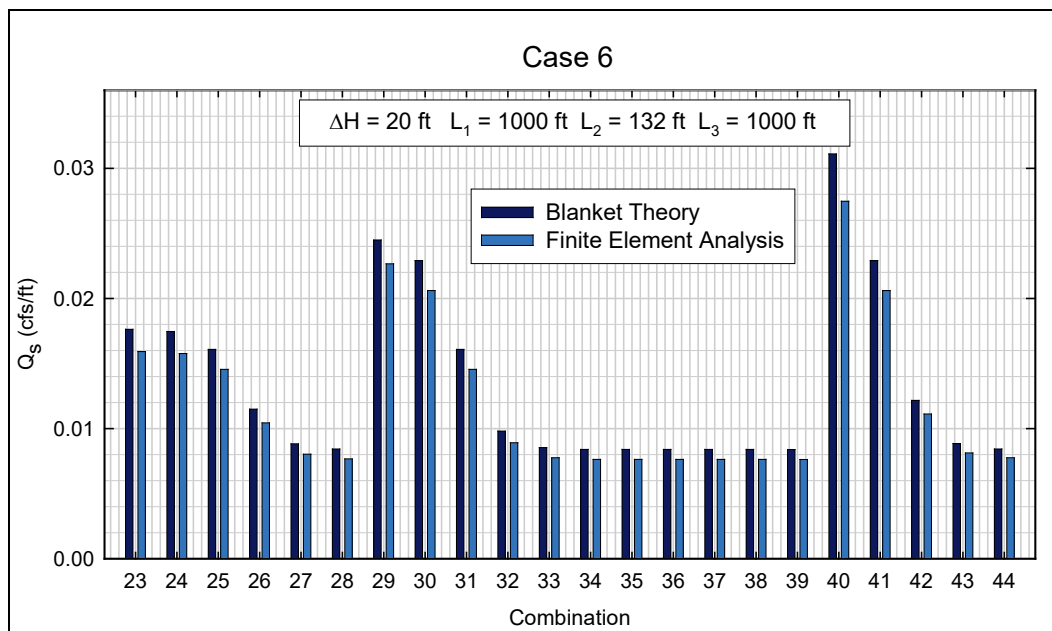


Figure 81. Excess head (h_o) or pressure head beneath blanket at toe for Case 6 calculated using finite element analysis and Blanket Theory for combinations 23 to 44.

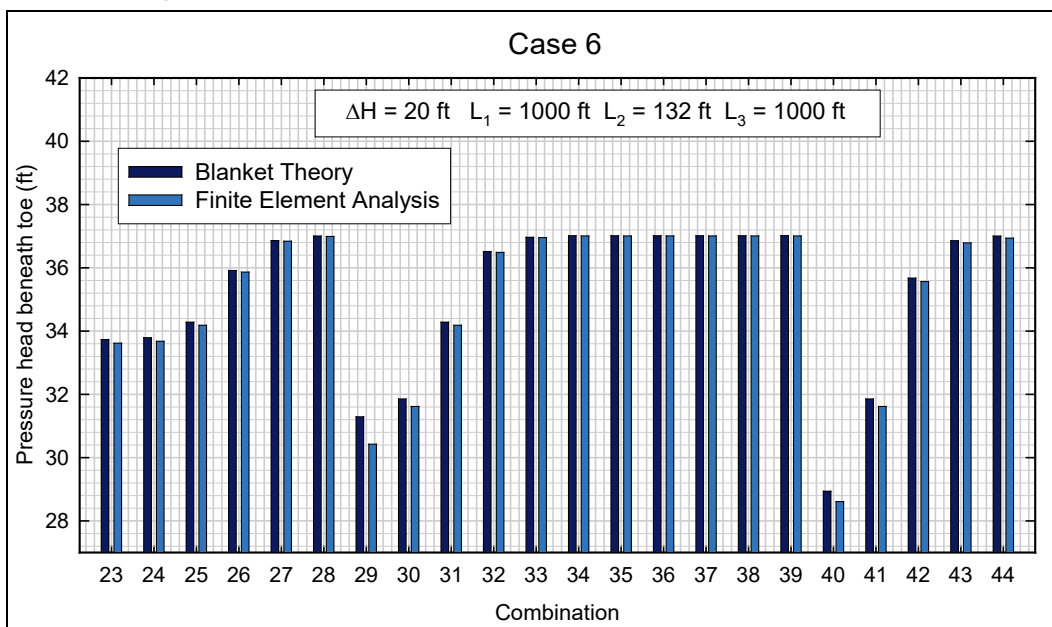


Figure 82. Calculated values of flow per unit length (Q_s) from Blanket Theory and finite element analysis for combinations 45 to 66 for Case 6.

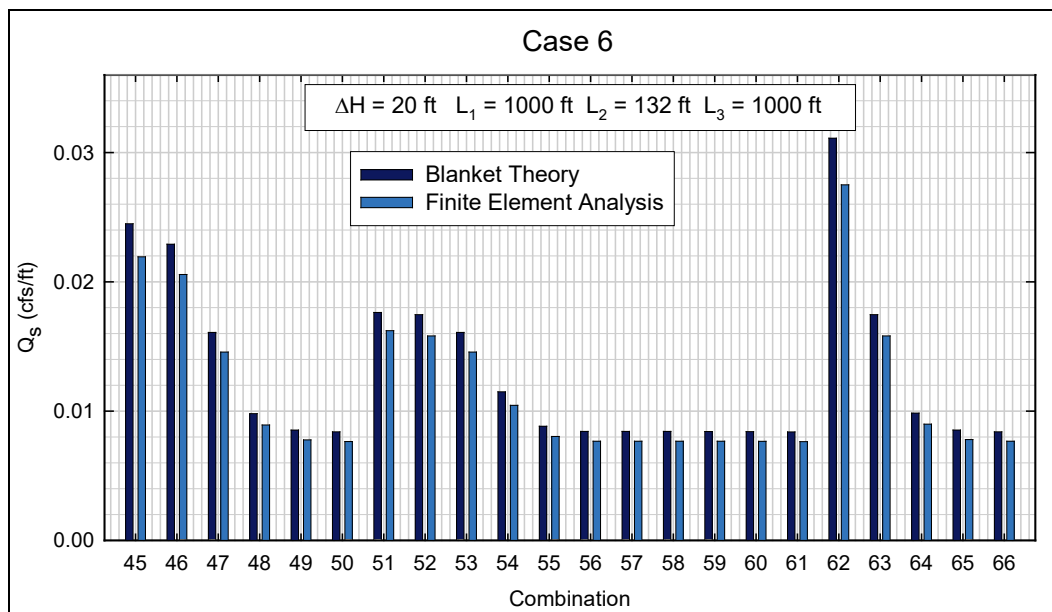
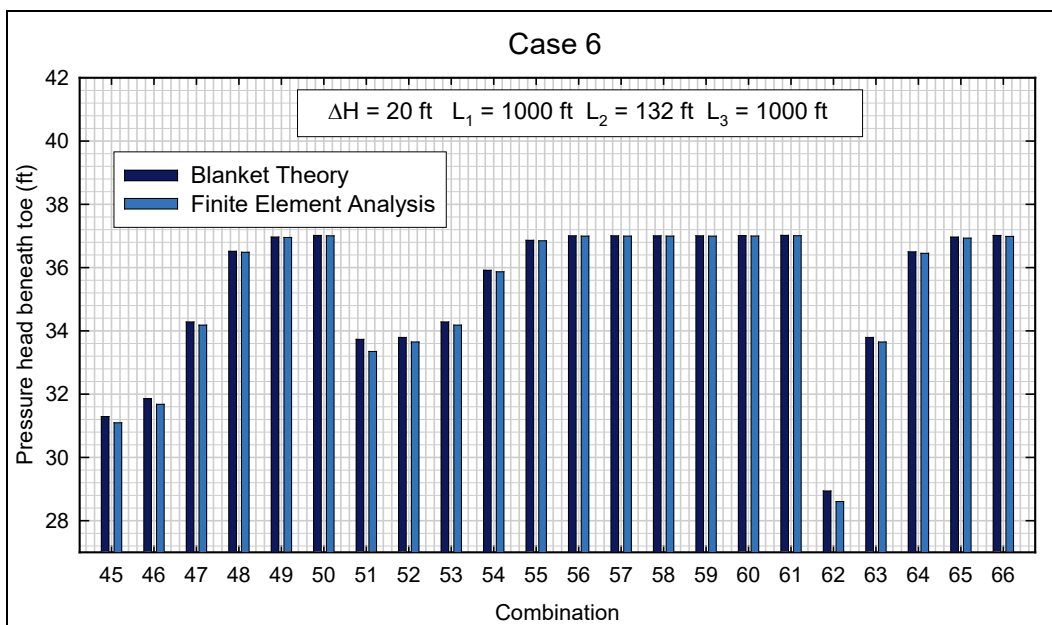


Figure 83. Excess head (h_o) or pressure head beneath blanket at toe for Case 6 calculated using FEA and Blanket Theory for combinations 45 to 66.



9 Finite Element Boundary Conditions for Outfall Canals

Considerable judgment is required to apply Blanket Theory for seepage analysis of outfall canals because the seepage boundary conditions used in the derivation of the Blanket Theory equations are not the same as the seepage boundary conditions at the outfall canals. The vertical boundary at the centerline of the canal would be a *no-flow* boundary, and none of the original Blanket Theory cases have a no-flow vertical boundary on the river or flood side. It is possible, with some effort, to modify existing cases to incorporate a vertical “seepage block” on the flood side.

If the bottom of the canal has direct hydraulic communication with the pervious layer, then Case 6 might provide reasonable results even though the vertical boundary conditions differ. If the canal is “silted in,” then Case 7c would be partially applicable. For the “silted in” condition, there would be some value of x_1 that could be used with Case 7c that may provide approximate results, but it is not possible to determine this value of x_1 based on site geometry because the boundary conditions for Case 7c and the outfall canals differ considerably.

The Interagency Performance Evaluation Task Force (IPET) formed to evaluate the levee performance of New Orleans levees during Hurricane Katrina used FEA to calculate pore pressures in the foundation sands of London Avenue Canal and Orleans Canal I-walls. In these analyses, the following boundary conditions were used:

- Constant head boundary for all points canal-side of the sheet pile to the centerline of the canal
- No-flow vertical boundary corresponding to the centerline of the canal (L_1 dimension in Blanket Theory)
- Potential seepage face boundary for surfaces on the landside of the I-wall
- Constant head vertical boundary at L_3 dimension as defined in Blanket Theory
- Sheet pile modeled as an impervious material.

In the case of a gap forming between the sheet pile and the levee fill, constant head boundary conditions, with a head equal to the canal water

level, were assigned to the depth of the gap on the flood-side boundary of the sheet pile. If the pervious layer is exposed in the bottom of the canal, then the presence of the gap has negligible effect on the calculated pore pressures. If the canal is “silted in,” then the gap can increase the pore pressures in the pervious layer if the gap extends down to this layer.

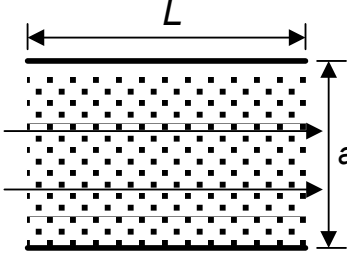
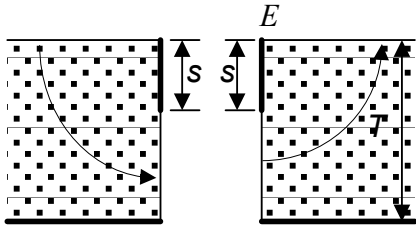
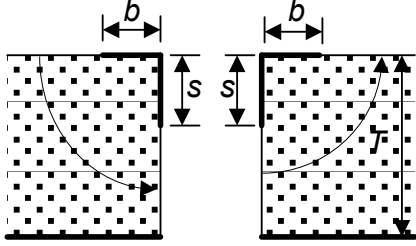
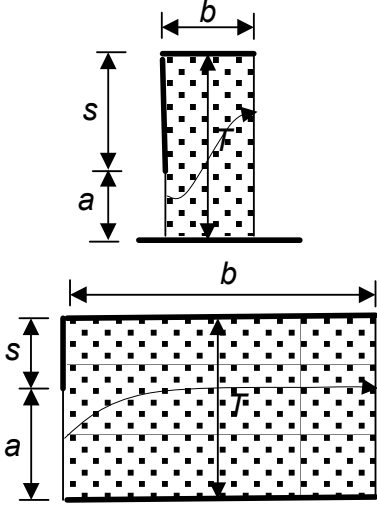
The distance to set the vertical boundary on the landside (L_3) requires some judgment. Ideally, it should be set at the minimum distance where the head is not affected by the canal water level. As the value of L_3 increases, the analysis becomes more conservative regarding the calculation of exit gradients, uplift pressures, and pore pressures. During the IPET study, the L_3 dimension was estimated based on piezometer data. A value of about 210 ft was used for London Avenue Canal analyses, and 135 ft was used for Orleans Canal analyses.

References

- Aravin, V. I., and Numerov, S. 1955. *Seepage computations for hydraulic structures*. Moscow: Stpoitel'stvu I Arkhitekture.
- Barron, R. A. 1948. The effect of a slightly pervious top blanket on the performance of relief wells. In *Proceedings of the Second International Conference on Soil Mechanics and Foundation Engineering, 21-30 June, Rotterdam, Netherlands*, 4:342.
- Bennett, P. T. 1946. *The effect of blankets on the seepage through pervious foundation*. Trans. ASCE 11. Reston, VA: American Society of Civil Engineers.
- Forchheimer, P. 1917. On the movement of groundwater according to sets of isothermal curves [in German]. *Sitzungsber K-K Akad der Wissenschaft* 126(4):409-40.
- Harr, M. E. 1962. *Groundwater and seepage*. New York: McGraw-Hill.
- Muskat, M. 1937. *The flow of homogeneous fluids through porous media*. New York: McGraw-Hill.
- Pavlovsky, N. N. 1935. *Principles of hydromechanical computation of Senkovtype barrages*. *Gidrotekh. Stroit.* Nos. 8-9.
- Pavlovsky, N. N. 1956. *Collected works*. Akad. Nauk. Leningrad: USSR.
- Spaulding, D. A. 1976. *Derivations of seepage equations*. TM-3-424, Personal Notes. St. Paul, MN: St. Paul District USACE.
- U.S. Army Corps of Engineers (USACE). 1956. *Investigation of underseepage and its control, lower Mississippi River levees*. Technical Memorandum No. 3-424. Vicksburg, MS: U.S. Army Engineer Waterways Experiment Station.
- U.S. Army Corps of Engineers (USACE). 2000. *Design and construction of levees*. Engineering Manual EM 1110-2-1913. Washington, DC: USACE HQ.

Appendix A: Fragment Types and Form Factors

Table A1. Summary of fragment type and form factors (Harr 1962).

Fragment Type	Illustration	Form Factor (Φ)
I		$\Phi = \frac{L}{a}$
II	 <p>Special Case $s = 0, \phi = 0.43$</p>	$\Phi = \frac{K}{K'}, m = \sin \frac{\pi s}{2T}$ $I_E = \frac{h\pi}{2KTm}$
III		$\Phi = \frac{K}{K'}$ $m = \cos \frac{\pi s}{2T} \sqrt{\tanh^2 \frac{\pi b}{2T} + \tan^2 \frac{\pi s}{2T}}$
IV		<p>Exact solution:</p> $\frac{\Lambda}{\Lambda'} = \frac{T}{b'}; modulus = \lambda$ $\Phi = \frac{K'(m)}{K(m)}; m = \lambda \sin \left(\frac{a}{T} \Lambda, \lambda \right)$ <p>Approximate solution:</p> <p>$S \geq b$:</p> $\Phi = \ln \left(1 + \frac{b}{a} \right)$ <p>$b \geq S$:</p> $\Phi = \ln \left(1 + \frac{s}{a} \right) + \frac{b-s}{T}$

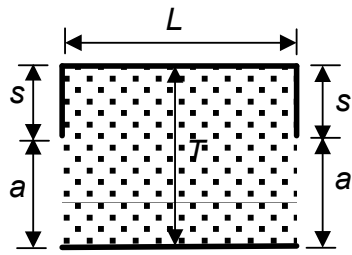
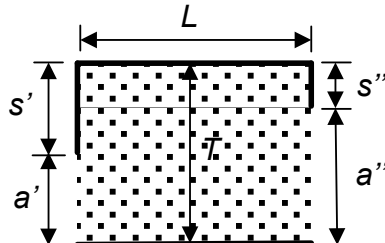
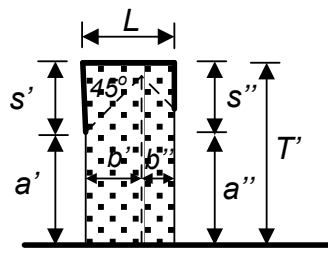
Fragment Type	Illustration	Form Factor (Φ)
V		$L \leq 2s:$ $\Phi = \ln \left(1 + \frac{b}{2a} \right)$ $b \geq 2s:$ $\Phi = 2 \ln \left(1 + \frac{s}{a} \right) + \frac{b - 2s}{T}$
VI	 	$L > s' + s'':$ $\Phi = \ln \left[\left(1 + \frac{s'}{a'} \right) \left(1 + \frac{s''}{a''} \right) \right] + \frac{L - (s' + s'')}{T}$ $L = s' + s'':$ $\Phi = \ln \left[\left(1 + \frac{s'}{a'} \right) \left(1 + \frac{s''}{a''} \right) \right]$ $L < s' + s'':$ $\Phi = \ln \left[\left(1 + \frac{b'}{a'} \right) \left(1 + \frac{b''}{a''} \right) \right]$ Where: $b' = \frac{L + (s' - s'')}{2}$ $b'' = \frac{L - (s' - s'')}{2}$

Table for complete elliptic integrals of the first kind

Table A2. Complete elliptic integrals of the first kind (Aravin and Numerov 1955).

m^2	K/K'	m^2	K/K'	m^2	K/K'	m^2	K/K'	m^2	K/K'
0.000	0.000	0.21	0.745	0.51	1.009	0.81	1.377	0.9993	3.195
0.001	0.325	0.22	0.754	0.52	1.018	0.82	1.397	0.9994	3.244
0.002	0.349	0.23	0.763	0.53	1.028	0.83	1.416	0.9995	3.302
0.003	0.366	0.24	0.773	0.54	1.037	0.84	1.439	0.9996	3.373
0.004	0.379	0.25	0.782	0.55	1.047	0.85	1.462	0.9997	3.465
0.005	0.389	0.26	0.791	0.56	1.057	0.86	1.484	0.9998	3.594
0.006	0.398	0.27	0.800	0.57	1.066	0.87	1.511	0.9999	3.814
0.007	0.406	0.28	0.808	0.58	1.076	0.88	1.538	1	∞
0.008	0.413	0.29	0.817	0.59	1.087	0.89	1.567		
0.009	0.420	0.30	0.826	0.60	1.098	0.90	1.600		
0.01	0.426	0.31	0.834	0.61	1.107	0.91	1.634		
0.02	0.471	0.32	0.843	0.62	1.118	0.92	1.672		
0.03	0.502	0.33	0.852	0.63	1.129	0.93	1.718		
0.04	0.526	0.34	0.860	0.64	1.140	0.94	1.770		
0.05	0.547	0.35	0.869	0.65	1.151	0.95	1.828		
0.06	0.565	0.36	0.877	0.66	1.162	0.96	1.901		
0.07	0.582	0.37	0.886	0.67	1.174	0.97	1.992		
0.08	0.598	0.38	0.895	0.68	1.186	0.98	2.123		
0.09	0.612	0.39	0.903	0.69	1.198	0.990	2.347		
0.10	0.625	0.40	0.911	0.70	1.211	0.991	2.381		
0.11	0.638	0.41	0.920	0.71	1.224	0.992	2.418		
0.12	0.650	0.42	0.929	0.72	1.237	0.993	2.461		
0.13	0.662	0.43	0.938	0.73	1.251	0.994	2.510		
0.14	0.674	0.44	0.946	0.74	1.265	0.995	2.568		
0.15	0.684	0.45	0.955	0.75	1.279	0.996	2.639		
0.16	0.695	0.46	0.964	0.76	1.294	0.997	2.731		
0.17	0.706	0.47	0.973	0.77	1.310	0.998	2.860		
0.18	0.716	0.48	0.982	0.78	1.326	0.999	3.081		
0.19	0.726	0.49	0.991	0.79	1.343	0.9991	3.115		
0.20	0.735	0.50	1.000	0.80	1.360	0.9992	3.152		

Notes: m is the modulus. To determine K/K' , compute the modulus (m) and then square it to find the K/K' from the above table.

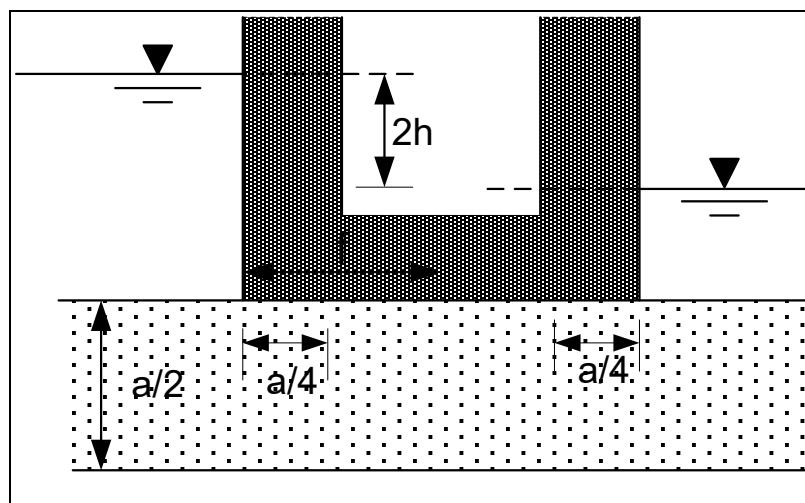
Appendix B: Derivation of Case 1

Introduction

The paper written by Forchheimer (1917) is in archaic technical German, and it was difficult to obtain a useful translation from current German-speaking engineers at our disposal. However, an effort was made to determine the origin of the equation presented in Muskat (1937), referenced to Forchheimer, which is similar to Case 1 of Blanket Theory. For this purpose, terminologies present in Muskat (1937) were related to those in Forchheimer (1917) for ease of understanding. The figure and equation numbers are also presented and cited as they appear in original paper.

The case having $L_2/d > 1$ will be discussed here as Blanket Theory is applicable only to such cases. However, it appears as $f/2a > 1/8$ in Forchheimer (1917), which is similar to $w/h > 1$ in Muskat (1937). Referring to Figure B1, Forchheimer considers the width of the levee as $2f$ and thickness of the pervious stratum as $a/2$. Therefore, for the case having $f/2a > 1/8$ (i.e., $w/h > 1$) where w =width of the structure and h is thickness of pervious substratum, we divide the length between $x=0$ and $x=f$ (the midpoint of levee) into an outer length of $a/4$ and an inner length of $f-a/4$ as shown the Figure B1 (Figure 11 of Forchheimer [1917]). The pressure loss is calculated for both the outer and inner lengths and is done by considering segments of $f = a/8$.

Figure B1. Figure indicating the outer and inner portions of the levee (Figure 11 in Forchheimer [1917]).



For the outer portion, pressure loss is calculated using Equation 38 of the paper, which is for the case $f/2a < 1/8$. This assumption is valid to some extent as the length of the outer portion is $a/4 < h$ ($a/2$). Equation 38 from Forchheimer (1917) is shown below:

$$h_{\Phi} = \frac{\pi q}{k \ln \frac{\cosh h \left(\frac{\pi f}{2a} \right) - 1}{3 \cosh h \left(\frac{\pi f}{2a} \right) - 1}} = \text{approximately } 1.364 \frac{q}{k} \frac{1}{\log \frac{\left(\frac{\pi f}{2a} \right)^2}{4 + 3 \left(\frac{\pi f}{2a} \right)^2}}$$

The pressure loss for the outer portion is equal to $0.673 \cdot q/k$ after substituting the value of $f = a/8$ in Equation 38 of Forchheimer (1917).

Similarly, for the inner portion, the pressure loss is again calculated by using a segment of length equal to $a/8$, and Darcy's Equation is used for this purpose:

$$q = kia$$

$$q = k \left(\frac{h}{l} \right) A$$

$$h = \frac{q}{k} \frac{l}{A}$$

where: $A = (a/2) \cdot 1$ and $l = a/8$

Substituting the values of A and l in the above expression, the pressure loss for the inner portion is equal to $0.25 \cdot q/k$.

Similarly, the collective pressure loss will be $0.923 \frac{q}{k}$, which is very close to the actual calculated value of $0.937 \frac{q}{k}$.

Note that the factor 0.937 is obtained by considering the flow net and then calculating the ratio of $\pi/2$ and mean potential difference $\left(\frac{\Phi_o + \Phi_f}{2} \right)$ as explained on Page 427 of Forchheimer (1917).

Equations 36 and 37 of Forchheimer (1917) are shown below:

$$\Phi_o = \ln \frac{\sin h\left(\frac{\pi f}{2a}\right)}{1 + \cos h\left(\frac{\pi f}{2a}\right)}$$

$$\Phi_f = \ln \frac{\sin h\left(\frac{\pi f}{2a}\right)}{\cos h\left(\frac{\pi f}{2a}\right) + \sqrt{\sin^2 h\left(\frac{\pi f}{2a}\right) + \cos^2 h\left(\frac{\pi f}{2a}\right)}} = \ln \frac{\sin h\left(\frac{\pi f}{2a}\right)}{\cos h\left(\frac{\pi f}{2a}\right) + \sqrt{\cos^2 h\left(\frac{\pi f}{a}\right)}}$$

Substituting the value of $f/2a = 1/8$ in Equations 36 and 37 of Forchheimer (1917), the mean potential difference is calculated as 1.6754 and the potential decrease (the ratio of $\pi/2$ and mean potential difference) as 0.937.

It is inferred that a correction is necessary for calculating the potential loss at the center of the structure because we are just considering segments of $a/8$ for the inner and outer distances are considered instead of the entire length for calculation of pressure loss.

It is presumed that correction for the outer section is incorporated in the calculated value of $0.937q/k$ by considering the flow from source to sink, with the source lying closer to the outer portion. However, for the correction of inner length, it is believed that the pressure loss has to be calculated for the length of $f-a/4$. This is again done by considering the Darcy's Law for the section of length equal to $f-a/4$.

$$q = kia$$

$$q = k \left(\frac{h}{l} \right) A$$

$$h = \frac{q}{k} \frac{l}{A}$$

where: $A = a/2$ and $l = f - a/4$. So, the pressure loss for this section will be:

$$\frac{q}{k} \frac{2}{a} \left(f - \frac{a}{4} \right) = \frac{q}{k} \left(\frac{2f}{a} - \frac{1}{2} \right)$$

Therefore, the pressure drop up to the center of the structure (i.e., the blanket) is calculated by using the following formula:

$$h = \frac{q}{k} \left(0.93 + \frac{2f}{a} - \frac{1}{2} \right)$$

Note that 0.93 is obtained by considering the mean of 0.923 and 0.937.

The above expression can be modified as follows:

$$h = \frac{q}{k} \left(0.43 + \frac{2f}{a} \right)$$

$$h \frac{k}{q} = \left(0.43 + \frac{2f}{a} \right)$$

$$\frac{q}{kh} = \frac{1}{\left(0.43 + \frac{2f}{a} \right)}$$

For $h = a/2$ and $w = 2f$:

$$\frac{q}{\Delta\Phi} = \frac{1}{\left(0.43 + \frac{w}{2h} \right)}$$

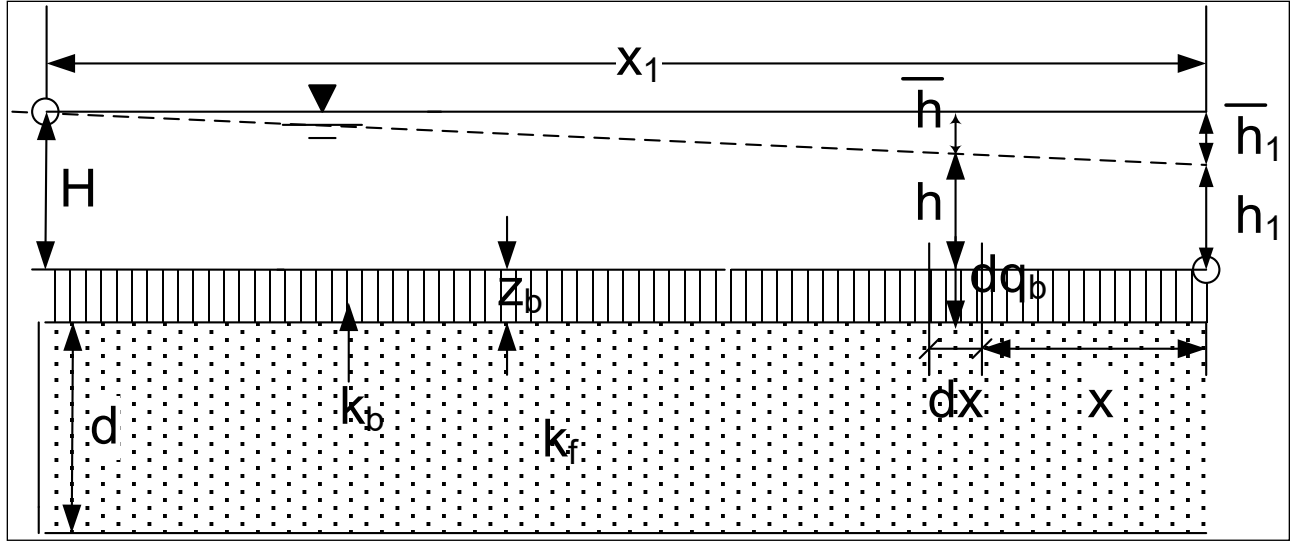
$$\frac{q}{\Delta\Phi} = \frac{1}{\left(0.86 + \frac{w}{h} \right)}$$

The above expression is similar to one that appears in Muskat (1937) and Case 1 of the Blanket Theory.

Determination of distance from effective seepage entry to riverside levee toe (x_1).

Consider the riverward side of the levee as shown in Figure B2

Figure B2. Riverward side of the levee.



Now, from Darcy's Law, the vertical flow through the top stratum is:

$$q = kiA$$

$$dq_b = k_{br} \left(\frac{H - h}{z_{br}} \right) dx$$

$$\frac{dq_b}{dx} = k_{br} \left(\frac{H - h}{z_{br}} \right) \quad (B1)$$

Similarly, the horizontal flow through the pervious substratum is:

$$q_f = k_f d \frac{dh}{dx}$$

$$\frac{dq_f}{dx} = k_f d \frac{d^2 h}{dx^2} \quad (B2)$$

The continuity equation for steady state will be:

$$\frac{dq_f}{dx} + \frac{dq_b}{dx} = 0$$

Putting the values of $\frac{dq_f}{dx}$ and $\frac{dq_b}{dx}$ from Equations B1 and B2, respectively:

$$k_f d \frac{d^2 h}{dx^2} + k_{br} \left(\frac{H-h}{z_{br}} \right) = 0$$

Dividing $k_f d$ on both sides of the equation:

$$\frac{d^2 h}{dx^2} + \frac{k_{br}}{k_f dz_{br}} (H-h) = 0$$

Let $\bar{h} = H - h$ and $\frac{d^2 \bar{h}}{dx^2} = -\frac{d^2 h}{dx^2}$

So,

$$\frac{d^2 \bar{h}}{dx^2} - c^2 \bar{h} = 0 \quad (B3)$$

where: $c = \sqrt{\frac{k_{br}}{k_f z_{br} d}}$

The differential equation is solved as follows:

Let $p = \frac{d\bar{h}}{dx}$ and the auxiliary equation is:

$$p^2 - c^2 = 0 \quad (p^1 = \frac{d\bar{h}}{dx}, p^2 = \frac{d^2 \bar{h}}{dx^2}, p^0 = \bar{h} = 1)$$

The roots of the above equation are c and $-c$;

The solution of the above differential equation is:

$$\bar{h} = m_1 e^{cx} + n_1 e^{-cx} \quad (B4)$$

Where, m_1 and n_1 are constants.

If the distance to the river from the riverside levee toe L_1 is known and no riverside borrow pits or seepage block exists, x_1 is determined as follows:

The boundary conditions for this case are:

$$\text{For } x = 0, \bar{h} = H - h_1$$

$$\text{For } x = L_1, \bar{h} = 0$$

Putting the first condition in Equation B4:

$$H - h_1 = m_1 + n_1$$

Similarly, putting the second condition in Equation B4:

$$0 = m_1 e^{cL_1} + n_1 e^{-cL_1}$$

Putting the value of m_1 in the above equation:

$$0 = (H - h_1 - n_1) e^{cL_1} + n_1 e^{-cL_1}$$

$$0 = He^{cL_1} - h_1 e^{cL_1} - n_1 e^{cL_1} + n_1 e^{-cL_1}$$

$$0 = He^{cL_1} - h_1 e^{cL_1} - n_1 (e^{cL_1} - e^{-cL_1})$$

$$He^{cL_1} - h_1 e^{cL_1} = n_1 (e^{cL_1} - e^{-cL_1})$$

$$n_1 = \frac{He^{cL_1} - h_1 e^{cL_1}}{(e^{cL_1} - e^{-cL_1})}$$

$$\text{As, } \sin hx = \frac{e^x - e^{-x}}{2}, \text{ Also, assume, } \bar{h}_1 = H - h_1 :$$

$$n_1 = \frac{\bar{h}_1 e^{cL_1}}{2 \sin h(cL_1)}$$

Putting the values of m_1 and n_1 in the solution of differential equation:

$$\bar{h} = \left(\bar{h}_1 - \frac{\bar{h}_1 e^{cL_1}}{2 \sin h(cL_1)} \right) e^{cx} + \frac{\bar{h}_1 e^{cL_1}}{2 \sin h(cL_1)} e^{-cx}$$

$$\bar{h} = \frac{\bar{h}_1}{2 \sin h(cL_1)} (2e^{cx} \sin h(cL_1) - e^{cL_1} e^{cx} + e^{cL_1} e^{-cx}) \quad (B5)$$

Now,

$$e^{cx} 2 \sin h(cL_1) = e^{cx} (e^{cL_1} - e^{-cL_1}) \text{ Because, } \sin hx = \frac{e^x - e^{-x}}{2}$$

$$e^{cx} 2 \sin h(cL_1) = e^{cx+cL_1} - e^{cx-cL_1}$$

Putting the value of above expression in Equation B5:

$$\bar{h} = \frac{\bar{h}_1}{2 \sin h(cL_1)} (e^{cx+cL_1} - e^{cx-cL_1} - e^{cL_1} e^{cx} + e^{cL_1} e^{-cx})$$

$$\bar{h} = \frac{\bar{h}_1}{\sin h(cL_1)} \frac{(e^{c(L_1-x)} - e^{-c(L_1-x)})}{2}$$

$$\bar{h} = \frac{\bar{h}_1 \sin h(c(L_1 - x))}{\sin h(cL_1)}$$

The distance from the riverside levee toe to the effective seepage entry (x_1) can be determined by extrapolating hydraulic grade line at $x = 0$ to the full head on river stage.

So,

$$\frac{d\bar{h}}{dx} = \frac{-\bar{h}_1}{x_1}$$

Also, we know that,

$$\bar{h} = \frac{\bar{h}_1 \sin h(c(L_1 - x))}{\sin h(cL_1)}$$

$$\frac{d\bar{h}}{dx} = \frac{\bar{h}_1}{\sin h(cL_1)} \frac{d}{dx} (\sin h(c(L_1 - x))) \quad (B6)$$

Now,

$$\sin h(c(L_1 - x)) = \frac{e^{cL_1} e^{-cx} - e^{-cL_1} e^{cx}}{2}$$

$$\frac{d}{dx} \sin h(c(L_1 - x)) = \frac{e^{cL_1} (-c) e^{-cx} - e^{-cL_1} (c) e^{cx}}{2}$$

$$\frac{d}{dx} \sin h(c(L_1 - x)) = \frac{-c}{2} [e^{c(-x+L_1)} + e^{-c(-x+L_1)}]$$

$$\frac{d}{dx} \sin h(c(L_1 - x)) = -c \cos hc(L_1 - x) \quad \cos hx = \frac{e^x + e^{-x}}{2}$$

Now, putting the value of above expression in Equation B6:

$$\frac{d\bar{h}}{dx} = \frac{\bar{h}_1}{\sin h(cL_1)} - c \cos hc(L_1 - x)$$

For x=0,

$$\frac{d\bar{h}}{dx} = \frac{\bar{h}_1}{\sin h(cL_1)} - c \cos h(cL_1)$$

$$\frac{d\bar{h}}{dx} = \frac{-c\bar{h}_1}{\tan h(cL_1)} \quad (B7)$$

As we know that,

$$\frac{d\bar{h}}{dx} = \frac{-\bar{h}_1}{x_1}$$

Putting the value of $\frac{d\bar{h}}{dx}$ in Equation B7:

$$\frac{-\bar{h}_1}{x_1} = \frac{-c\bar{h}_1}{\tan h(cL_1)}$$

$$x_1 = \frac{\tan h(cL_1)}{c}$$

where:

$$c = \sqrt{\frac{k_{br}}{k_f z_{br} d}}$$

where:

k_{br} = Transformed vertical permeability of riverside top stratum

k_f = Horizontal permeability of pervious substratum

d = Thickness of pervious substratum

z_{br} = Transformed thickness of riverside top stratum

If the seepage block exists between the riverside levee toe and the river so as to prevent any seepage entrance into pervious foundation beyond the point, x_1 can be determined as follows:

From above case, we know that:

$$\bar{h} = m_1 e^{cx} + n_1 e^{-cx}$$

where: m_1 and n_1 are constants.

The boundary conditions for this case are as follows:

$$\text{For } x = 0, \bar{h} = H - h_1$$

$$\text{For } x = L_1, \frac{d\bar{h}}{dx} = 0$$

Putting the first condition in Equation B4:

$$H - h_1 = m_1 + n_1$$

Similarly, putting the second condition in Equation B4:

$$\frac{d\bar{h}}{dx} = m_1 c e^{cx} - n_1 c e^{-cx}$$

$$0 = m_1 c e^{cL_1} - n_1 c e^{-cL_1}$$

Putting the value of m_1 in the above equation:

$$0 = (H - h_1 - n_1) c e^{cL_1} + n_1 c e^{-cL_1}$$

$$0 = H c e^{cL_1} - h_1 c e^{cL_1} - n_1 c e^{cL_1} - n_1 c e^{-cL_1}$$

$$0 = H c e^{cL_1} - h_1 c e^{cL_1} - n_1 c (e^{cL_1} - e^{-cL_1})$$

$$H c e^{cL_1} - h_1 c e^{cL_1} = n_1 c (e^{cL_1} + e^{-cL_1})$$

Multiplying by $1/2$ on both sides:

$$\frac{1}{2} (H c e^{cL_1} - h_1 c e^{cL_1}) = \frac{1}{2} n_1 c (e^{cL_1} + e^{-cL_1})$$

As we know that,

$$\cos hx = \frac{e^x + e^{-x}}{2}$$

And we also assume $\bar{h}_1 = H - h_1$

So,

$$n_1 \cos h(cL_1) = \frac{1}{2} \bar{h}_1 e^{cL_1}$$

$$n_1 = \frac{\bar{h}_1 e^{cL_1}}{2 \cos h(cL_1)}$$

Substituting the values of m_1 and n_1 in the solution of differential equation:

$$\bar{h} = \left(\bar{h}_1 - \frac{\bar{h}_1 e^{cL_1}}{2 \cosh(cL_1)} \right) e^{cx} + \frac{\bar{h}_1 e^{cL_1}}{2 \cosh(cL_1)} e^{-cx}$$

$$\bar{h} = \frac{\bar{h}_1}{2 \cosh(cL_1)} (2e^{cx} \cosh(cL_1) - e^{cL_1} e^{cx} + e^{cL_1} e^{-cx}) \quad (\text{B8})$$

Now,

$$e^{cx} 2 \cosh(cL_1) = e^{cx} (e^{cL_1} + e^{-cL_1}) \quad \text{Because, } \cosh x = \frac{e^x + e^{-x}}{2}$$

$$e^{cx} 2 \cosh(cL_1) = e^{cx+cL_1} + e^{cx-cL_1}$$

Putting the value of above expression in Equation B8:

$$\bar{h} = \frac{\bar{h}_1}{2 \cosh(cL_1)} (e^{cx+cL_1} + e^{cx-cL_1} - e^{cL_1} e^{cx} + e^{cL_1} e^{-cx})$$

$$\bar{h} = \frac{\bar{h}_1}{\cosh(cL_1)} \frac{(e^{-c(-x+L_1)} + e^{c(-x+L_1)})}{2}$$

$$\bar{h} = \frac{\bar{h}_1 \cosh(c(L_1 - x))}{\cosh(cL_1)}$$

For $x = L_1$

$$\bar{h}_x = \frac{\bar{h}_1}{\cosh(cL_1)} \quad (\text{Since } \cosh(0) = 1)$$

The distance from the riverside levee toe to the effective seepage entry (x_1) can be determined by extrapolating hydraulic grade line at $x = 0$ to the full head on river stage.

So,

$$\frac{d\bar{h}}{dx} = -\frac{\bar{h}_1}{x_1}$$

Also, we know that,

$$\bar{h} = \frac{\bar{h}_1 \cosh(c(L_1 - x))}{\cosh(cL_1)}$$

$$\frac{d\bar{h}}{dx} = \frac{\bar{h}_1}{\cosh(cL_1)} \frac{d}{dx} (\cosh(c(L_1 - x))) \quad (\text{B9})$$

Now,

$$\cosh(c(L_1 - x)) = \frac{e^{cL_1}e^{-cx} + e^{-cL_1}e^{cx}}{2}$$

$$\frac{d}{dx} \cosh(c(L_1 - x)) = \frac{e^{cL_1}(-c)e^{-cx} + e^{-cL_1}(c)e^{cx}}{2}$$

$$\frac{d}{dx} \cosh(c(L_1 - x)) = \frac{-c}{2} [e^{c(-x+L_1)} - e^{-c(-x+L_1)}]$$

$$\frac{d}{dx} \cosh(c(L_1 - x)) = -c \sinh(c(L_1 - x)) \quad \sinh hx = \frac{e^x - e^{-x}}{2}$$

For $x = 0$,

$$\frac{d}{dx} \cosh(c(L_1 - x)) = -c \sinh(cL_1)$$

Now, putting the value of above expression in the Equation B9:

$$\frac{d\bar{h}}{dx} = \frac{\bar{h}_1}{\cosh(cL_1)} - c \sinh(cL_1)$$

$$\frac{d\bar{h}}{dx} = -c\bar{h}_1 \tanh(cL_1) \quad (\text{B10})$$

As we know that,

$$\frac{d\bar{h}}{dx} = \frac{-\bar{h}_1}{x_1}$$

Putting the value of $\frac{d\bar{h}}{dx}$ in Equation B10:

$$-\frac{\bar{h}_1}{x_1} = -c\bar{h}_1 \tan h(cL_1)$$

$$x_1 = \frac{1}{c \tan h(cL_1)}$$

where:

$$c = \sqrt{\frac{k_{br}}{k_f z_{br} d}}$$

where:

k_{br} = transformed vertical permeability of riverside top stratum

k_f = horizontal permeability of pervious substratum

d = thickness of pervious substratum

z_{br} = transformed thickness of riverside top stratum

Appendix C

Additional figures comparing FEA and Blanket Theory

Figure C1. Calculated values of flow per unit length (Q_s) for different values of L_2/d for Case 1.

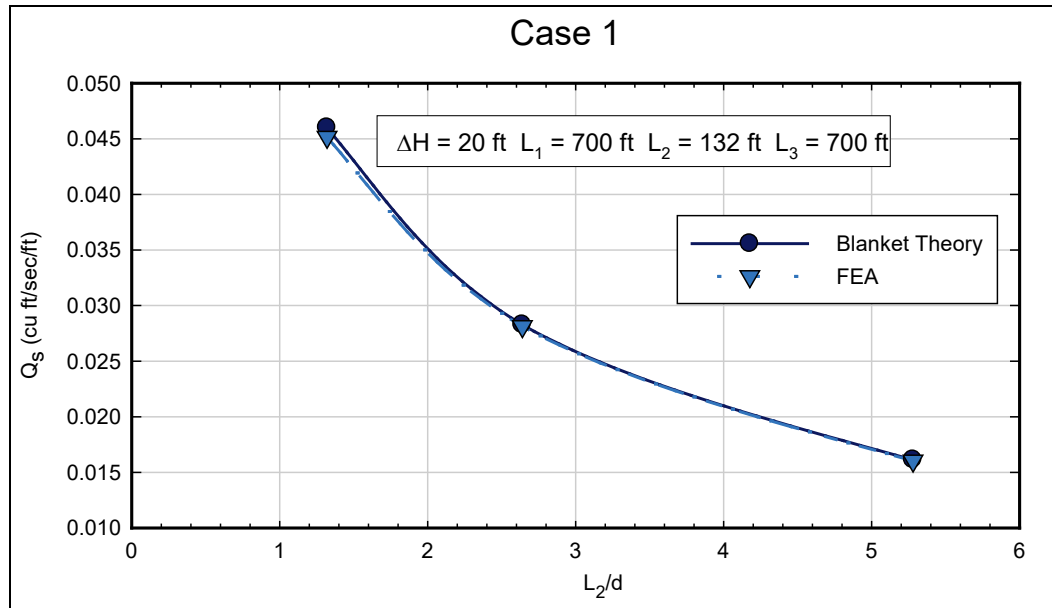


Figure C2. Calculated values of flow per unit length (Q_s) for different values of L_2/d for Case 1.

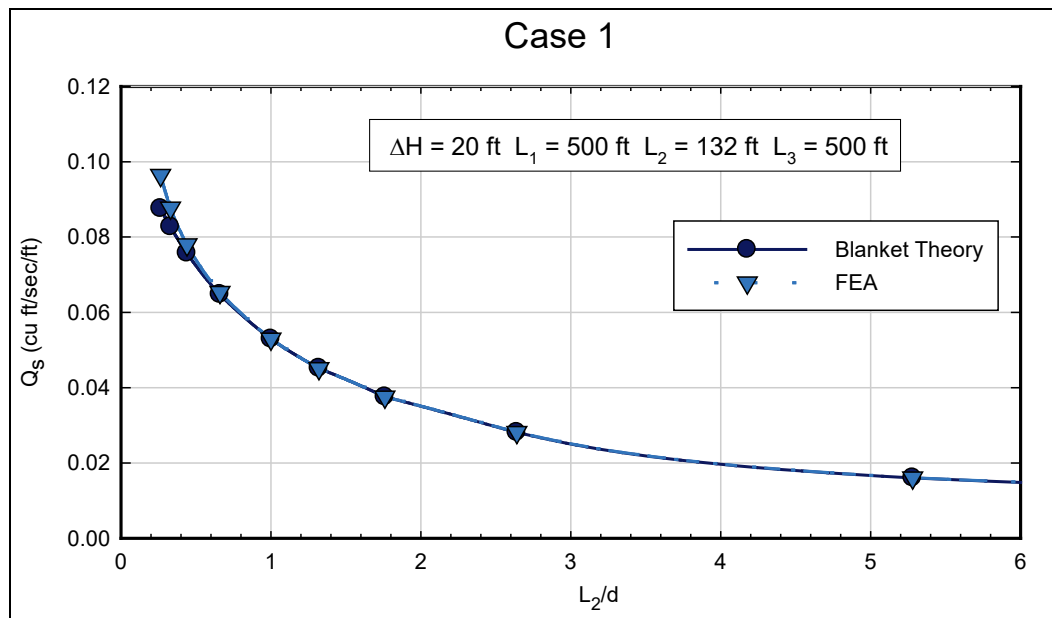


Figure C3. Calculated values of flow per unit length (Q_s) from Blanket Theory and finite element analysis for different values of L_3 for Case 2.

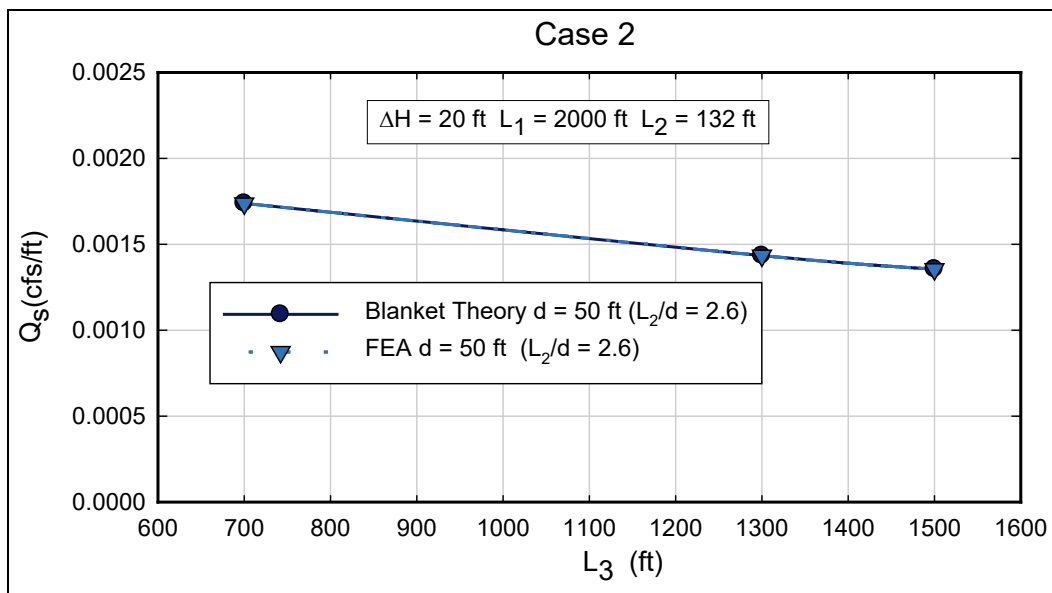


Figure C4. Excess head (h_b) or pressure head beneath blanket at toe for Case 2 calculated using FEA and Blanket Theory for different values of L_3 for $d = 50$ ft.

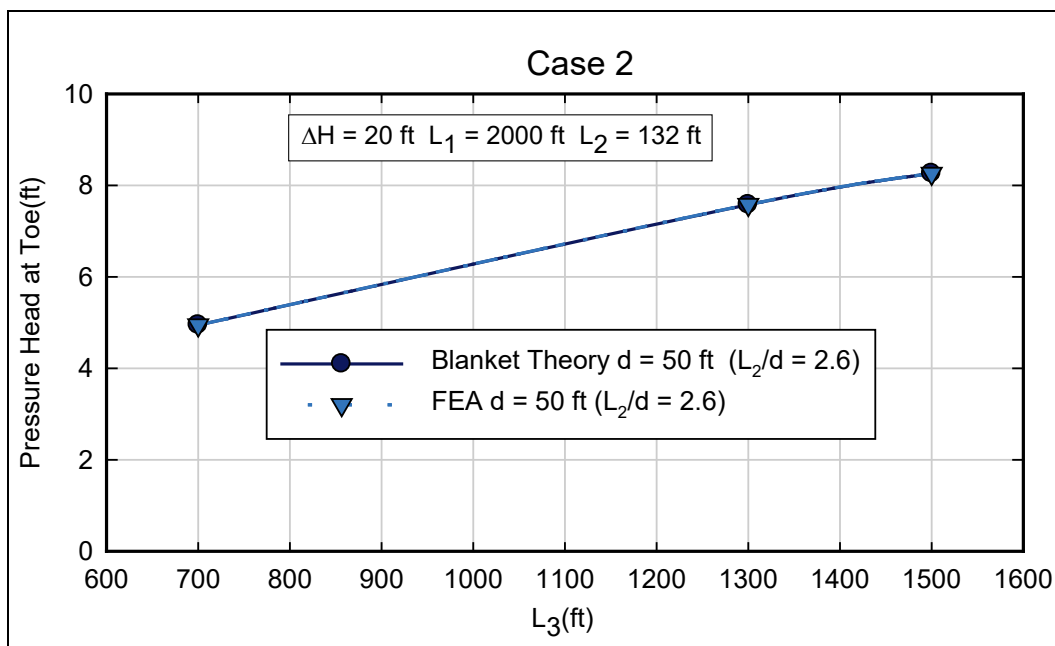


Figure C5. Calculated values of flow per unit length (Q_s) from Blanket Theory and finite element analysis for different values of L_3 for Case 2 having k_r as 0.00328 ft/sec.

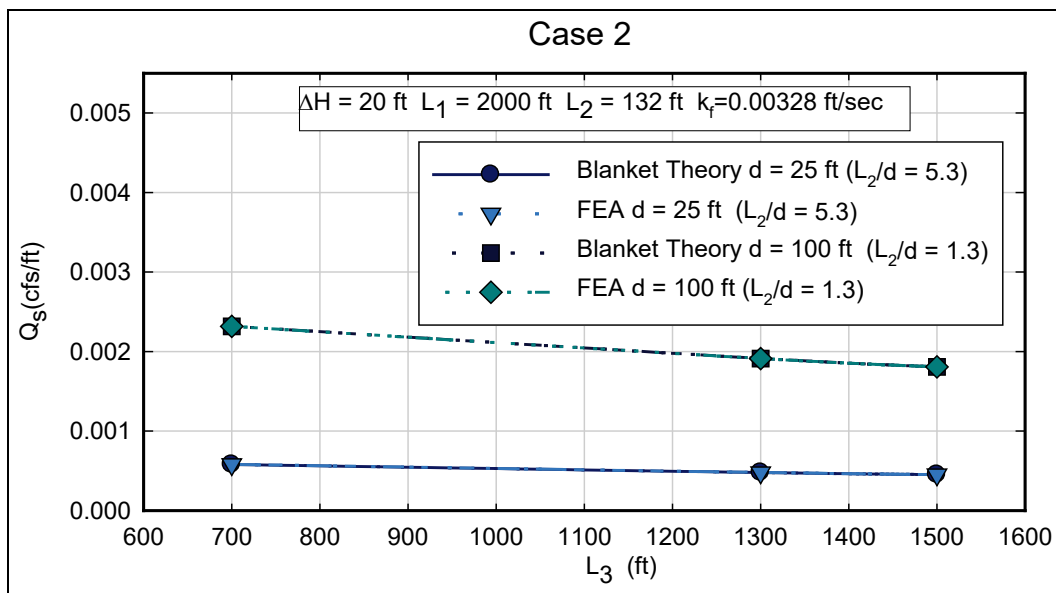


Figure C6. Excess head (h_o) or pressure head beneath blanket at toe for Case 2 calculated using FEA and Blanket Theory for different values of L_3 for k_r as 0.00328 ft/sec.

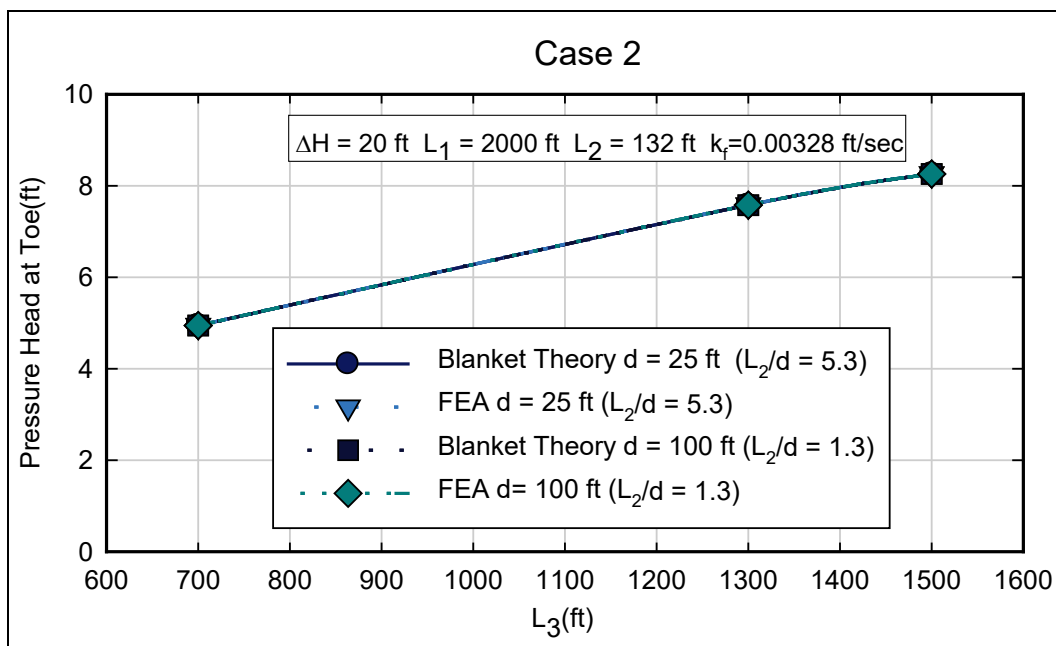


Figure C7. Calculated values of flow per unit length (Q_s) from Blanket Theory and finite element analysis for different values of L_1 for Case 3.

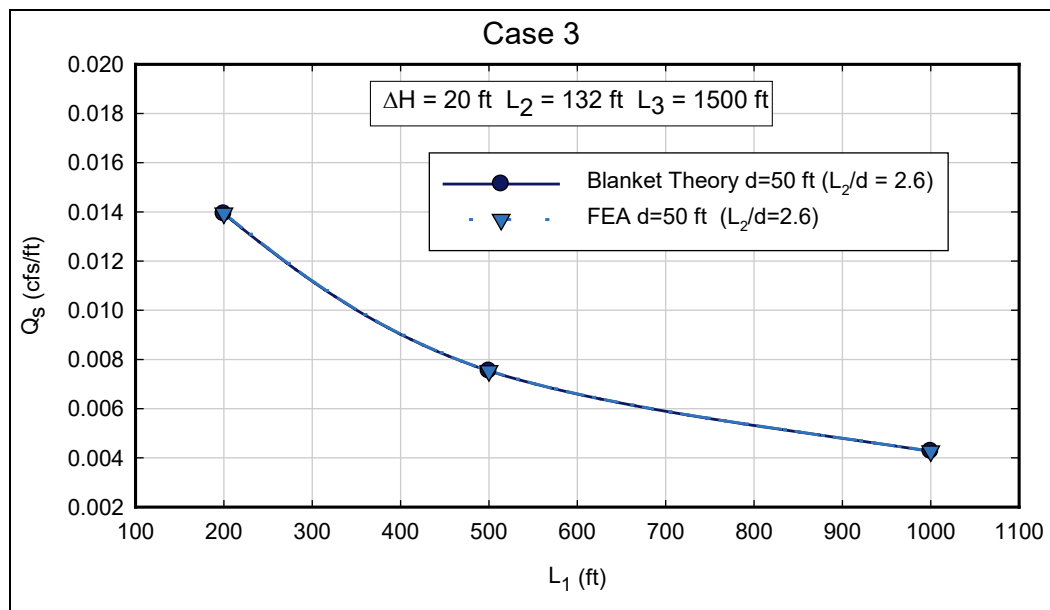


Figure C8. Calculated values of flow per unit length (Q_s) from Blanket Theory and finite element analysis for different values of L_3 for Case 4.

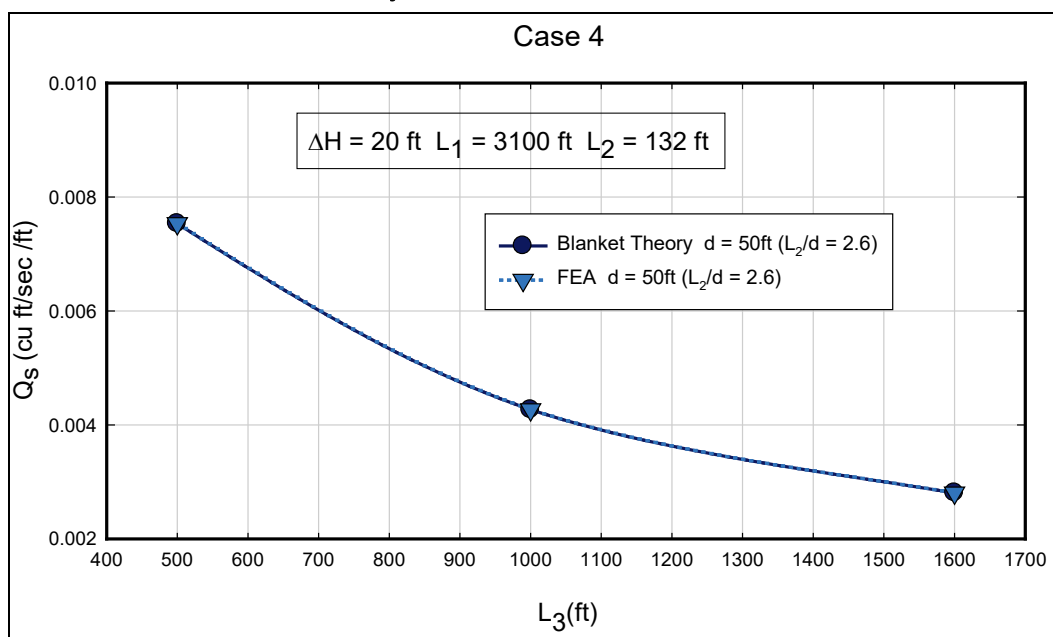


Figure C9. Excess head (h_o) or pressure head at toe calculated using FEA and Blanket Theory for different values of L_3 .

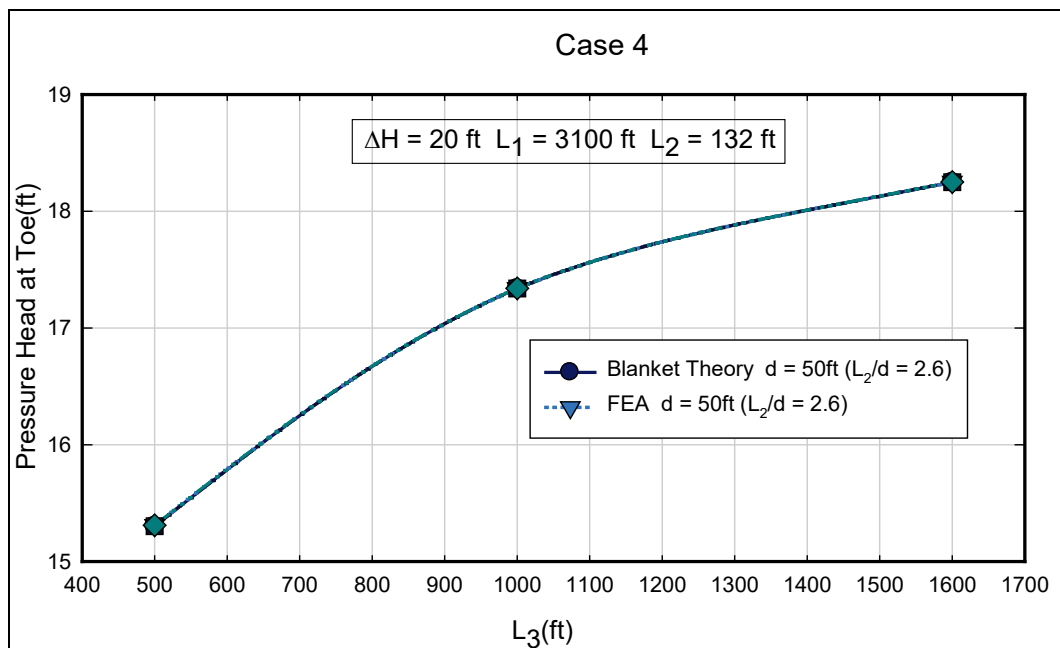


Figure C 10. Calculated values of flow per unit length (Q_s) from Blanket Theory and finite element analysis for different values of L_3 for Case 4 having k_f as 0.00328 ft/sec.

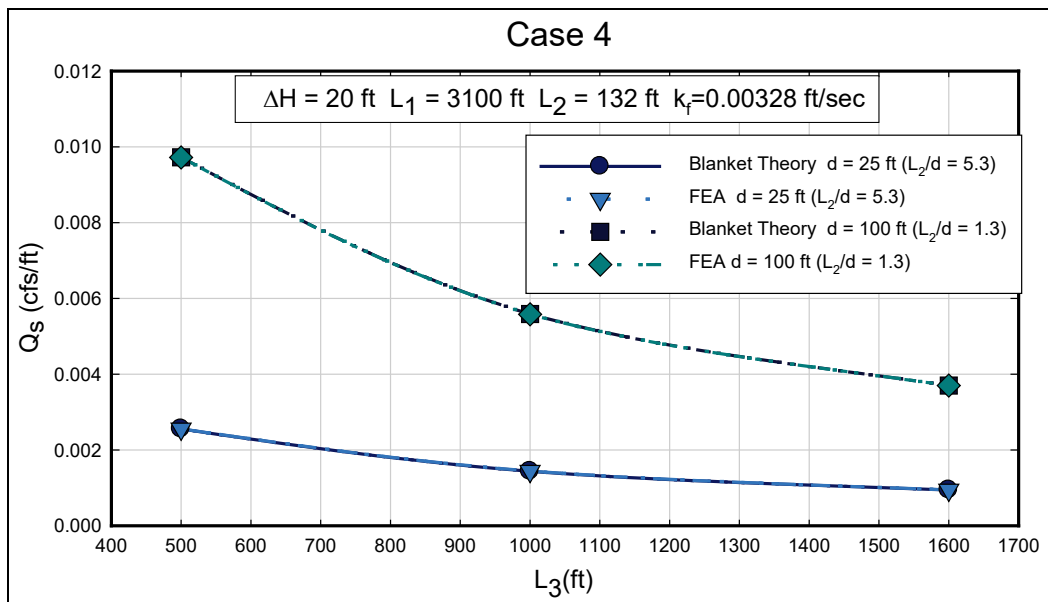


Figure C11. Excess head (h_o) or pressure head at toe calculated using FEA and Blanket Theory for different values of L_3 having k_r as 0.00328 ft/sec.

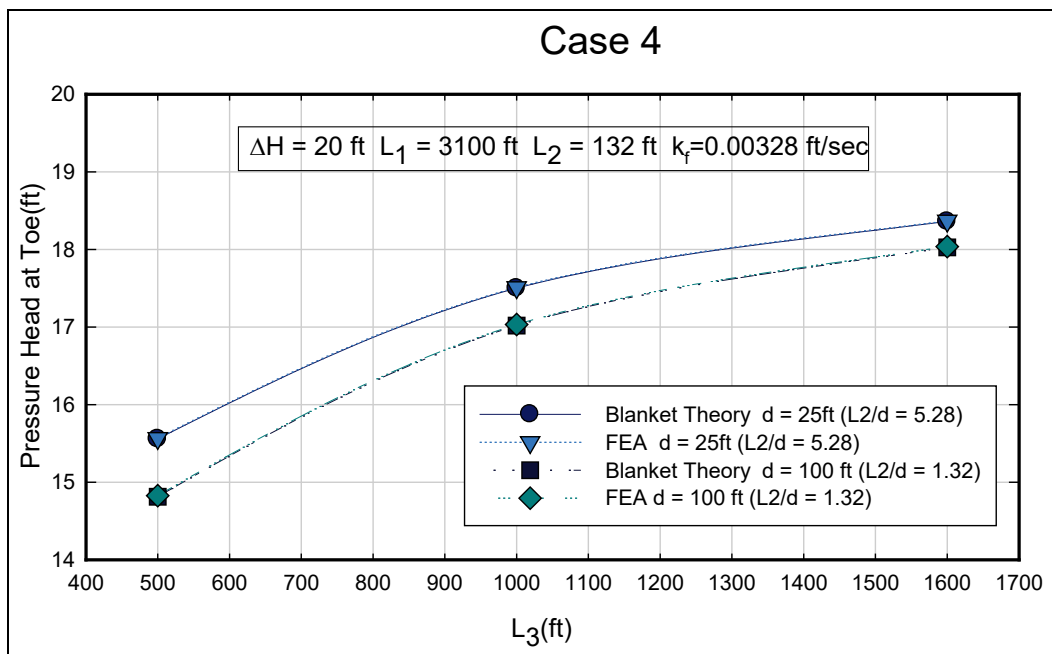


Figure C12. Calculated values of flow per unit length (Q_s) for various permeability ratios from Blanket Theory and finite element analysis for Case 5 for $z_b = 10$ ft and $L_1 = 500$ ft.

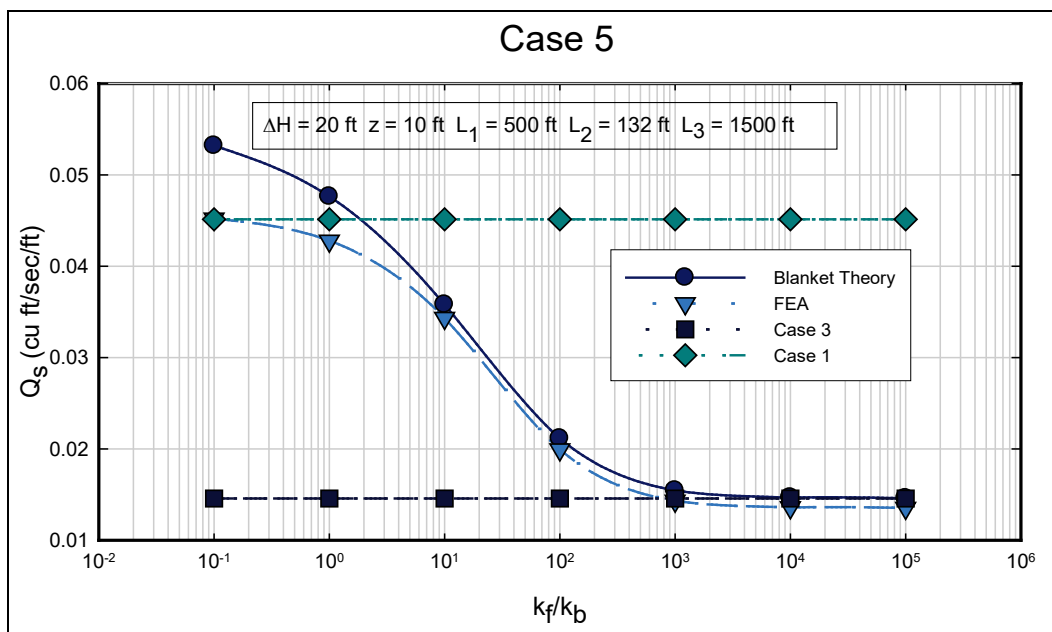


Figure C13. Calculated values of flow per unit length (Q_s) for various permeability ratios from Blanket Theory and finite element analysis for Case 5 for $z_b = 20$ ft and $L_1 = 500$ ft.

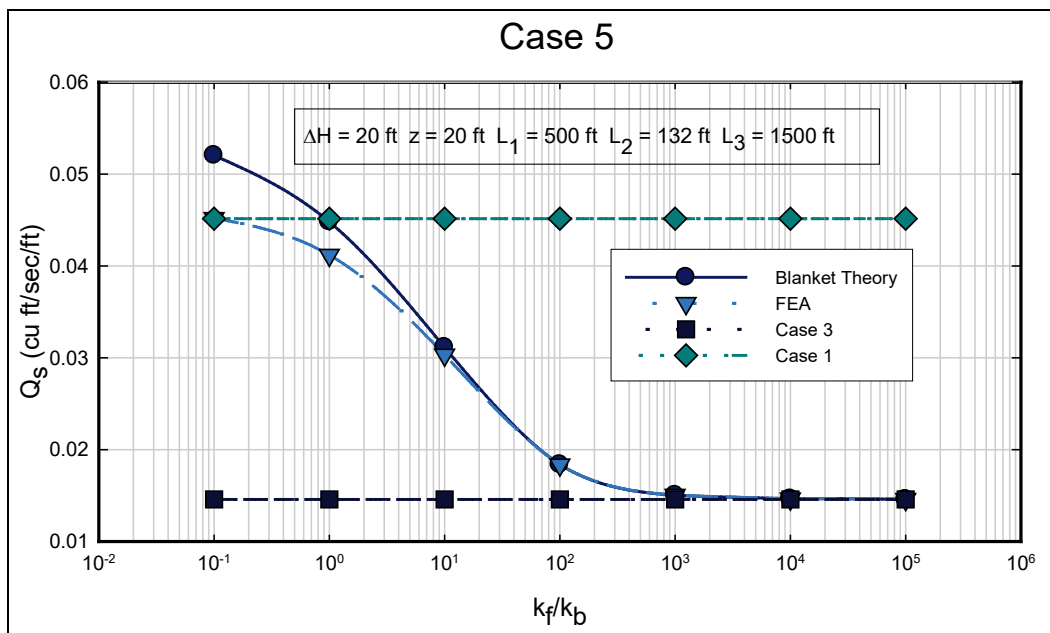


Figure C14. Calculated flows for SLIDE and SEEP/W for Case 5.

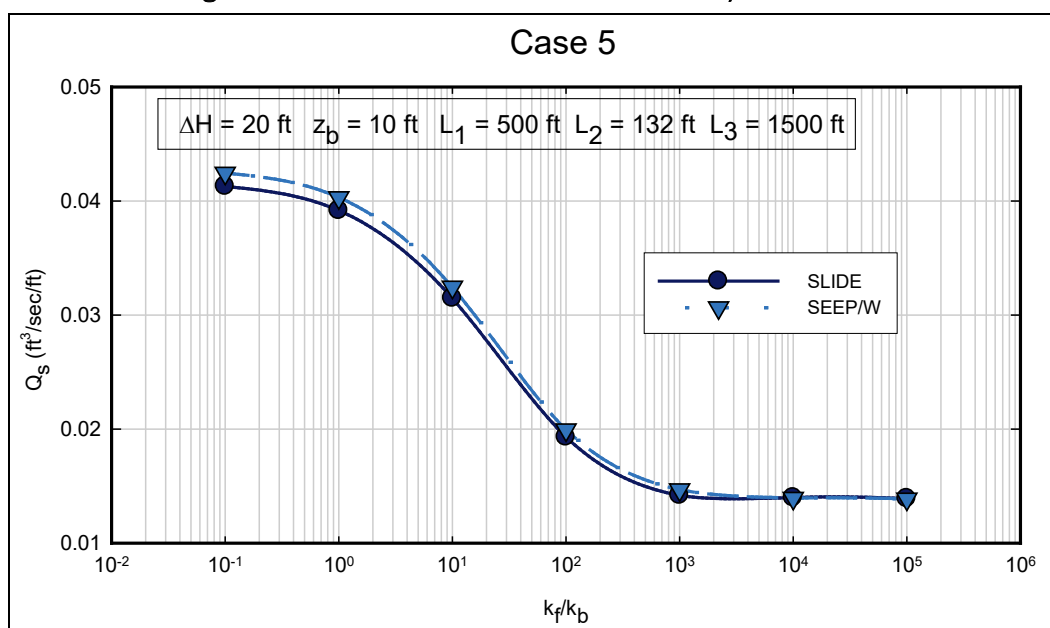


Figure C15. Calculated values of flow per unit length (Q_s) for various permeability ratios from Blanket Theory and finite element analysis for Case 6 for $z_b = 10$ ft and $L_3 = 200$ ft.

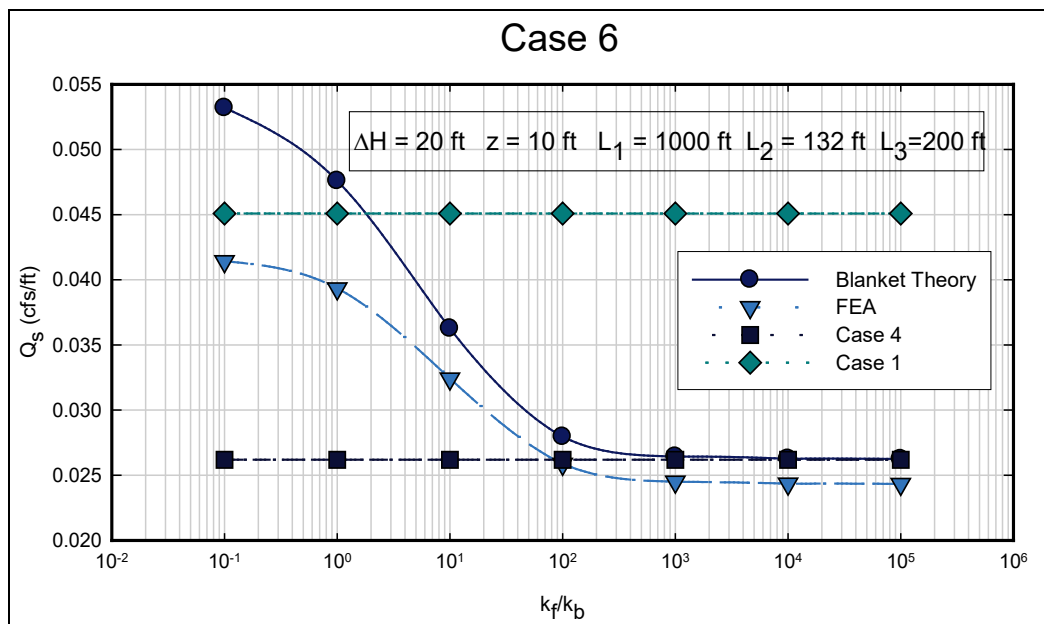


Figure C16. Calculated values of flow per unit length (Q_s) for various permeability ratios from Blanket Theory and finite element analysis for Case 6 for $z_b = 10$ ft and $L_3 = 500$ ft.

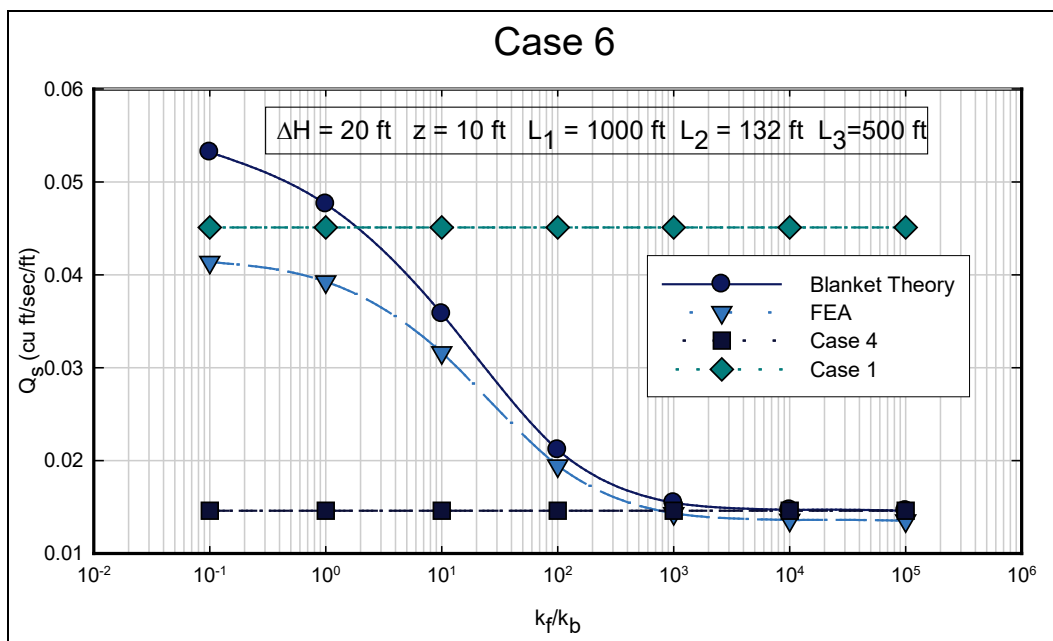


Figure C17. Excess head (h_b) or pressure head beneath blanket at toe for Case 6 calculated using FEA and Blanket Theory for different permeability ratios for $z_b = 10$ ft and $L_3 = 200$ ft.

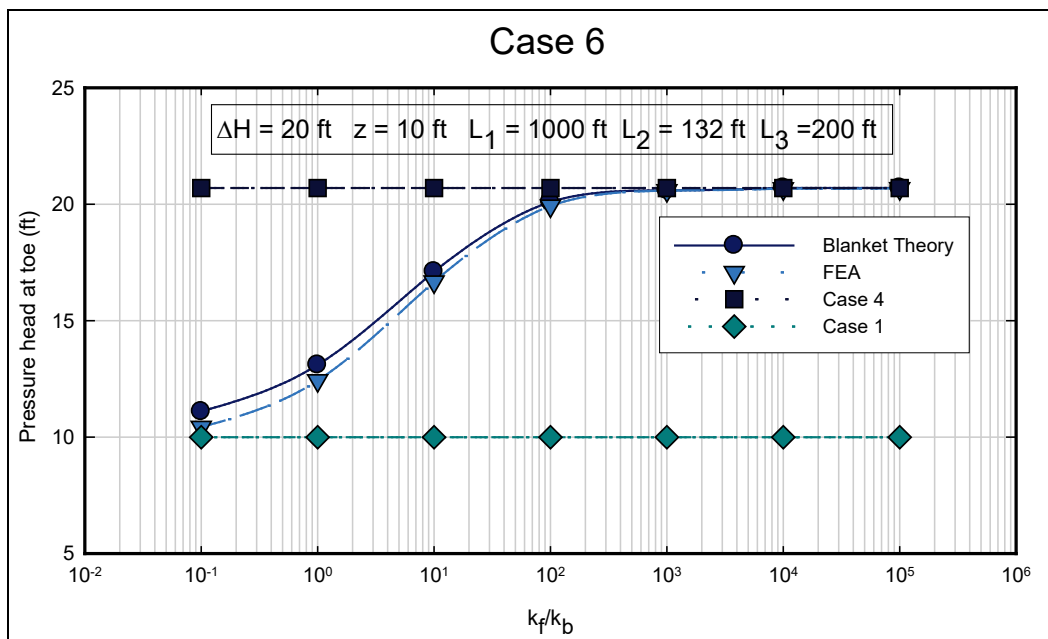


Figure C18. Excess head (h_b) or pressure head beneath blanket at toe for Case 6 calculated using FEA and Blanket Theory for different permeability ratios for $z_b = 10$ ft and $L_3 = 500$ ft.

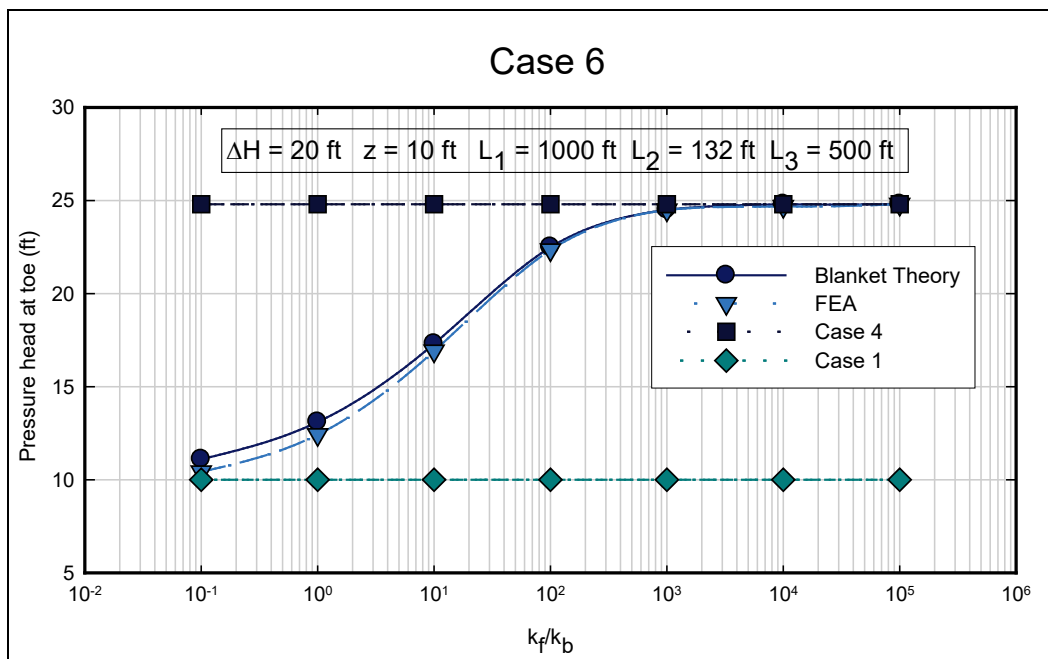


Figure C19. Calculated values of flow per unit length (Q_s) for various permeability ratios from Blanket Theory and finite element analysis for Case 6 for $z_b = 20$ ft and $L_3 = 200$ ft.

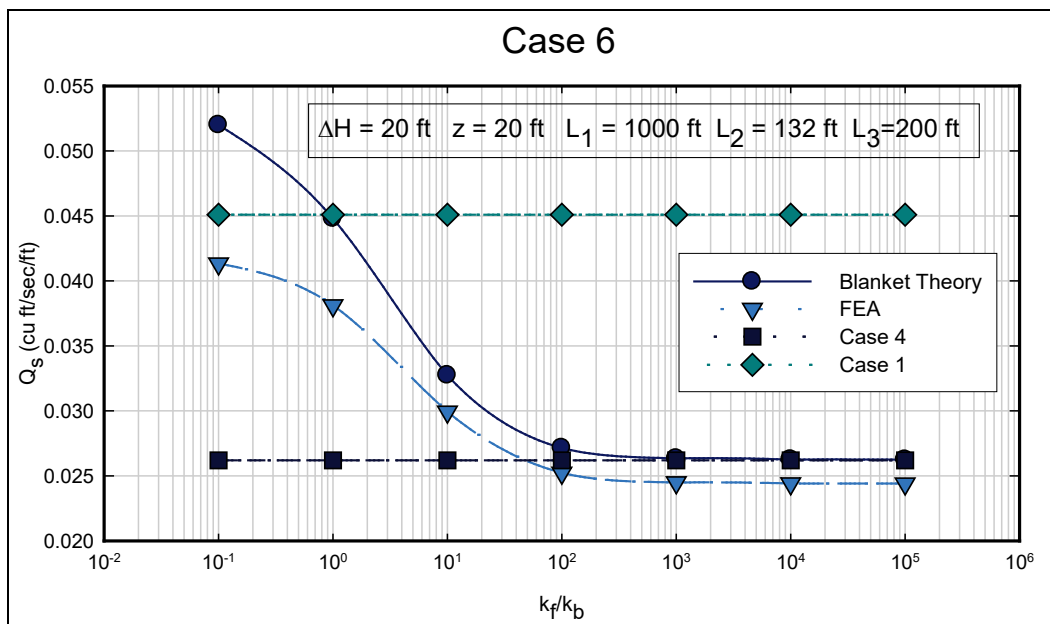


Figure C20. Calculated values of flow per unit length (Q_s) for various permeability ratios from Blanket Theory and finite element analysis for Case 6 for $z_b = 20$ ft and $L_3 = 500$ ft.

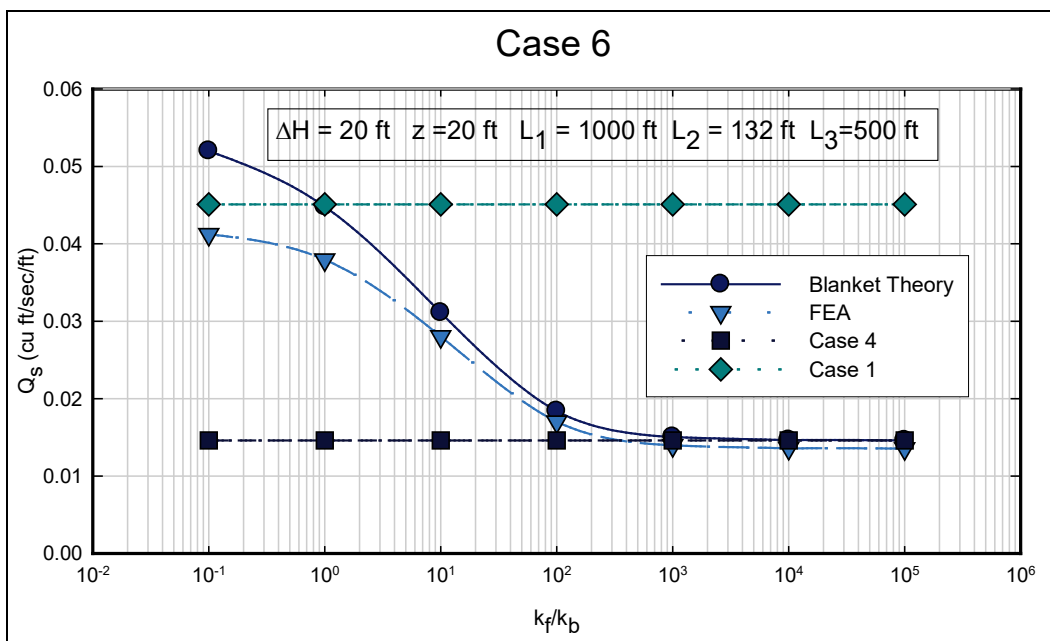


Figure C21. Excess head (h_b) or pressure head beneath blanket at toe for Case 6 calculated using FEA and Blanket Theory for different permeability ratios for $z_b = 20$ ft and $L_3 = 200$ ft.

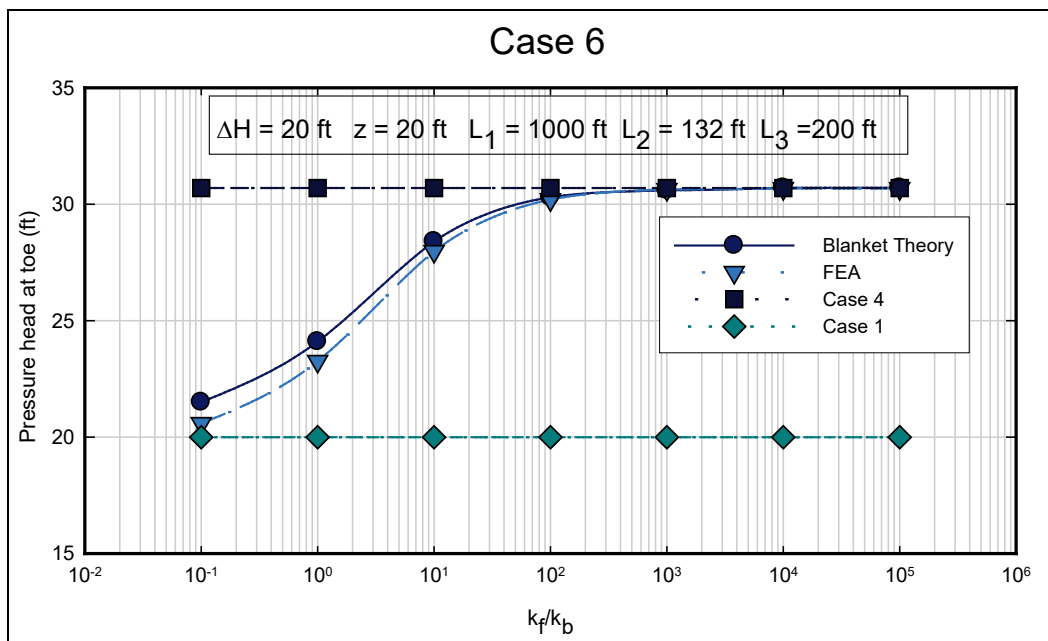


Figure C22. Excess head (h_b) or pressure head beneath blanket at toe for Case 6 calculated using FEA and Blanket Theory for different permeability ratios for $z_b = 20$ ft and $L_3 = 500$ ft.

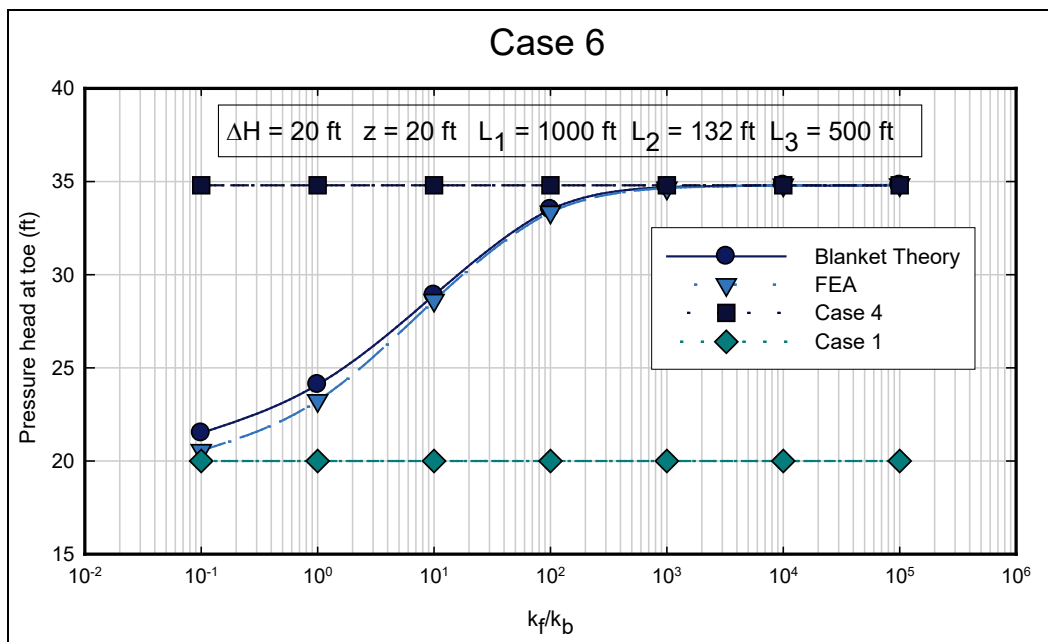


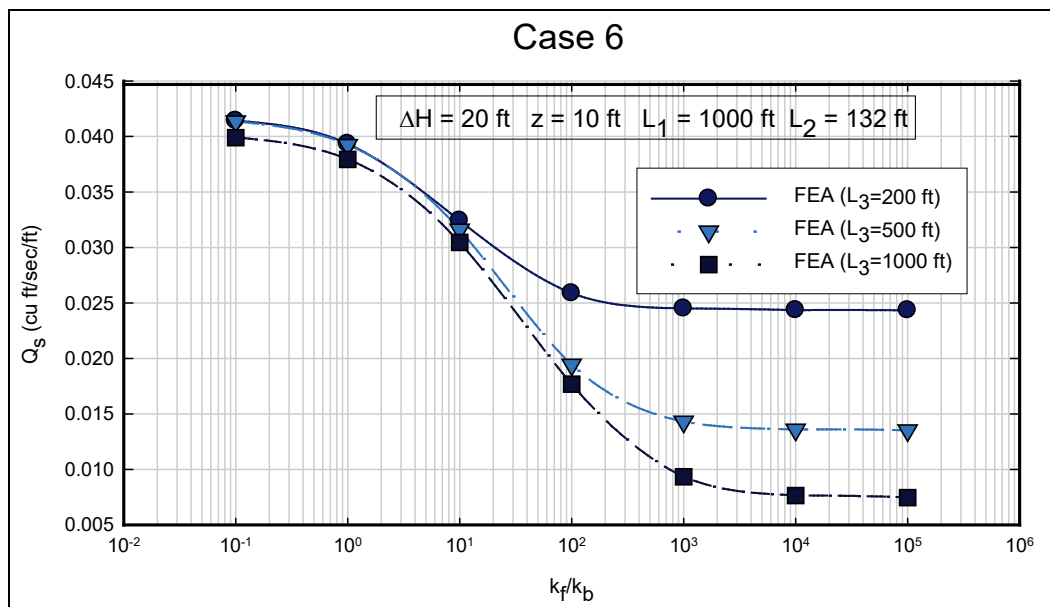
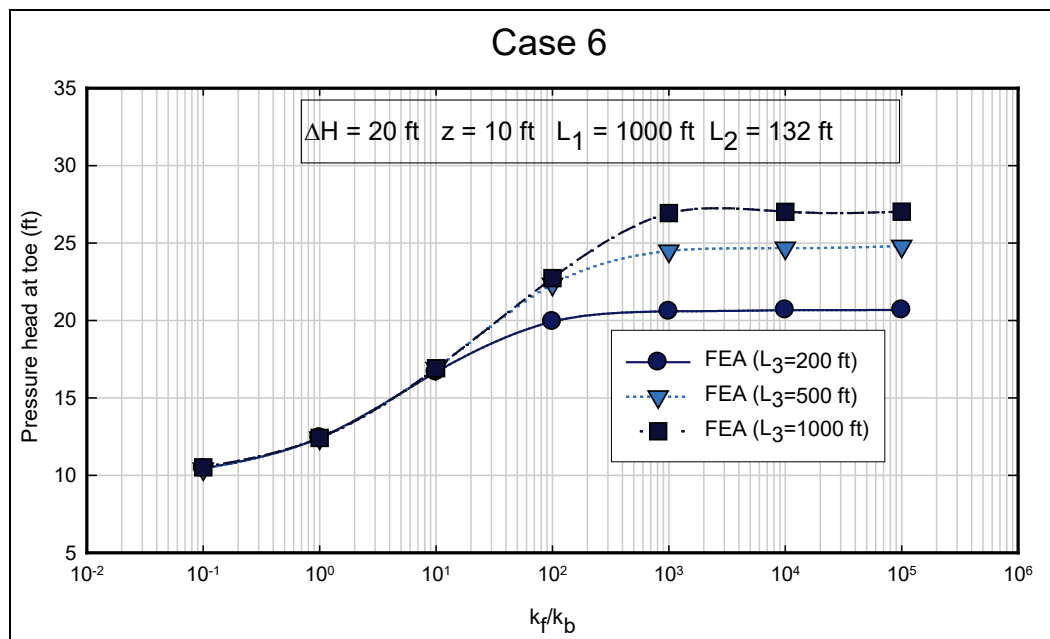
Figure C23. Comparison of flows for different values of L_3 for Case 6 for $z_b=10$ ft.Figure C24. Comparison of excess head (h_o) for different values of L_3 for Case 6 for $z_b=10$ ft.

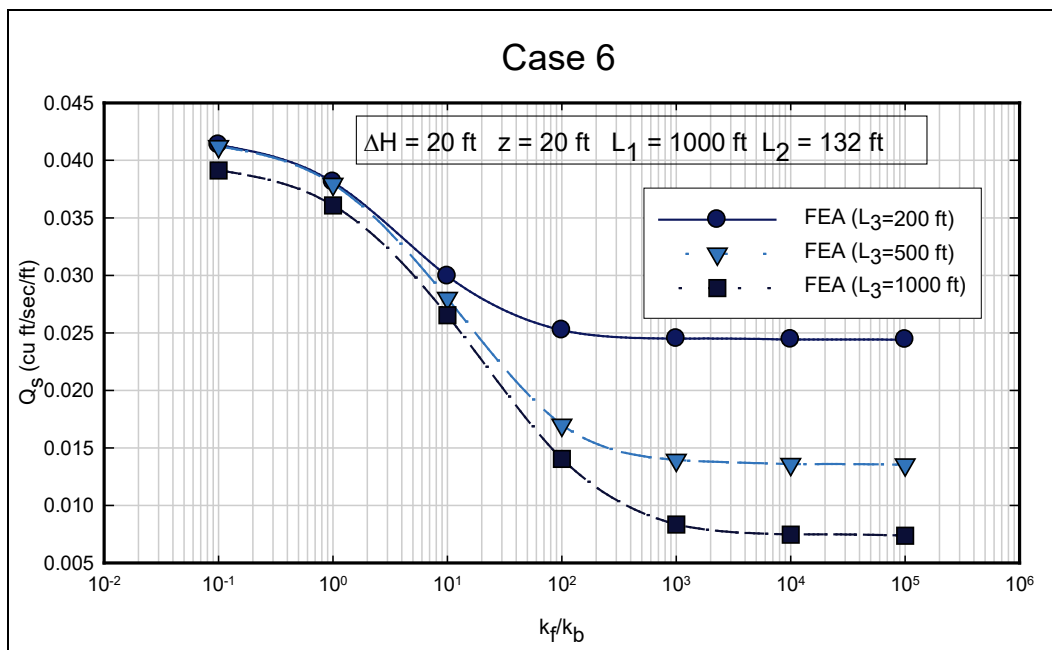
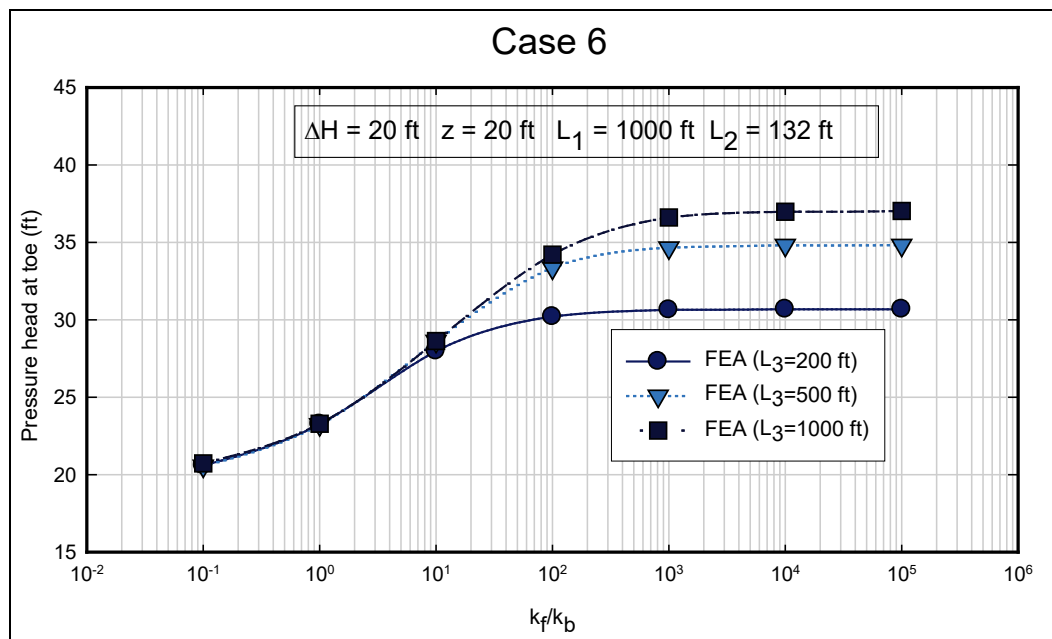
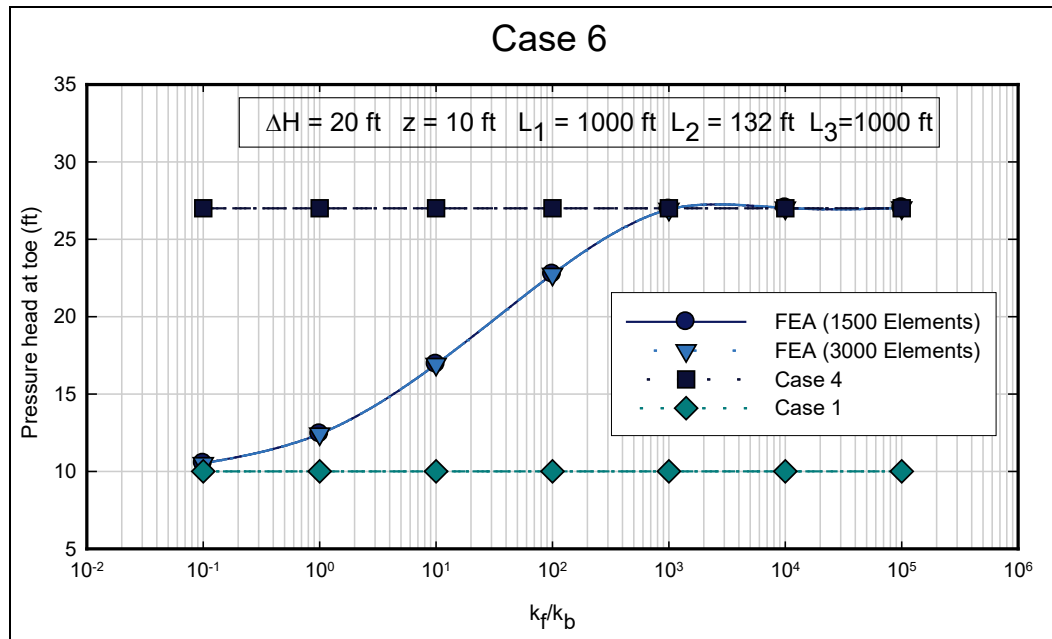
Figure C25. Comparison of flows for different values of L_3 for Case 6 for $z_b=20$ ft.Figure C26. Comparison of excess head (h_o) for different values of L_3 for Case 6 for $z_b=20$ ft.

Figure C27. Calculated excess head (h_e) for Case 6 showing the effect of number of elements.

REPORT DOCUMENTATION PAGE

Form Approved
OMB No. 0704-0188

Public reporting burden for this collection of information is estimated to average 1 hour per response, including the time for reviewing instructions, searching existing data sources, gathering and maintaining the data needed, and completing and reviewing this collection of information. Send comments regarding this burden estimate or any other aspect of this collection of information, including suggestions for reducing this burden to Department of Defense, Washington Headquarters Services, Directorate for Information Operations and Reports (0704-0188), 1215 Jefferson Davis Highway, Suite 1204, Arlington, VA 22202-4302. Respondents should be aware that notwithstanding any other provision of law, no person shall be subject to any penalty for failing to comply with a collection of information if it does not display a currently valid OMB control number. **PLEASE DO NOT RETURN YOUR FORM TO THE ABOVE ADDRESS.**

1. REPORT DATE (DD-MM-YYYY) August 2018		2. REPORT TYPE Final		3. DATES COVERED (From - To)	
4. TITLE AND SUBTITLE Comparison of Levee Underseepage Analysis Methods Using Blanket Theory and Finite Element Analysis				5a. CONTRACT NUMBER	
				5b. GRANT NUMBER	
				5c. PROGRAM ELEMENT NUMBER	
6. AUTHOR(S) Thomas L. Brandon, Abeera Batool, Martha Jimenez, and Noah D. Vroman				5d. PROJECT NUMBER	
				5e. TASK NUMBER	
				5f. WORK UNIT NUMBER	
7. PERFORMING ORGANIZATION NAME(S) AND ADDRESS(ES) Geotechnical and Structures Laboratory U.S. Army Engineer Research and Development Center 3909 Halls Ferry Road Vicksburg, MS 39180-6199				8. PERFORMING ORGANIZATION REPORT NUMBER ERDC/GSL TR-18-24	
9. SPONSORING / MONITORING AGENCY NAME(S) AND ADDRESS(ES) Headquarters, U.S. Army Corps of Engineers Washington, DC 20314-1000				10. SPONSOR/MONITOR'S ACRONYM(S) HQ-USACE	
				11. SPONSOR/MONITOR'S REPORT NUMBER(S)	
12. DISTRIBUTION / AVAILABILITY STATEMENT Approved for public release; distribution is unlimited.					
13. SUPPLEMENTARY NOTES					
14. ABSTRACT This report provides a comparison of levee underseepage analysis methods using Blanket Theory and finite element analysis. Blanket Theory is a set of closed-form solutions for computing seepage pressures and flows beneath levees. These solutions were introduced in a U.S. Army Corps of Engineers (USACE) 1956 technical manual and are also shown in the 2000 version of USACE Engineering Manual, Design and Construction of Levees. Derivations of Blanket Theory, which have not been previously documented, are thoroughly documented in this report. These derivations include the standard seven Blanket Theory cases and provide the key assumptions necessary for the accuracy of the solution; they highlight the errors in the Blanket Theory equations shown in the 2000 USACE engineering manual. An additional Blanket Theory case, which included a cutoff wall located beneath the levee, was derived in this re-port. Subsequently, an evaluation of the Blanket Theory solutions is made using finite element analysis. This evaluation included the standard seven Blanket Theory cases, the additional Blanket Theory case, and layered strata. This evaluation demonstrated where the analysis methods did or did not produced similar results. The finite element analysis method is further evaluated comparing different finite element analysis software. Finally, general guidelines for performing levee underseepage finite element analysis are provided in this report.					
15. SUBJECT TERMS Blanket Theory Underseepage		United States – Army Corps of Engineers Levee Finite Element Analysis		Seepage – analysis Seepage – mathematical models Finite element method – computer program	
16. SECURITY CLASSIFICATION OF:			17. LIMITATION OF ABSTRACT	18. NUMBER OF PAGES 145	19a. NAME OF RESPONSIBLE PERSON
a. REPORT Unclassified	b. ABSTRACT Unclassified	c. THIS PAGE Unclassified			19b. TELEPHONE NUMBER (include area code)